

**MATHEMATICAL MODELING OF COVID-19 TRANSMISSION
DYNAMICS BETWEEN HEALTHCARE WORKERS AND
COMMUNITY**

Lemjini Masandawa

**A Dissertation Submitted in Partial Fulfillment of the Requirements for the Degree of
Master's in Mathematical and Computer Sciences and Engineering of the Nelson Mandela
African Institution of Science and Technology**

Arusha, Tanzania

June, 2022

ABSTRACT

COVID-19 pandemic has posed an unprecedented threat to global public health. Health professionals caring for COVID-19 patients face insomnia, mental stress, physical exhaustion, stigma, the pain of losing patients and colleagues. Many of them acquired SARS-CoV-2 and some died. Protection of this workforce is of paramount importance to ensure optimal care to patients. Thus, this study contributes to the subject by formulating a deterministic mathematical model $SWEI_sI_aHRR$ (Susceptible - Healthcare workers - Exposed - Symptomatic - Asymptomatic - Hospitalized - Recovered) that combines both healthcare workers (as an independent compartment) and community and focuses on the protection of the healthcare workforce against SARS-COV-2. Benefiting the next generation matrix method, the basic reproduction number (R_0) was computed. Routh-Hurwitz criterion and stable Metzler matrix theory revealed that disease-free equilibrium point is locally and globally asymptotically stable whenever $R_0 < 1$, respectively. Lyapunov function depicted that the endemic equilibrium point is globally asymptotically stable when $R_0 > 1$. Further, the dynamics behavior of R_0 was explored when varying the use personal protective equipment (ξ) and physical distancing (θ). In the absence of protective measures (ξ and θ), the value of R_0 was 6.7125 which implies the expansion of the disease. When θ and ξ were introduced in the model, R_0 was 0.6713, indicating the decrease of the disease in the community. Numerical solutions were simulated by using Runge-Kutta fourth-order method. The numerical results illustrated mathematically that protection of health care workers can be achieved through effective use of personal protective equipment and minimization of transmission of COVID-19 in the community.

DECLARATION

I, **Lemjini Masandawa** do hereby declare to the Senate of Nelson Mandela African Institution of Science and Technology that this dissertation is my own original work and that it has neither been submitted nor being concurrently submitted for degree award in any other institution.



Signature.....

Date..20..07.2022

Lemjini Masandawa
(The name of the candidate)


The above declaration is confirmed.



Signature.....

Date..20..07.2022

Dr. Silas Steven Mirau
(Supervisor 1)



Signature.....

Date..22..07.2022

Dr. Isambi Sailon Imbalawata
(Supervisor 2)

COPYRIGHT

This dissertation is copyright material protected under the Berne Convention, the Copyright Act of 1999 and other international and national enactments, in that behalf, on intellectual property. It must not be reproduced by any means, in full or in part, except for short extracts in fair dealing; for researcher private study, critical scholarly review or discourse with an acknowledgment, without a written permission of the Deputy Vice Chancellor for Academic, Research and Innovation, on behalf of both the author and the Nelson Mandela African Institution of Science and Technology.

CERTIFICATION

The undersigned certify that they have read and hereby recommend for acceptance by the Nelson Mandela African Institution of Science and Technology the dissertation entitled: *Mathematical Modeling of COVID-19 Transmission Dynamics Between Healthcare Workers and Community*, in fulfillment of the requirements for the degree of Master in Mathematical and Computer Sciences and Engineering of the Nelson Mandela African Institution of Science and Technology.

Signature.....

Date.....20 .07.2022

Dr. Silas Steven Mirau
(Supervisor 1)

Signature.....

Date.....20 .07.2022

Dr. Isambi Sailon Mbalawata
(Supervisor 2)

ACKNOWLEDGMENTS

First and foremost, I have to thank my creator, the Almighty God for His protection, grace, and provision over my life and studies.

I am extremely thankful to my supervisors, Dr. Silas Steven Mirau of NM-AIST and Dr. Isambi Sailon Mbalawata of AIMS Rwanda for their noble guidance, support with full encouragement and enthusiasm. I will forever be grateful to them for their expertise, generous help, suggestion and positive attitude towards my abilities. I have benefited greatly from their wealth of knowledge.

My deepest appreciation goes to all the lecturers at the NM-ASIT for teaching and introducing me to the research world. Thank you very much.

I am deeply obliged to thank Lambura A, H Mlyashimbi, J Mwasunda, Miracle Amadi, Jean P, Jean Claude, Taiwo Adedipe for all support and contribution made during the preparation of this work.

Very special thanks to Mr. James P Shekaoneka an inspiring friend and a colleague for his camaraderie and support. Your friendship made writing less of an isolating slog through hell.

I would also like to thank all of my classmates for encouraging, supporting me whenever I needed, and cherished time spent together in the entire duration of my studies in NM-AIST.

Finally, I am more grateful to my family, my lovely wife Janeth, and children Emanuel and Noel for their love, support motivation, prayers, and patience as I spent time away while pursuing my studies. I am forever thankful to my parents and family members for their love and support.

DEDICATION

I dedicate this work to my precious wife, my beloved brothers, sisters and in memory of my late beloved father and mother.

TABLE OF CONTENTS

ABSTRACT	i
DECLARATION	ii
COPYRIGHT	iii
CERTIFICATION	iv
ACKNOWLEDGMENTS	v
DEDICATION	vi
TABLE OF CONTENT	vii
LIST OF TABLES	x
LIST OF FIGURES	xi
LIST OF ABBREVIATIONS	xiii
CHAPTER ONE	1
INTRODUCTION	1
1.1 Background of the Problem	1
1.1.1 History of Coronavirus	1
1.1.2 Historical Background, Transmission Route and Symptoms of COVID-19	2
1.1.3 Prevalence of COVID-19 Among Healthcare Workers and Protection Measures	3
1.1.4 The Disease Control Strategies	6
1.2 Statement of the Problem	7
1.3 Rationale of the Study	8
1.4 Objectives	8
1.4.1 Main Objective	8
1.4.2 Specific Objectives	9
1.5 Research Questions	9
1.6 Significance of the Study	9
1.7 Delineation of the Study	9
CHAPTER TWO	11
LITERATURE REVIEW	11

2.1	History of Mathematical Models in Epidemiology	11
2.2	Mathematical Models for COVID-19	12
2.2.1	Stochastic Models for COVID-19	12
2.2.2	Deterministic Models for COVID-19	13
2.2.3	Hybrid Model for COVID-19	18
2.3	Summary	18
CHAPTER THREE		19
MATERIALS AND METHODS		19
3.1	Mathematical Model for COVID-19 Dynamics	19
3.2	Mathematical Model Development	19
3.2.1	Model Assumptions	20
3.2.2	Illustrative Scheme for $SWEI_sI_aHR$ Model and Equations	21
3.2.3	Model Variables Description	22
3.3	Qualitative Analysis of the Proposed COVID-19 Model	24
3.3.1	Positiveness of Model Solutions	24
3.3.2	Invariant Region	28
3.3.3	Existence and Uniqueness for $SWEI_sI_aHR$ Model Solution	30
3.3.4	Disease-Free Equilibrium (DFE)	35
3.3.5	Basic Reproduction Number (R_0)	35
3.3.6	Local Stability at Disease-Free Equilibrium (DFE)	38
3.3.7	Existence and Uniqueness of Endemic Equilibrium	41
3.3.8	Global Stability of Disease-Free Equilibrium	42
3.3.9	Global Stability of Endemic Equilibrium	44
3.4	Summary	48
CHAPTER FOUR		49
RESULTS AND DISCUSSION		49
4.1	Numerical Results	49
4.2	Numerical Simulation for the Model (3.1)	49
4.2.1	Sensitivity and Uncertainty Analysis	49
4.2.2	Dynamics of Human Populations	53
4.2.3	Global Stability at Endemic Equilibrium (EE) for the Proposed Model (3.1)	54
4.2.4	Impact of Control Parameters on the COVID-19 Model (3.1)	56
4.2.5	The Identifiability of Model Parameters	61
4.3	Discussion	63
4.4	Summary	63

CHAPTER FIVE	64
CONCLUSION AND RECOMMENDATIONS	64
5.1 Conclusion	64
5.2 Recommendations	65
5.2.1 Limitation of the Study	65
5.2.2 Future Work	65
REFERENCES	67
APPENDICES	78
RESEARCH OUTPUT	86

LIST OF TABLES

Table 1:	Detailed description of state variables of the proposed model (3.1)	23
Table 2:	Detailed description of the parameters used in the proposed Model (3.1) . .	23
Table 3:	Relevant model's parameters and their indices values	50
Table 4:	Parameter identifiability of the COVID-19 proposed model.	62

LIST OF FIGURES

Figure 1:	Images for COVID-19 (Ford, 2020)	3
Figure 2:	A photograph of a healthcare worker full of PPE (Herron <i>et al.</i> , 2020) . . .	5
Figure 3:	The compartmental model for COVID-19	22
Figure 4:	Normalized local sensitivity indices of R_0 for each parameter	51
Figure 5:	Dependence of R_0 on recruitment rate (Λ)	51
Figure 6:	Dependence of R_0 on healthcare workers transmission probability (β_2) . .	51
Figure 7:	Effect of recovery rate (η) for I_s population on R_0	52
Figure 8:	Dependence of R_0 on disease transmission rate (β_1)	52
Figure 9:	Dependence of R_0 on healthcare workers recruitment rate (b)	52
Figure 10:	Dependence of R_0 on disease induced death rate (d)	52
Figure 11:	Effect of hospitalizing symptomatic infected population (ν) on R_0	52
Figure 12:	Effect of progression rate (ρ) from E to I_a on R_0	52
Figure 13:	Effect of progression rate (α) from E to I_s on R_0	53
Figure 14:	Dependence of R_0 on natural mortality rate (μ)	53
Figure 15:	Effect of a proportional of health workers (r) on R_0	53
Figure 16:	Effect of physical distancing (θ) on R_0	53
Figure 17:	Profile for the dynamics of $SWEI_sI_aHR$ sub-populations	54
Figure 18:	Profile of global stability at EEP for susceptible population	55
Figure 19:	Profile of global stability at EEP for healthcare workers population	55
Figure 20:	Profile of global stability at EEP for exposed population	55
Figure 21:	Profile of global stability at EEP for symptomatic infected population . . .	55
Figure 22:	Profile of global stability at EEP for asymptomatic infected population . .	55
Figure 23:	Profile of global stability at EEP for hospitalized population	55
Figure 24:	Profile of global stability at EEP for recovered population	56
Figure 25:	Profile showing the impact of θ on susceptible population	57
Figure 26:	Profile showing the impact of θ on symptomatic population	57
Figure 27:	Profile for the impact of θ on hospitalized humans	57
Figure 28:	Profile for the impact of θ on recovered humans	57
Figure 29:	Profile for the impact of treatment (δ) on asymptomatic infected population	57
Figure 30:	Profile for the impact of treatment (δ) on recovered population	57
Figure 31:	Profile for the impact of treatment (η) on symptomatic infectious	58
Figure 32:	Profile for the impact of treatment (η) on recovered population	58
Figure 33:	Profile for the impact of (ξ) on healthcare workers population	58
Figure 34:	Profile for the impact of (ω) on hospitalized population	58
Figure 35:	3D dynamics behavior of R_0 for ω and θ along with contour plot	59
Figure 36:	3D dynamic behavior of R_0 for θ and η along with contour plot	60
Figure 37:	3D dynamic behavior of R_0 for ν and θ	60

Figure 38: Model fitting 62

LIST OF ABBREVIATIONS

WHO	World Health Organization
COVID	Coronavirus Disease-2019
SARS-COV-2	Severe Acute Respiratory Syndrome Coronavirus -2
SARS-COV-1	Severe Acute Respiratory Syndrome Coronavirus -1
MERS-COV	Middle East Respiratory Syndrome Coronavirus
WWI	World War 1
NMAIST	The Nelson Mandela Africa Institution of Science and Technology
HIV	Human Immunodeficiency Virus
PPE	Personal Protective Equipment
ODE	Ordinary Differential Equation
US	United State
HBV	Hepattis B Virus
3D	Three Dimension
MATLAB	Mathematics Laboratory

CHAPTER ONE

INTRODUCTION

1.1 Background of the Problem

In recent times, the globe is facing challenges of emerging and re-emerging infectious diseases which posed a devastating impact on global public health. These diseases threaten the lives of people socially and economically (Adekola *et al.*, 2020; Omar *et al.*, 2021). Some examples of these diseases are HIV, H1N1, HBV, Malaria, and Ebola which advance to the global community at much remarkable rate with the ability to spread rapidly to many countries in the world within a short period (He *et al.*, 2020; Naik *et al.*, 2020). Since today's world is characterized by mutual dependence and interconnectedness, this leads to high human mobility (Zhao *et al.*, 2020; Tatem *et al.*, 2006). The greatest human interaction globally accelerates the spread of infectious diseases, for example, if an outbreak is detected in one part of the world, the movement of people transmits it to the other part of the globe within few hours or days (Asamoah *et al.*, 2020). Further, the ability of bacteria, viruses, and parasites to keep changing over time made infectious diseases difficult to completely control. Despite the effort made in the world of developing antibiotics and vaccines, yet infectious diseases count the second in the number of death worldwide after cardiovascular diseases (Fauci *et al.*, 2005). The newest of these viruses is called SARS-COV-2.

1.1.1 History of Coronavirus

Coronaviruses are a group of enveloped viruses with positive sense, uniquely grounded, affirmative sense RNA virus with the diameter of 60-140nm which is either elliptical or round in shape (Shayak *et al.*, 2020). These viruses cause respiratory illness in many animal species, including humans. It is named coronavirus because of the crown structure when viewed through an electronic microscope (Wan *et al.*, 2020). Coronavirus belongs to the biological family of *coronaviridae* with two subfamily which are *torovirinae* and *coronavirinae* (Mishal *et al.*, 2020). The subfamily *coronavirinae* has four classes which are: alpha, beta, gamma, and delta coronavirus. Alpha coronavirus includes human coronavirus such as HCoV-NL63 and HCoV-229E (Harapan *et al.*, 2020). On other hand, beta coronavirus contains human coronavirus such as HCoV-HKU1, Severe Acute Respiratory Syndrome Human Coronavirus (SARS-HCoV), and Middle Eastern Respiratory Syndrome Coronavirus (MERS-CoV). Delta coronavirus contains viruses extracted from birds and pigs while gamma coronavirus contains viruses from birds and whales (Harapan *et al.*, 2020).

At first, coronaviruses were discovered as human pathogens in the mid-1960s (Steardo *et al.*, 2020). There are seven types of coronaviruses which are SARS-COV-1, MERS-CoV, SARS-COV-2, HCoV-229E, HCoV-HKU1, HCoV-OC43, and HCoV-NL63 (Steardo *et al.*, 2020). SARS-COV-1, MERS-CoV, and SARS-COV-2 are well-known coronaviruses compared to others.

SARS-COV-1 emerged in Guangdong, the southern part of China in November 2002 and then spread to Vietnam, Canada, Singapore, and other countries in the world (Koh *et al.*, 2005). In March 2003, one of the conducted research evinced that the novel coronavirus was a causative agent of SARS-COV-1, where the palm civet cats and dromedary camels were the intermediary animal sources (Peiris *et al.*, 2003). Research suggested that bats might be a natural reservoir of SARS-CoV-1 (Garba *et al.*, 2020). This virus is transmitted from human to human through respiratory droplet fomite-based contact and direct contact. SARS-CoV-1 spread to 29 countries causing 8096 confirmed cases with 774 deaths and disappearing in the year 2004 (Tsang *et al.*, 2003).

MERS-CoV was first detected in September 2012 in Saudi Arabia and spread to 27 countries of the world causing 2494 confirmed cases and 858 deaths (Garba *et al.*, 2020). Still, dromedary camels and civet cats were important natural sources of the virus. One research revealed that the novel beta coronavirus was discovered from a male patient who died because of serious pneumonia contributed to the failure of many parts of his body organs (Hui *et al.*, 2021). MERS-CoV is transmitted through close contact via droplets or contact with fomite (Zaki *et al.*, 2012).

1.1.2 Historical Background, Transmission Route and Symptoms of COVID-19

Coronavirus Disease 2019 (COVID-19) is a respiratory illness that emerged on 31 December, 2019 in China and spread to many parts of the world within a short period (Oud *et al.*, 2021; Mahmoudi *et al.*, 2021). It is the newest kind of virus caused by Severe Acute Respiratory Syndrome Coronavirus 2 (SARS COV-2) (Bubar *et al.*, 2021; Ivorra *et al.*, 2020). COVID-19 can affect either the lower respiratory tract (lungs and windpipes) or the upper respiratory tract (throat, sinuses, and nose). It started as unusual pneumonia of unknown etiology in Wuhan City in central China. On 7 January, 2020 it was discovered that the cause of the new outbreak of pneumonia is called the novel coronavirus (2019-nCoV) and later, on 11 February, 2020 an International Committee on Taxonomy of Viruses gave the disease a name called Coronavirus Disease 2019 (COVID-19) (Abioye *et al.*, 2021). Some studies suggested that the potential intermediary source of the novel infection is pangolins (Shayak *et al.*, 2020; Mahmoudi *et al.*, 2021). In spite of the fact that the Chinese government imposed a strong lockdown, yet the disease spread very quickly throughout China and many other parts of the world through travelers from Wuhan. The outbreak was declared as Public Health of International Concern (PHIC) on 30 January, 2020 and due to the high rate of the global spread of the virus, WHO announced it as pandemic on 11 March, 2020. As of 15 November, 2021 there have been more than 254 million confirmed cases of COVID-19 and more than 5.1 million death reported globally (Coronavirus, 2020).

COVID-19 is transmitted from one person to another via breathing in respiratory droplets released from the mucous membrane (eye, mouth, and nose) of an infected person when sneezing, coughing, talking, or exhaling (Peter *et al.*, 2021). These respiratory droplets are too heavy to hang in the

air so, the force of gravity influences and travel not more than one meter before quickly falling on the floor or surface thus, a social distance of 2 meters is a precaution. Further, the disease can be acquired through fomite transmission (Mbogo & Odhiambo, 2021). Predominantly transmission occurs through inhaling respiratory droplets from an infected person in close contact.

Zamir *et al.* (2021) in their research presented that about 75% of COVID-19 victims do not show symptoms but recover naturally from the disease, only 20% can develop symptoms. The infected person will take 2-14 days to manifest full symptoms of the disease (Ahmad *et al.*, 2021). About 80% of infected individuals recover without any treatment (Ahmad *et al.*, 2021). Mid-infected individuals recover within two weeks while critical cases recover within 3 to 6 weeks.

The disease is much severe to the age group of 65 and above compared to young people. The human population having a long-term illness that weakens the body immunity such as cancer, chronic respiratory disease, diabetes, hypertension, and cardiovascular are most likely to experience severe illness (Peter *et al.*, 2021). Common symptoms for this disease include tiredness, sleep disorders, throat infection, nausea, vomiting, diarrhea, severe headache, muscles ache, runny nose, dry cough, red eyes, fatigue, sneezing, losing smell, and test (Gostic *et al.*, 2020; Ahmad *et al.*, 2021). The very serious clinical symptoms include breathing problems, persistent pain in the chest, blood pressure, kidney failure, and lack of voluntary movement (Baba *et al.*, 2021). Figure 1 shows the images of COVID-19 with crown-like spikes on their surface.



Figure 1: Images for COVID-19 (Ford, 2020)

1.1.3 Prevalence of COVID-19 Among Healthcare Workers and Protection Measures

Public health experts are in a frontline fight against the COVID-19 pandemic. The fight against the pandemic subjected the healthcare workforce to be the most vulnerable group. For example, Park (2020) in his study indicated that the proportional of healthcare workers who are infected in Spain and the US are 20% and 3% of all cases of COVID-19, respectively. On other hand, one

study depicted that as of May 2020, out of 11 086 the total number of COVID-19 confirmed cases in the Philippines, 1996 (17.96%) were healthcare workers (Buhat *et al.*, 2021). Another study revealed that as of 3 April, 2020 in Italy there were around 10 000 healthcare workers who have been infected with COVID-19 and 74 death (Chersich *et al.*, 2020). As of 20 September, 2020 one study conducted in Mexico City revealed that there were around 17 531 healthcare workers who have been infected (Antonio-Villa *et al.*, 2021). The Chinese Centre for Disease Control and Prevention (CCDC) showed that by early February 2020, out of 72 000 confirmed COVID-19 cases, 3000 healthcare workers had become infected which is 3.8% of all cases of the disease (Kursumovic *et al.*, 2020). Poukka *et al.* (2022) conducted cohort study in Finland evinced that 3874 healthcare workers tested positive of SARS-COV-2. Frequently interaction of healthcare workers in close proximity puts them at a higher risk of getting infected. Once the healthy person is infected unceasingly contact with the patient and the community facilitates more transmission of the disease, hence medical staffs are likely to become super spreaders. Also, the daily activities of healthcare workers at their workplace such as placing respiratory devices on patients and physical examinations put them at unimaginable risks. Further, Patients seeking medical services though not revealing COVID-19 symptoms put this workforce a risk of getting infected. In addition, healthcare workers are faced with risks of becoming infected because of inadequate availability of protective measures and lack of diagnostic tests (Buhat *et al.*, 2021). Unknowingly exposure of the healthcare workers to the virus threatens the patients and the general community at large since this workforce transmit the virus unintentionally.



(a)



(b)

Figure 2: A photograph of a healthcare worker full of PPE (Herron *et al.*, 2020)

Protection of healthcare staff is essential in order to ensure and maintain the provision of optimal care to patients. Shortening the work shift could be one of the alternatives to protect the medical

staff though this approach was not feasible during the COVID-19 pandemic due to overwhelmed number of patients (Dy and Rabajante, 2020). Protection of healthcare workers against COVID-19 results in a robust healthcare staff that can endure a long period of war against the disease. Public health experts can be protected by using Personal Protective Equipment (PPE) (Asamoah *et al.*, 2020; Park, 2020). PPE are tools or garments designed to protect wearers from infection or any injury. These are essential items used to protect individuals from pathogens and contaminants (Singh *et al.*, 2020). The purpose of PPE is to reduce the wearer's exposure hazard. N95 masks, eye shields, medical gowns, isolation booths, and gloves are among the protective equipment. The N95 mask is a kind of respirator that protects the user from breathing in contaminated air. N stands for not resistant to oil while 95 is the percentage of its minimum efficacy in protecting a wearer. Eyeshield protects the eye of the wearers from any hazard. Medical gowns are worn by health professionals to act as a barrier between a patient and health workers. Gloves protect a user from touching contaminated particles (Park, 2020). Figure 2 (a) shows a photograph of a healthcare worker full of personal protective equipment when recording a temperature of a patient. Figure 2 (b) depicts an image for N95 mask.

1.1.4 The Disease Control Strategies

Regarding the minimization of the COVID-19 outbreak in the general community, WHO recommended the following measures: Covering a cough or sneeze with inner elbow or tissue, cleaning hand with soap and running water or with alcohol-based hand rub, keeping unwashed hand away from the mouth, eye, and face, maintain a physical distance of at least 1 meter between you and another person coughing or sneezing, avoidance of gathering which bring many people together, lockdown, rapid testing, wearing of medical masks in the public, and isolation (Bakar & Rosbi, 2020).

Physical distancing refers to measures aiming at minimizing interactions within a community, which can include infected human population as yet unidentified, hence not in isolation (Aquino *et al.*, 2020). Since COVID-19 is transmitted to a healthy person through respiratory droplets there is a need of having certain physical proximity which reduces the spread of the disease. Physical distancing allows the spread to be minimized. Examples of physical distancing suppression measures that have been adopted include cancellation of events to avoid mass gatherings, the closure of learning institutions, workplaces, and closure of certain businesses (Abrams *et al.*, 2021; Imai *et al.*, 2020). Physical distancing is specifically useful in settings where there is community transmission of the virus, where the suppression measures imposed on the most vulnerable segments of the population are regarded insufficient to prevent new transmissions (Aquino *et al.*, 2020). The total lockdown is the most extreme case of physical distancing which can be applied either in the entire community, region, or city by forbidding people to leave their homes except to purchase basic supplies or to access emergency services. Lockdown enables social contact to be substantially reduced.

Many research groups dedicated much of their effort to developing vaccines (Shahzad *et al.*, 2021). Pfizer, Moderna, Gamaleya, and AstraZeneca are some of the vaccines developed in less than a year (da Silveira *et al.*, 2021). Even after the discovery of COVID-19 vaccines, yet non-pharmaceutical strategies have a significant on containing the spread of the COVID-19. During this pandemic, several researchers deployed mathematical models which incorporate the control measures stipulated by WHO to study the dynamics transmission of COVID-19.

Mathematical modeling is an essential theoretical tool in analyzing the spread of COVID-19 and suggesting suppression measures (Shahzad *et al.*, 2021). Some mathematical models decompose the entire population which is under consideration into groups where the assumptions on-time rate of transfer among the population and their nature are made (Olivares & Staffetti, 2021). Models have been used in implementing, planning, evaluating, optimizing detection, and therapy. At the same time, they have been used to analyze the spreads of viruses (Singh *et al.*, 2021; Danane *et al.*, 2021). After the COVID-19 outbreak chemists, epidemiologists, pharmacists, mathematicians, biologists paid much attention to mathematical modeling to defeat the pandemic (Bastos & Cajueiro, 2020; Tang & Wang, 2020; Faranda & Alberti, 2020; Redhwan *et al.*, 2020; Ud Din *et al.*, 2020; Atangana & Atangana, 2020).

There exist few mathematical models on the transmission dynamics among the healthcare workers (Chatterjee *et al.*, 2020; Gozalpour *et al.*, 2021). Dy and Rabajante (2020) in their study, they estimated the number of newly infected healthcare workers within a short duration of fewer than 48 hours. Other authors in their study, proposed that work shifts as a good strategy to protect healthcare workers against COVID-19 (Sánchez-Taltavull *et al.*, 2021).

1.2 Statement of the Problem

COVID-19 epidemic has posed an unprecedented threat to global public health. Healthcare workers caring for COVID-19 patients face insomnia, stigma, mental stress, physical exhaustion, separation from families, and the pain of losing patients and colleagues (Chersich *et al.*, 2020). Many of them acquired SARS-CoV-2 and some died. From the outset of the outbreak to 8 May, 2020 there were around 152 888 infected healthcare workers with a total of 1 413 death globally (Bandyopadhyay *et al.*, 2020). On other hand, as of 20 September, 2020 one study conducted in Mexico City revealed that there were around 17 531 healthcare workers who have been infected (Antonio-Villa *et al.*, 2021). Public health experts are at risk for increased exposure to COVID-19 compared to other members in the community, and they may serve as vectors for transmission of these illnesses (Kim *et al.*, 2020). An insufficient number of diagnostic tests, inadequate protective equipment, and a COVID-19 asymptomatic infectious population put the healthcare workers at the greatest risk of being infected (Heinzerling *et al.*, 2020). Also, frequent interaction in close proximity between healthcare and COVID-19 infected individuals puts this workforce at higher risk of contracting the disease.

Much researches conducted on mathematical models of COVID-19 concentrated on minimization of the disease spread among the public members. The study at hand formulated a deterministic model with focus on minimizing the COVID-19 infections among the healthcare workers and also the community at large.

1.3 Rationale of the Study

The core function of healthcare workers during the COVID-19 epidemic subjected them to be the most vulnerable group against the disease. Healthcare workers are on the frontline in the battle against the COVID-19 pandemic. This motivated us to investigate the transmission dynamics of COVID-19 between the healthcare workers and the community in a mathematical language. The mathematical model developed is utilized to analyze the transmission dynamics of COVID-19 between healthcare workers and the community in order to examine the impact of protective measures.

Few kinds of research have been done on mathematical modeling between frontlines and the general public. For example, Buhat *et al.* (2021) conducted a study on the dynamics of COVID-19 between frontlines and the public when regarding two mutually exclusive populations. They studied the dynamics when having the general public population alone and the frontlines compartment alone. Another study determined only the number of newly infected individuals one cycle of the day job (a short period of only less than 48 hours) (Dy and Rabajante, 2020). This study did not focus on the dynamics of the disease rather the estimation of risk among healthcare workers. However, the aforementioned models did not reflect the clear spread of COVID-19 between healthcare workers and the general community since their models lack a compartment of healthcare workers who interact directly with the general community. The presents study developed and explored a mathematical model in which healthcare workers interact directly with the community for the sake of studying transmission dynamics of COVID-19. The proposed $SWEI_sI_aHR$ model is applied to analyze the impact of implementing the use of personal protective equipment among healthcare professionals. Further, the effect of control measures among the community members is investigated.

1.4 Objectives

To solve the stated research problem, there is a need to have general and specific objectives.

1.4.1 Main Objective

The main objective of the presents study is to develop and analyze a mathematical model for COVID-19 transmission dynamics between healthcare workers and the community.

1.4.2 Specific Objectives

The specific objectives of this study are:

- (i) To develop a mathematical model for COVID-19 transmission dynamics between healthcare workers and community which includes protective measures.
- (ii) To determine the existence and stability of the equilibrium points of the model formulated in (i).
- (iii) To identify sensitive parameters of the developed model by using sensitivity analysis.
- (iv) To perform numerical simulation of the model using MATLAB solver ODE45 Runge-Kutta fourth-order scheme.

1.5 Research Questions

The study is guided by the following questions:

- (i) What is the deterministic model for the transmission of COVID-19?
- (ii) What are the conditions for the existence and stability of the equilibrium points?
- (iii) What is the sensitivity indices of the developed model?
- (iv) Which kind of information do the simulations convey?

1.6 Significance of the Study

The significance of this study are :

- (i) To inform the public of the importance of protective measures (i.e physical distancing (θ) and the use of protective equipment (ξ)) in curtailing the transmission of COVID-19.
- (ii) To researchers, the current study act as a base for further investigations.
- (iii) To help the society to get a deeper understanding of the novel coronavirus.
- (iv) It helps the governments and policymakers all over the world to establish and put in place policies, programs for disease prevention and control.

1.7 Delineation of the Study

COVID-19 is an infectious disease that has affected different groups of humankind such as farmers, soldiers, drivers, educators, students, healthcare workers, and many others. Healthcare workers are much affected compared to other groups. Their protection against the disease maintains

the care given to patients in the health system. Without adequate protection, the COVID-19 mortality rate may be high among medical staff and their children, families, and friends (Chersich *et al.*, 2020). They may also serve as a vector for disease transmission. Much could be done to protect health care workers. The study at hand developed and analyzed a deterministic model for COVID-19 among the health care workers and the community. Two protective measures ξ and θ were incorporated to both health care workers and susceptible compartments when exposed to the disease. The two parameters quantify the level of protection against the disease.

CHAPTER TWO

LITERATURE REVIEW

2.1 History of Mathematical Models in Epidemiology

In epidemiology, mathematical modeling gives a comprehension of the fundamental process that governs the transmission of the disease and proposes control strategies. Managing infectious diseases through mathematical models has a long history and notable success. Epidemiological models can be expressed in mathematical languages in two ways: (a) compartmental models, where members of the group are divided into different sections called classes. (b) Agent-based modeling, this is based on the interaction among the members of the group (Gozalpour *et al.*, 2021). Generally, mathematical models can be used to evince a specific behavior that is not clear in experimental data since the data are non-reproducible, limited, and sometimes subjected to error when measuring. These models range from simple to detailed. The detailed models are very valuable since they can be used to give recommendations about specific strategies to deal with a certain outbreak in the community (Brauer *et al.*, 2012).

The pioneering work of mathematical modeling in epidemiology was done by Swiss mathematician Daniel Bernoulli who is trained as a physician in 1760. He published a paper that focused on the prediction of the impact of immunization with cowpox by examining the expected life of the population which is immunized (Scherer & McLean, 2002). After around 150 years later, nearly to the first World War (WW1), Ronald Ross presented several mathematical models to explore the transmission dynamics of malaria. These models laid down a good foundation for the modern theory of how to control infectious diseases. Ross' models suggested that malaria can be prevented by controlling mosquitoes. This work got great recognition in the public health (Scherer & McLean, 2002). McKendrick and Kermack (1927) proposed *SIR* which laid down the complete foundation of compartmental models in epidemiology. In their model, they assumed that *S* gets an infection at a rate that is proportional to the total number of contact between *S* and *I* (Brauer *et al.*, 2012). They wrote classical papers in 1932 and 1933 which influenced the development of mathematical models for the spread of infectious diseases.

Communicable diseases disseminate through the vector to human or human-human transmission. Depending on whether an infected person will acquire or not acquire immunity after recovery, the basic models in modeling are *SIS* and *SIR*. The *SIS* describes diseases with no immunity against reinfection while *SIR* explains diseases that confers immunity. Other models can be obtained by extending the two aforesaid models depending on the needs and number of compartments required for example Exposed- Infectious- Quarantined- Recovered (*SEIQR*), Susceptible-Exposed- Infectious (*SEI*), Susceptible- Exposed- Infectious- Susceptible (*SEIS*), Susceptible-Exposed- Infected- Recovered- Deceased (*SEIRD*), Susceptible- Infectious- Recovered- Susceptible (*SIRS*), Susceptible- Undetected- Isolated- Hospitalized- Threatened- Extinct- Recovered

(*SUIHTER*) and many others (Parolini *et al.*, 2021; Hethcote, 2000).

2.2 Mathematical Models for COVID-19

Recently, many scholars have developed several mathematical models of COVID-19 such as classical integer-order derivatives, non-integer derivatives, stochastic, and many others. These models are formulated for the sake of better understanding the transmission dynamics of COVID-19. To generate a clear gap in the present study, there was paramount importance of literature review.

2.2.1 Stochastic Models for COVID-19

Oka *et al.* (2021) presented a modified SIR spatial model for studying the propagation of COVID-19 within 33 provincial regions of China. The multivariate discrete-time Markov model which authors developed here assumed a heterogeneous transmission within and across all 33 provinces. In their paper, they employed the Bayesian Markov Chain Monte-Carlo methods (MCMC) to estimate the model parameters and transmission dynamic network to evaluate the effect of different policies which may curtail the epidemic. In their findings, They demonstrated that movement restriction within and outside the regions and lock-down were important measures to suppress the pandemic.

Hellewell *et al.* (2020) formulated a stochastic model of the COVID-19 outbreak. In their paper, they assessed the feasibility of COVID-19 by using case isolation and contact tracing. Further, they examined the effectiveness of contact tracing and isolation on suppressing SARS-COV-2. The results indicated that these two aforementioned control measures were insufficient to control the pandemic but reduced the initial number of cases and this made the outbreak simple to be controlled.

Channapathi and Thatikonda (2020) developed a SEIR stochastic model to assess early transmission of the novel coronavirus. In their study, they evaluated the effectiveness of control measures adopted by individuals, governments, and organizations to contain COVID-19. In their findings, they demonstrated that apart from the government and organization action plans, individual precautionary measures such as self-quarantine of individuals were very important for controlling the spread of COVID-19 in the community.

Hussain *et al.* (2020) presented a SIR stochastic model for COVID-19 transmission dynamics. They are motivated to have this study since any number related to the total infected population, number of death, and recovered population is certain. These numbers can be obtained through estimation and the Poisson process. Models which deploy the Poisson process and estimation technique are stochastic in nature. The stability of the formulated model was provided. Their results revealed that implementation of lockdown, hygiene, sanitation, physical distancing, and sensitization of the public about the pandemic decreased transmission and individual susceptibil-

ity. They concluded that the management of these control measures minimized the number of infectious individuals.

Abrams *et al.* (2021) scrutinized a stochastic model for SARS-COV-2. They deployed a compartmental model with the age-structured discrete-time with real data from Belgium to explore the transmission dynamics of the current disease now and in the future. They investigated the impact of lockdown when effectively implemented by the general population. In addition, they estimated the impact of exit mitigation strategies for the future SARS-COV-2 waves. Their results showed that lockdown and social distancing minimized the pandemic.

Girona (2020) proposed a stochastic model to estimate the time required for confinement which may stop the occurrence of the second wave of SARS-COV-2 in the USA and Spain. The targeted cities for the aforesaid purpose are the most populated cities such as New York (US), San Francisco (US), and Madrid (Spain). In their study, they considered a population that is not detected but remains a circulating infection within the community. The results depicted that proper handling of suppression strategies was effective in reducing the time for confinement. Based on their model assumption, the time required for home confinement and social distancing before the second wave was ≈ 110 days in New York, ≈ 80 days in San Francisco, and ≈ 70 days in Madrid.

Balsa *et al.* (2021) composed a stochastic SEIR model for computing simulation on COVID-19 pandemic. Authors in their study assessed the impact of quarantine and vaccines in reducing SARS-COV-2 transmission in the community. They deployed MCMC for simulation with a medium-sized population of 20 000. The results indicated that the pandemic can be reduced through a large-scale quarantine of infectious individuals obtained by administering testing on a daily basis. Moreover, they concluded that a combination of the two aforementioned strategies prevented an outbreak in the community.

2.2.2 Deterministic Models for COVID-19

Mahikul *et al.* (2021) developed a mathematical model of COVID-19 in Thailand to appraise the impact of interventions strategies in the first wave and predict the second wave of COVID-19. The analyzed interventions were quarantine, hand washing, physical distancing, and wearing face masks. Their findings suggested that the second wave surges can be prevented through the implementation of physical distancing, wearing of face masks, and contact tracing.

Dwomoh *et al.* (2021) provided a deterministic model to explore transmission dynamics of COVID-19 in Ghana. In their study, they examined the impact of interventions strategies categorized at an individual and government level. Hospitalization, treatment, quarantine, self-isolation closure of schools, and provision of personal protective equipment (PPE) to health workers are classified as government intervention strategies while the use of hand sanitizers, hand washing, and social distancing and intensive media education are grouped as individual mitigation measures. They

illustrated in their finding that government intervention alone may not curtail the spread of infection. Furthermore, they concluded that the community should adhere to the prevention protocol while the media intensify daily reports in order to improve community behavioral change.

Riyapan *et al.* (2021) recommended a classical integer-order derivatives model as a good approach in studying COVID-19 transmission dynamics, a case study in Thailand. The formulated model divided its population into seven compartments. In their study, they computed the basic reproductive rate using the next-generation matrix. Also, they used the proposed model to predict infected individuals in real life by fitting the real data from Thailand. Their numerical results depicted that continuous and proper use of face masks were significant in reducing the spread of the novel coronavirus.

Gathungu *et al.* (2020) suggested a deterministic model for COVID-19 to examine the impact of several control measures such as physical distancing, awareness to the community about the pandemic, isolating infected people, and taking into quarantine those who came into contact with the infectious group in curtailing the novel coronavirus. The simulated results stipulated that isolating infected people reduced the spread. Furthermore, quarantining people who came into contact with the infectious populations was the other strategy that has a fundamental role in controlling the novel coronavirus.

Garba *et al.* (2020) established a COVID-19 model to scrutinize the role of environmental contamination in spreading the disease. The model deployed real data from South Africa to study the dynamics of the disease in presence of different control strategies. The results stipulated that lockdown was an effective way to curtail the current disease. Moreover, contact tracing and testing of the general population are emphasized as the other means to cut down the epidemic.

He *et al.* (2020) explored the SEIR model for COVID-19 and its transmission dynamics. In this study estimation of parameters was done using a particle swarm optimization algorithm. Moreover, treatment and quarantine were observed as the control strategies which were so suitable in the dynamics of COVID-19. In their study, they observed chaos in the system when seasonality and stochastic infections of parameters are introduced in the model. Further, their findings denoted that changing the parameters will result in a change in the dynamics of the model.

Kucharski *et al.* (2020) proposed a mathematical modeling study of COVID-19 to analyse the effect of combining several control strategies in curbing the disease. They examined the role of digital tracing and a minimum social distancing as means of reducing the transmission. In their findings, they suggested that combining contact tracing, self-isolation, and tolerable physical distancing should be used to cut down the pandemic. Further, they proposed that in a situation in which the number of cases is high, contact tracing strategies should be used to get newly infectious and quarantine them.

Mumbu and Hugo (2020) formulated a modified kind of SEIR deterministic model for COVID-19 dynamics with two interventions strategies in Tanzania. Both quantitative and qualitative analyses were examined. In their study, they examined the impact of wearing masks and isolation of sick individuals as strategies to contain the pandemic. Numerical results recommended the regular use of face masks in the public as well as isolating COVID-19 infectious after identification were good strategies to contain the disease.

Titus *et al.* (2020) composed a mathematical model of COVID-19 to examine the effect of different interventions strategies such as isolating infected people, educating the human population, testing, quarantining, treatment of infected group, practicing the habit of wearing face masks, and physical distancing in controlling the disease. The results revealed that the disease can be controlled by isolating infected people from the general population after doing extensive testing. Also, their findings indicated that combining more than two of the aforementioned interventions work best in a long way of managing the disease.

Agaba (2020) generated a compartmental model for COVID-19 which incorporated two intervention measures such as educating people about the pandemic and medication. Further, the estimation of parameters is presented in the formulated SEIR model. The results revealed that awareness dissemination reduced the spread of the disease. Additionally, medication of infected people demonstrated a significant effect in managing the epidemic in the population.

Kumar *et al.* (2021) investigated the role of the vaccine in their developed SEIR model of COVID-19. They formulated classical integer-order derivatives and non-integer order-derivatives. They have the idea that the two models may give a clear picture of the role of vaccines in curbing the pandemic. The model's existence of solutions is established. The real data from Spain is deployed in the formulated model. The numerical results are obtained through a predictor-corrector algorithm. Their finding depicted different behavior of the model when fractional-order and vaccine rate is varied.

Lopman *et al.* (2021) scrutinized a study on mathematical modeling of COVID-19 by deploying the population of three universities. Three intervention strategies were taken into consideration in the formulated model. These interventions include testing, isolating infected people, and quarantine of people who contracted with infectious. They pointed out the sensitive parameters through the sensitivity analysis approach. Their outcome stipulated that the proper implementation of control measures such as powerful testing, isolation, and quarantine completely minimized the spread of COVID-18 introduced to the campus by the infected population from the community.

Aldila *et al.* (2020) presented a model with optimal control for SARS-COV-2. Several interventions and control strategies were introduced in the formulated model. These control techniques ranged from pharmaceutical to non-pharmaceutical intervention. Two kinds of models have been formulated in which one model included only intervention strategies such as effective testing,

treatment, and use of medical masks. They assessed the impact of these strategies in defeating the pandemic. The other model incorporated human awareness together with the aforementioned intervention strategies. The results from the initial model pointed out that masks have a significant impact in controlling the epidemic while the results from the second model showed that human awareness has a fundamental role in the eradication of the epidemic in the human population.

Djaoue *et al.* (2020) in Cameroon explored mathematical model for COVID-19 transmission dynamics. Different interventions such as lockdowns, wearing of face masks, isolation after contact tracing, reasonable testing of the human population, and practicing health hygiene were analyzed in the formulated model. They discovered that the asymptomatic infectious of the novel coronavirus play a major role in the transmission of the disease. In regard to which intervention measures are effective, the results pointed out that isolating infected people may reduce the epidemic by 80% and the disease will disappear after only 100 hundred days. Tracing infected people and isolating them will control the disease by only 90 days. Finally, they concluded that hygiene protocol when being practiced and wearing medical masks were among the most important strategies to control the disease.

Lin *et al.* (2020) proposed a deterministic mathematical model to analyses the impact of medical resources on the spread of COVID-19 in Hubei province in China. In their model, they put under consideration different resources such as human resources like health workers, materials resources like medicine, and masks. Other interventions which were included in the model are quarantine and treatment to the individuals infected population. China built a big hospital after the outbreak of coronavirus disease in 2019 as means of hospitalizing the detected case and give them treatment. This hospital was being used as a place to quarantine people suspected to meet with infected people. Their fundings revealed that hospitalization plays a fundamental role in slowing down the quick spread of the disease.

Ghosh and Martcheva (2021) established a model on the effect of generous awareness on COVID-19 dynamics. The proposed model has four equilibrium states based on several parametric conditions. The local and global stability condition for awareness and disease-free equilibrium is studied. By using Lyapunov function theory and LaSalle Invariance Principle, the endemic equilibrium is shown to be globally asymptotically stable under some parametric constraints. The existence of unique awareness, endemic equilibrium, and unique endemic equilibrium is presented. Sensitivity analysis indicated that the rate of transmission and learning factors related to awareness of susceptible populations is very important in order to reduce disease-related deaths. Their results indicated that awareness has big importance in flattening the curve.

In Ontario, Canada, Tuite *et al.* (2020) analyzed a compartmental model for the spread of the disease and control approach. In their model, they considered a number of interventions such as social distancing, isolating infected population and taking much care of the hospital population who are severely sick. Their model results showed that social distancing has a great significance in

controlling the epidemic. Also, strengthening detection together with isolating infected individual has fundamental role in controlling COVID-19.

Traoré and Konané (2020) studied a deterministic model to assess the effectiveness of contact tracing on transmission dynamics of COVID-19. They compared the basic reproduction number R_0 of a basic model with an induced basic reproductive number R_c after having incorporated contact tracing. It was observed that a large value of R_c is required when R_0 is very large. The results indicated that in order to control the pandemic, the value of R_0 should be small and contact tracing must be at a higher rate.

Aldila (2020) in his study presented a model on the effect of education on the community and impressive testing for COVID-19. Different interventions strategies such as educating the community and effective testing were incorporated in the formulated model. They conducted parameter estimation. Their results revealed that a combination of both education and effective testing for identifying infectious have a significant impact in reducing the pandemic.

Mbogo and Odhiambo (2020) explored a deterministic model for coronavirus spread. Two interventions such as mass testing and physical distancing were included in their model. They studied the variation of spread from time to time. Their results suggested that mass testing should focus on a specific group of people. Furthermore, their findings showed that the Kenya government should focus on the community in the non-formal settlement for large-scale testing and provide them clean water and hands sanitizers. Moreover, the model results revealed that special medical care should be given to the population with pre-existing non-communicable diseases.

Dy and Rabajante (2020) presented a theoretical model for COVID-19 infection risk for frontline health workers. In the developed model, they calculated the risk of being infected in health facilities. They considered many factors which lead an individual to be infected. They considered the time in which the COVID-19 victim interact with health personal, exposure time, the average number of infected individuals per one health personal per hour, presence of protective gears, and other facilities given to health workers. The fourth-order Runge-Kutta scheme was used in the simulation. Their simulated results indicated that there was a need to reduce interaction time between health workers and patients, increase social distance and provision of facilities, and effective protective gears. This study focused only on risk assessment rather than simulating the pandemic in the general public.

Buhat *et al.* (2021) developed a conceptual mathematical model for COVID-19 transmission between frontlines and the general public. In their study, they modified the SEIR model with two mutually exclusive populations which are frontlines alone as well as the general public. It was estimated that the frontlines (transport workers, food providers, health workers, customer services, and retail personnel) have a basic reproduction ratio of 4 while 1.5 is the value of R_0 for the general public. The simulated results showed that the reduction of infections can be acquired by

decreasing the average number of secondary infections in the population.

2.2.3 Hybrid Model for COVID-19

Sánchez-Taltavull *et al.* (2021) studied both deterministic and stochastic models for COVID-19. In their studies, they first formulated a deterministic model followed by stochastic in which modeling the strategies to organize the health care workers during the epidemic is presented. These organizational strategies are paramount since the issue of social distancing is not possible in the health professional compared to others. The health workforce is protected through these strategies. Also, in their models, they assessed whether desynchronization healthcare teams by dichotomizing the workers may protect the workforce. Furthermore, the study examined the productivity of the workforce and their efficiency while working at home during the pandemic. Their numerical results revealed that the healthcare workforce can be protected having two teams working alternatively in seven days a week.

2.3 Summary

In this chapter, mathematical models of COVID-19 with one or more intervention strategies were reviewed. Every author proposed a mathematical model and effective control measure of COVID-19 depending on their findings. Face masks, hygiene, sanitation, isolation, avoidance of mass gathering, lockdown, banning of international airlines, tracing and physical distancing are the among of intervention strategies that were mentioned mostly by the scholars as strategies for curtailing COVID-19.

Also, these reviews helped in pointing out the research gap for this work. Since little is known on transmission dynamics among healthcare workers, the presents study formulate a mathematical of the novel coronavirus with the main goal of protecting healthcare providers to ensure and maintaining functioning of the health system.

CHAPTER THREE

MATERIALS AND METHODS

3.1 Mathematical Model for COVID-19 Dynamics

The study at hand presented a deterministic model of seven compartments whose size change with time namely; Susceptible population $S(t)$, Healthcare workers population $W(t)$, Exposed individuals $E(t)$, Symptomatic infected population $I_s(t)$, Asymptomatic infected population $I_a(t)$, Hospitalized population $H(t)$ and Recovered population $R(t)$. The susceptible population refers to individuals who are healthy but they are at the risk of being infected and denoted by $S(t)$. The population at an incubation period but not yet infectious is placed in a class called exposed $E(t)$. The healthcare workers population are individuals who work in health facilities and these include nurses, medical technologists, radiation technologists, nursing assistants, doctors, and hospital janitors. The human population which does not show the disease symptoms but infectious are referred to the class $I_a(t)$ while those who revealed the disease symptoms are placed in a class $I_s(t)$, those individuals with COVID-19 who are isolated from the general population in order to receive treatment are referred to the class $H(t)$, and recovered individuals denoted by $R(t)$ are people who were previously detected as infectious, survived the disease, there are no longer infectious and have developed a temporary natural immunity to the virus.

Also, this chapter presents an analysis of the feasibility and positiveness of the solution by using the calculus technique. Further, the existence of equilibria points was provided. The next-generation method was employed to compute R_0 while Wolfram Mathematica 12 was utilized to simplify it. The model stability at disease-free and endemic equilibrium points at the local and global levels was established. Routh-Hurwitz criterion and stable Metzler matrix theory are used to investigate local and global stability at DFE, respectively. On other hand, the Lyapunov direct method combined with LaSalle's Invariance Principle is deployed to compute global stability at an endemic point.

3.2 Mathematical Model Development

Modeling is an abstract science that embodies mathematics to be applied in solving real-life problems. For many years application of modeling to study the transmission dynamics of infectious has become a topic of much interest. Despite the fact that modeling does not provide a cure for a specific infectious disease, it can be used to design and analyze an epidemiological survey, identify the trend of the disease, make a general forecast, suggest very important data that should be collected. For better understanding COVID-19 transmission dynamics, the presents study developed a deterministic model with seven sub-population which are: Susceptible-Health workers-Exposed-Symptomatic-asymptomatic-hospitalized-Recovered. The total sum of seven

compartments is symbolized by $N(t)$ and given as:

$$N(t) = S(t) + W(t) + E(t) + I_s(t) + I_a(t) + H(t) + R(t).$$

The number of susceptible individuals from the community is denoted by S while W presents the number of susceptible from the healthcare workers. The susceptible class is increased by birth at a rate of Λ and also from the recovered individuals by losing temporary immunity with the rate γ . For the sake of direct interaction between healthcare workers and the community, we assumed to have a proportional r of healthcare workers who join the susceptible class. The parameter b represents the recruitment rate of healthcare workers. Parameter β_1 and β_2 present the exposure rate for susceptible community and healthcare workers, respectively. Exposure rate refers to the total number of newly exposed individuals caused by one individual per unit time. This occurs only when there is enough contact between S , W , and infected class I_s . Susceptible compartment move to exposed class after enough interaction between S and I_s . Also, healthcare workers are transferred to the exposed class after enough interaction between the compartment W and I_s . The parameter θ presents the rate at which the susceptible community practice physical distancing. We assumed this control measure minimizes the transmission of the disease in the general community. The parameter ξ presents a proportion of public healthcare workers who implement the use of PPE. Exposed individuals who manifested the light symptoms such as fever of the disease are transferred to the symptomatic class I_s at a rate of α while those who did not reveal any symptoms after 14 days move to asymptomatic class I_a a rate of ρ . Both symptomatic and asymptomatic infected individuals are admitted to the hospital after suffering severe symptoms of COVID-19 such as breathing problems at the rate of ν and ϵ , respectively, otherwise, they move to recovered class at a rate of η and δ , respectively. After recovery, hospitalized individuals are discharged and join the recovered class at the rate of ω . In all classes, individuals die with a natural mortality rate of μ while infected individuals (I_s and I_a) and hospitalized humans decrease as a result of COVID-19 related death at a rate of d .

3.2.1 Model Assumptions

The formulation of deterministic models are preceded by assumptions. The following are assumptions to be taken into consideration before formulating the proposed model (3.1):

- (i) The pandemic process of COVID-19 is deterministic. The characteristic of the population depends on the rule that describes the model and its history.
- (ii) The total population in each compartment should be a differentiable function of time. This is only true after a clear establishment of the disease.
- (iii) The demographic effects such as death and natural birth are considered while emigration and immigration are ignored.

- (iv) The whole population except infectious (I_s and I_a) and H has an equal death rate.
- (v) The members of the population mix homogeneously within a closed system. Here we assumed no inlet or outlet of individuals within the area of studies.
- (vi) All individuals are born susceptible.
- (vii) The formulated model has no vertical transmission, that is, all new recruitment in the population is susceptible to the disease.
- (viii) Cases detected from infected class are taken into hospitalization for treatment or quarantined in their home and recovered with temporary natural immunity.
- (ix) Transmission is only through human-human transmissions within close contact with an infected individual and this is considered to be the main transmission of this infectious disease. Fomite transmission is considered a secondary order genesis of infections.
- (x) Each infectious individual causes an average R_0 secondary infections.
- (xi) The virus-infected person is not infectious during the incubation period.
- (xii) The rate of spread of COVID-19 in the I_a class was assumed to be very small compared to the rate of the disease in the I_s class due to the fact that I_s individuals sneeze or cough frequent than I_a individual (Mugisha *et al.*, 2021).

3.2.2 Illustrative Scheme for $SWEI_sI_aHR$ Model and Equations

The illustrative scheme found in Fig. 3 was deployed to formulate the system of ordinary differential equations which represent parameters and change of state variables in the non-linear deterministic proposed mathematical model. The time t is considered as an independent variable when formulating differential equations in the model (3.1). The transfer rate between each compartment was expressed mathematically as derivative with respect to the time of the size of the compartment.

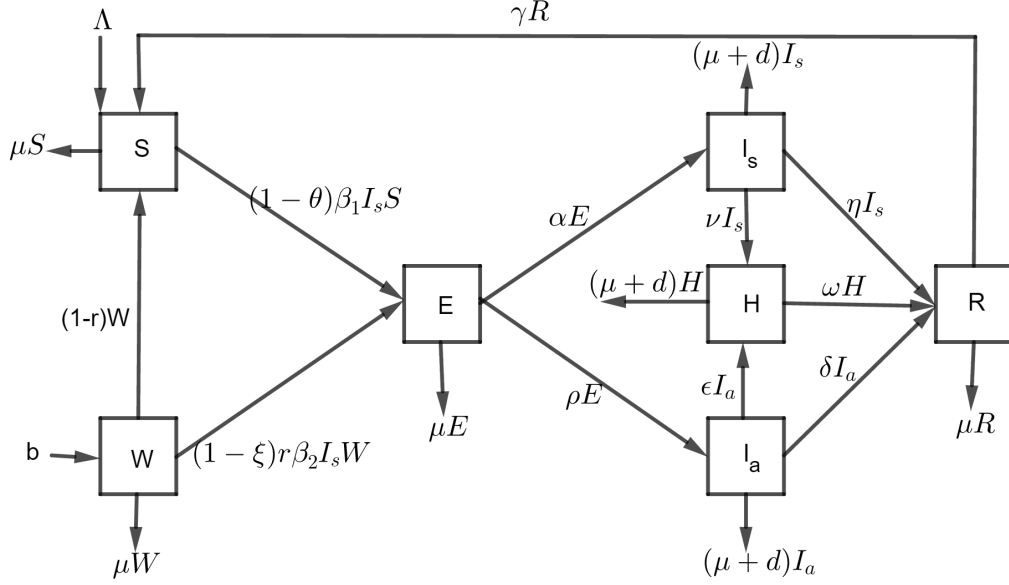


Figure 3: The compartmental model for COVID-19

$$\begin{aligned}
 \frac{dS}{dt} &= \Lambda + (1-r)W + \gamma R - (\mu + (1-\theta)\beta_1 I_s)S, \\
 \frac{dW}{dt} &= b - \mu W - (1-r)W - (1-\xi)r\beta_2 W I_s, \\
 \frac{dE}{dt} &= (1-\theta)\beta_1 I_s S + (1-\xi)r\beta_2 W I_s - (\alpha + \mu + \rho)E, \\
 \frac{dI_s}{dt} &= \alpha E - (d + \nu + \mu + \eta)I_s, \\
 \frac{dI_a}{dt} &= \rho E - (\mu + d + \delta + \epsilon)I_a, \\
 \frac{dH}{dt} &= \nu I_s + \epsilon I_a - (\mu + d + \omega)H, \\
 \frac{dR}{dt} &= \eta I_s + \omega H + \delta I_a - (\mu + \gamma)R.
 \end{aligned} \tag{3.1}$$

The Equation (3.1) was subjected to positive initial conditions: $S(0) = S_0 \geq 0, W(0) = W_0 \geq 0, I_a(0) = (I_a)_0 \geq 0, I_s = (I_s)_0 \geq 0, E(0) = E_0 \geq 0, H(0) = H_0 \geq 0, R(0) = R_0 \geq 0$.

3.2.3 Model Variables Description

Variables for the model (3.1) are described in Table 1.

Table 1: Detailed description of state variables of the proposed model (3.1)

Variable	Description
$N(t)$	Total population at given time t
$S(t)$	Susceptible population at time t
$E(t)$	Exposed population at a given time t
$W(t)$	Healthcare workers at a given time t
$I_a(t)$	Asymptomatic infected population at a given time t
$I_s(t)$	symptomatic infected population at time t
$H(t)$	Hospitalized population at time t
$R(t)$	Recovered population at time t

The parameters for the system of model (3.1) are described in Table 2.

Table 2: Detailed description of the parameters used in the proposed Model (3.1)

Parameter	Description
d	COVID-19 mortality rate
γ	The rate at which recovered become susceptible
Λ	The recruitment rate into the susceptible compartment
α	The rate in which exposed become symptomatic infected individuals
θ	The rate of physical distancing
r	The percentage of healthcare workers who are becoming susceptible
b	The rate at which healthcare workers are recruited
ξ	A fraction indicating effective use of personal protective equipment
ω	The rate at which admitted individuals in hospital recover
β_1	The effective contact rate for susceptible population
δ	Recovery rate of asymptomatic infected individuals
β_2	Healthcare workers contact rate
μ	The natural death rate for all individuals
ρ	The rate at which exposed become asymptomatic infected individuals
ν	The rate at which symptomatic infected individuals are hospitalized
η	Recovery rate of symptomatic infected population
ϵ	The rate in which asymptomatic infected individuals are hospitalized

3.3 Qualitative Analysis of the Proposed COVID-19 Model

This subsection presents the stability analysis of the proposed model (3.1). In epidemiology and immunology, knowledge of the stability of a system is useful in examining the behavior of the system in disease dynamics. Besides positiveness, boundedness, existence, and uniqueness of the solution, a basic reproduction number is also provided. Furthermore, the determination of the stability of the model solution is investigated.

3.3.1 Positiveness of Model Solutions

The formulated model (3.1) is epidemiologically realistic whenever all state variables are proved to always remain positive at every point in time t . The aforesaid statement is preceded with an assumption that the initial conditions of the proposed model are positive for all time $t > 0$.

Theorem 1: let $\mathbb{R}_+^7 = \{\pi(t) \in \mathbb{R}^7 : \pi(t) \geq 0\}$ and

$$\pi(t) = [S(t), W(t), E(t), I_a(t), I_s(t), H(t), R(t)]^T$$

then the solution set for the model Equation (3.1) subjected to the positive initial conditions is positive $\forall t \geq 0$.

Proof: In proofing for the existence of positivity of the solution in the model system (3.1), all classes must be non-negative. Consider the first the model Equation (3.1) given as:

$$\frac{dS}{dt} = \Lambda + (1-r)W + \gamma R - (\mu + (1-\theta)\beta_1 I_s)S. \quad (3.2)$$

Omitting the positive terms and introduce inequality in Equation (3.2) yields:

$$\frac{dS}{dt} \geq -(\mu + (1-\theta)\beta_1 I_s)S. \quad (3.3)$$

Then solving by using separation of variable Equation (3.3) and introducing initial condition results to:

$$\int_{S(0)}^{S(t)} \frac{dS}{S} \geq - \int_0^t (\mu + (1-\theta)\beta_1 I_s) dt.$$

This simplifies into:

$$S(t) \geq S(0)e^{-(\mu+(1-\theta)\beta_1 I_s)t} \geq 0.$$

Applying similar approach on the second equation of model (3.1), we have:

$$\frac{dW}{dt} = b - \mu W - (1-r)W - (1-\xi)r\beta_2 W I_s,$$

that is:

$$\frac{dW}{dt} = b - \mu W - (1 - r)W - (1 - \xi)r\beta_2 W I_s.$$

Omitting the positive term results to:

$$\frac{dW}{dt} \geq -(\mu + 1 - r + (1 - \xi)r\beta_2 I_s)W.$$

Introducing the variable separable and apply integral both side with limit gives:

$$\int_{W(0)}^{W(t)} \frac{dW}{W} \geq \int_0^t -(\mu + 1 - r + (1 - \xi)r\beta_2 I_s)dt.$$

$$\ln W(t) - \ln W(0) \geq -(\mu + 1 - r + (1 - \xi)r\beta_2 I_s)(t - 0).$$

$$\frac{W(t)}{W(0)} \geq \exp -(\mu + 1 - r + r\beta_2 I_s)t.$$

$$W(t) \geq W(0) \exp -(\mu + 1 - r + (1 - \xi)r\beta_2 I_s)t \geq 0.$$

Moreover, considering the third equation model (3.1) we have:

$$\frac{dE}{dt} = (1 - \theta)\beta_1 I_s S + (1 - \xi)r\beta_2 W I_s - (\alpha + \mu + \rho)E.$$

Exclusion of non-negative terms results to:

$$\frac{dE}{dt} \geq -(\alpha + \mu + \rho)E.$$

Applying the separating variable technique leads to:

$$\int_{E(0)}^{E(t)} \frac{dE}{E} \geq \int_0^t -(\alpha + \mu + \rho)dt.$$

Introducing the limit both sides guide to:

$$\ln \frac{E(t)}{E(0)} \geq -(\alpha + \mu + \rho)(t - 0),$$

further simplification gives:

$$E(t) \geq E(0)e^{-(\alpha + \mu + \rho)t} \geq 0.$$

The fourth equation of the model (3.1) implies that:

$$\frac{dI_s}{dt} = \alpha E - (d + \nu + \mu + \eta)I_s,$$

or

$$\frac{dI_s}{dt} = \alpha E - (d + \nu + \mu + \eta)I_s \geq -(d + \nu + \mu + \eta)I_s.$$

After dropping αE we got:

$$\frac{dI_s}{dt} \geq -(d + \nu + \mu + \eta)I_s.$$

Inserting variable separable technique and integral both side yields:

$$\int_{I_s(0)}^{I_s(t)} \frac{dI_s}{I_s} \geq - \int_0^t (d + \nu + \mu + \eta) dt.$$

$$\ln I_s(t) - \ln I_s(0) \geq -(d + \nu + \mu + \eta)(t - 0).$$

$$\ln\left(\frac{I_s(t)}{I_s(0)}\right) \geq -(d + \nu + \mu + \eta)t.$$

$$I_s(t) \geq I_s(0)e^{-(d+\nu+\mu+\eta)t} \geq 0.$$

Considering the fifth differential for model (3.1) implies:

$$\frac{dI_a}{dt} = \rho E - (\mu + d + \delta + \epsilon)I_a,$$

Also, can be written as:

$$\frac{dI_a}{dt} = \rho E - (\mu + d + \delta + \epsilon)I_a \geq -(\mu + d + \delta + \epsilon)I_a.$$

Omitting the positive term gives:

$$\frac{dI_a}{dt} \geq -(\mu + d + \delta + \epsilon)I_a,$$

can be written as:

$$\frac{dI_a}{I_a} \geq -(\mu + d + \delta + \epsilon)dt.$$

Introducing variable separable and limit both sides yields:

$$\int_{I_a(0)}^{I_a(t)} \frac{dI_a}{I_a} \geq \int_0^t -(\mu + d + \delta + \epsilon) dt.$$

$$\ln I_a(t) - \ln I_a(0) \geq -(\mu + d + \delta + \epsilon)(t - 0).$$

$$\frac{I_a(t)}{I_a(0)} \geq \exp -(\mu + d + \delta + \epsilon)t.$$

$$I_a(t) \geq I_a(0) \exp -(\mu + d + \delta + \epsilon)t \geq 0.$$

Furthermore, by considering the sixth equation for model (3.1), we have:

$$\frac{dH}{dt} = \nu I_s + \epsilon I_a - (\mu + d + \omega)H,$$

that is:

$$\frac{dH}{dt} = \nu I_s + \epsilon I_a - (\mu + d + \omega)H \geq -(\mu + d + \omega)H.$$

Through omission of positive terms results to:

$$\frac{dH}{dt} \geq -(\mu + d + \omega)H.$$

After separating the variable introduce integral with initial limit both sides leads to:

$$\int_{H(0)}^{H(t)} \frac{dH}{H} \geq - \int_0^t (\mu + d + \omega) dt.$$

After that, we have:

$$\ln H(t) - \ln H(0) \geq -(\mu + d + \omega)(t - 0).$$

$$\ln\left(\frac{H(t)}{H(0)}\right) \geq -(\mu + d + \omega)t.$$

$$\frac{H(t)}{H(0)} \geq e^{-(d+\mu+\omega)t}.$$

$$H(t) \geq H(0)e^{-(\omega+\mu+d)t},$$

which implies

$$H(t) \geq 0.$$

From the last equation of model (3.1) we have:

$$\frac{dR}{dt} = \eta I_s + \omega H + \delta I_a - (\mu + \gamma)R,$$

moreover, it can be rewritten as:

$$\frac{dR}{dt} = \eta I_s + \omega H + \delta I_a - (\mu + \gamma)R \geq -(\mu + \gamma)R.$$

After omitting positive terms and introduce variable separable technique with initial limit results to:

$$\int_{R(0)}^{R(t)} \frac{dR}{R} \geq - \int_0^t (\mu + \gamma) dt.$$

Thereafter, yields:

$$\ln R(t) - \ln R(0) \geq -(\mu + \gamma)(t - 0).$$

$$\ln \frac{R(t)}{R(0)} - \geq -(\mu + \gamma)t.$$

$$\frac{R(t)}{R(0)} \geq e^{-(\mu+\gamma)t}.$$

$$R(t) \geq R(0)e^{-(\mu+\gamma)t} \geq 0.$$

Consequently, susceptible human $S(t)$, healthcare workers $W(t)$, Exposed $E(t)$ asymptomatic infectious $I_a(t)$, symptomatic infectious $I_s(t)$, hospitalized $H(t)$ and recovered $R(t)$ are positive $\forall t \geq 0$. Hence, $(S(t), W(t), E(t), I_s(t), I_a(t), H(t), R(t))$ in Equation (3.1) is positive at every point in time t . The proof is complete. \square

3.3.2 Invariant Region

The invariant region illustrates the feasible region in which the proposed model of COVID-19 solutions are mathematically significant. Since the formulated model is concerned with living organisms then, we made an assumption that all parameters and states variables are positive at every point of time t .

Theorem 2: *The solutions of system model (3.1) with initial condition enters and remain in the region given by $\psi = \{(S(t), W(t), E(t), I_s(t), I_a(t), H(t), R(t)) \in \mathbb{R}_+^7 : N(t) \leq \frac{\Lambda+b}{\mu}\}$.*

Proof: Considering the region $\psi = (S(t), W(t), E(t), I_s(t), I_a(t), H(t), R(t)) \in \mathbb{R}_+^7$ for for all $t \geq 0$. At every point in time t , the total sum of human population is given as:

$$N(t) = S(t) + W(t) + E(t) + I_a(t) + I_s(t) + H(t) + R(t).$$

Differentiate $N(t)$ with respect to t yield:

$$\frac{dN}{dt} = \frac{dS}{dt} + \frac{dW}{dt} + \frac{dE}{dt} + \frac{dI_s}{dt} + \frac{dI_a}{dt} + \frac{dH}{dt} + \frac{dR}{dt}. \quad (3.4)$$

Then substitute Equation (3.1) into Equation (3.4), then further simplification results to:

$$\frac{dN}{dt} = \Lambda + b - \mu(S + W + E + I_s + I_a + H + R) - (I_s + I_a + H)d. \quad (3.5)$$

Since $N = S + W + E + I_s + I_a + H + R$, then Equation (3.5) is reduced to:

$$\frac{dN}{dt} = b + \Lambda - \mu N - (I_s + I_a + H)d. \quad (3.6)$$

Assume that there is no COVID-19 induced death ($d = 0$) then, introducing inequalities in Equation (3.6) leads to:

$$\frac{dN}{dt} \leq \Lambda + b - \mu N. \quad (3.7)$$

Then solving by separation of variable Equation (3.7) and introducing initial condition yields:

$$\int_{N_0}^{N(t)} \frac{dN}{b + \Lambda - \mu N} \leq \int_0^t dt. \quad (3.8)$$

$$\frac{-1}{\mu} \ln(\Lambda + b - \mu N(t)) + \frac{1}{\mu} \ln(\Lambda + b - \mu N_0) \leq (t - 0). \quad (3.9)$$

Multiply by $-\mu$ both sides Equation (3.9) gives:

$$\ln(\Lambda + b - \mu N(t)) - \ln(\Lambda + b - \mu N_0) \geq -\mu t.$$

$$\ln\left(\frac{\Lambda + b - \mu N(t)}{\Lambda + b - \mu N_0}\right) \geq -\mu t.$$

$$\frac{\Lambda + b - \mu N(t)}{\Lambda + b - \mu N_0} \geq e^{-\mu t}. \quad (3.10)$$

Multiply by $\Lambda + b - \mu N_0$ both sides Equation (3.10) arises to:

$$\Lambda + b - \mu N(t) \geq (\Lambda + b - \mu N_0)e^{-\mu t}.$$

After rearranging, we have:

$$-\mu N(t) \geq (\Lambda + b - \mu N_0)e^{-\mu t} - (\Lambda + b). \quad (3.11)$$

Divide by $-\mu$ both side Equation (3.11) yields:

$$N(t) \leq \frac{-(\Lambda + b)e^{-\mu t}}{\mu} + \frac{\Lambda + b}{\mu} + N_0 e^{-\mu t}.$$

Further simplification yields:

$$N(t) \leq \frac{\Lambda + b}{\mu}(1 - e^{-\mu t}) + N_0 e^{-\mu t}.$$

Taking limit as $t \rightarrow \infty$, the population size becomes:

$$N(t) \rightarrow \frac{\Lambda + b}{\mu}.$$

Thereafter, the feasible solution set of the system Equation (3.1) enters and remain in the region:

$$\psi = \{(S(t), W(t), E(t), I_s(t), I_a(t), H(t), R(t)) \in \mathbb{R}_+^7 : N(t) \leq \frac{\Lambda + b}{\mu}\}.$$

Consequently, the model is well posed mathematically and it is a sufficient condition to study the dynamics of the model Equation (3.1) in ψ . The proof is complete. \square

3.3.3 Existence and Uniqueness for $SWEI_s I_a HR$ Model Solution

Consider ordinary differential equation in the form of:

$$\frac{dy}{dt} = f(t, y), y(t_0) = y_0. \quad (3.12)$$

Theorem 3 and 4 is used to investigate whether they exist a unique solution in Equation (3.1).

Theorem 3: (*uniqueness of solution*)

Using the approach found in Zhang *et al.* (2021), Let use D to denote the confined domain of the form:

$$|t - t_0| \leq a, \|y - y_0\| \leq b, y = (y_1, y_2, \dots, y_n), y_0 = (y_{10}, y_{20}, \dots, y_{n0}), \quad (3.13)$$

and presume that $f(t, y)$ satisfies the Lipschitz condition:

$$\|F(t, y_2) - F(t, y_1)\| \leq k \|y_2 - y_1\|, \quad (3.14)$$

and if the set of $(t, y_1) \in D$ and $(t, y_2) \in D$, where k is a Lipschitz constant. consequently, there is a constant $\delta > 0$ in such a manner that there exists a continuous vector solution $y(t)$ of the differential equation in (3.12) in the interval $|t - t_0| \leq \delta$ which is unique. It is important to observe that the Lipschitz condition in (3.14) is satisfied by the requirement that:

$$\left[\frac{\partial F_i}{\partial y_j}, i, j = 1, 2, \dots, 7 \right]$$

be continuous and bounded within the domain D.

Lemma 1: *Whenever $F(t, y)$ has continuous partial derivative $\frac{\partial F_i}{\partial y_j}$ on a bounded closed convex domain \mathbb{R} , where \mathbb{R} is used to denote real numbers, then it satisfies a Lipschitz condition in \mathbb{R} . The interest was on the domain:*

$$1 < \epsilon < \infty. \quad (3.15)$$

On this account, we looked for solution in the interval $0 < \mathbb{R} < \infty$ which is bounded as suggested by Zhang *et al.* (2021). We proved **Lemma 1** by using **Theorem 4**.

Theorem 4: (*Existence of the solution*)

Let D symbolize the domain described in (3.13) in such a manner that Equation (3.14) and (3.15) hold. In that case, there is an existence of a solution of the differential equations in (3.1) which is confined in the region of the domain D. Equation (3.1) can be written in the form of:

$$\begin{aligned}
F_1 &= \Lambda + \gamma R - \mu S - (1 - \theta)\beta_1 I_s S + (1 - r)W, \\
F_2 &= b - \mu W - (1 - r)W - (1 - \xi)r\beta_2 W I_s, \\
F_3 &= (1 - \theta)\beta_1 I_s S + (1 - \xi)r\beta_2 W I_s - (\mu + \alpha + \rho)E, \\
F_4 &= \alpha E - (\mu + \nu + d + \eta)I_a, \\
F_5 &= \rho E - (\mu + d + \delta + \epsilon)I_a, \\
F_6 &= \epsilon I_a + \nu I_s - (\mu + d + \omega)H, \\
F_7 &= \omega H + \delta I_a + \eta I_s - (\gamma + \mu)R.
\end{aligned} \tag{3.16}$$

We showed that:

$$\left[\frac{\partial F_i}{\partial y_j}, i, j = 1, 2, \dots, 7 \right]$$

are continuous and bounded. For this reason, we performed partial derivatives of F_1 to F_7 from Equation (3.16) with respect to the state variables S, W, E, I_s, I_a, H, R .

Proof: Taking into consideration F_1 in Equation (3.16) we have:

$$F_1 = \Lambda + \gamma R + (1 - r)W - (\mu + (1 - \theta)\beta_1 I_s)S.$$

The partial derivatives of F_1 was performed as follows:

$$\begin{aligned}
\frac{\partial F_1}{\partial S} &= -(\mu + (1 - \theta)\beta_1 I_s), \left| \frac{\partial F_1}{\partial S} \right| = |-(\mu + (1 - \theta)\beta_1 I_s)| < \infty, \\
\frac{\partial F_1}{\partial W} &= 1 - r, \left| \frac{\partial F_1}{\partial W} \right| = |1 - r| < \infty, \\
\frac{\partial F_1}{\partial E} &= 0, \left| \frac{\partial F_1}{\partial E} \right| = |0| < \infty, \\
\frac{\partial F_1}{\partial I_s} &= -(1 - \theta)\beta_1 S, \left| \frac{\partial F_1}{\partial I_s} \right| = |(1 - \theta)\beta_1 S| < \infty, \\
\frac{\partial F_1}{\partial I_a} &= 0, \left| \frac{\partial F_1}{\partial I_a} \right| = |0| < \infty, \\
\frac{\partial F_1}{\partial H} &= 0, \left| \frac{\partial F_1}{\partial H} \right| = |0| < \infty, \\
\frac{\partial F_1}{\partial R} &= \gamma, \left| \frac{\partial F_1}{\partial R} \right| = |\gamma| < \infty.
\end{aligned}$$

Similarly, from F_2 we also have:

$$\begin{aligned}
\frac{\partial F_2}{\partial S} &= 0, \left| \frac{\partial F_2}{\partial S} \right| = |0| < \infty, \\
\frac{\partial F_2}{\partial W} &= -(\mu + 1 - r + (1 - \xi)r\beta_2 I_s), \left| \frac{\partial F_2}{\partial W} \right| = |-(\mu + 1 - r + (1 - \xi)r\beta_2 I_s)| < \infty, \\
\frac{\partial F_2}{\partial E} &= 0, \left| \frac{\partial F_2}{\partial E} \right| = |0| < \infty, \\
\frac{\partial F_2}{\partial I_s} &= -(1 - \xi)r\beta_2 W, \left| \frac{\partial F_2}{\partial I_s} \right| = |-(1 - \xi)r\beta_2 W| < \infty, \\
\frac{\partial F_2}{\partial I_a} &= 0, \left| \frac{\partial F_2}{\partial I_a} \right| = |0| < \infty, \\
\frac{\partial F_2}{\partial H} &= 0, \left| \frac{\partial F_2}{\partial H} \right| = |0| < \infty, \\
\frac{\partial F_2}{\partial R} &= 0, \left| \frac{\partial F_2}{\partial R} \right| = |0| < \infty.
\end{aligned}$$

From F_3 we are going to have:

$$\begin{aligned}
\frac{\partial F_3}{\partial S} &= (1 - \theta)\beta_1 I_s, \left| \frac{\partial F_3}{\partial S} \right| = |(1 - \theta)\beta_1 I_s| < \infty, \\
\frac{\partial F_3}{\partial W} &= (1 - \xi)r\beta_2 I_s, \left| \frac{\partial F_3}{\partial W} \right| = |(1 - \xi)r\beta_2 I_s| < \infty, \\
\frac{\partial F_3}{\partial E} &= -(\alpha + \rho + \mu), \left| \frac{\partial F_3}{\partial E} \right| = |-(\alpha + \rho + \mu)| < \infty, \\
\frac{\partial F_3}{\partial I_s} &= (1 - \theta)\beta_1 S + (1 - \xi)r\beta_2 W, \left| \frac{\partial F_3}{\partial I_s} \right| = |(1 - \theta)\beta_1 S + (1 - \xi)r\beta_2 W| < \infty, \\
\frac{\partial F_3}{\partial I_a} &= 0, \left| \frac{\partial F_3}{\partial I_a} \right| = |0| < \infty, \\
\frac{\partial F_3}{\partial H} &= 0, \left| \frac{\partial F_3}{\partial H} \right| = |0| < \infty, \\
\frac{\partial F_3}{\partial R} &= 0, \left| \frac{\partial F_3}{\partial R} \right| = |0| < \infty.
\end{aligned}$$

For F_4 from Equation (3.16) we obtained:

$$\begin{aligned}
\frac{\partial F_4}{\partial S} &= 0, \left| \frac{\partial F_4}{\partial S} \right| = |0| < \infty, \\
\frac{\partial F_4}{\partial W} &= 0, \left| \frac{\partial F_4}{\partial W} \right| = |0| < \infty, \\
\frac{\partial F_4}{\partial E} &= \alpha, \left| \frac{\partial F_4}{\partial E} \right| = |\alpha| < \infty, \\
\frac{\partial F_4}{\partial I_s} &= -(\mu + d + \eta + \nu), \left| \frac{\partial F_4}{\partial I_s} \right| = |-(\mu + d + \eta + \nu)| < \infty, \\
\frac{\partial F_4}{\partial H} &= 0, \left| \frac{\partial F_4}{\partial H} \right| = |0| < \infty, \\
\frac{\partial F_4}{\partial I_a} &= 0, \left| \frac{\partial F_4}{\partial I_a} \right| = |0| < \infty, \\
\frac{\partial F_4}{\partial R} &= 0, \left| \frac{\partial F_4}{\partial R} \right| = |0| < \infty.
\end{aligned}$$

Moreover, F_5 results to:

$$\begin{aligned}
\frac{\partial F_5}{\partial S} &= 0, \left| \frac{\partial F_5}{\partial S} \right| = |0| < \infty, \\
\frac{\partial F_5}{\partial W} &= 0, \left| \frac{\partial F_5}{\partial W} \right| = |0| < \infty, \\
\frac{\partial F_5}{\partial E} &= \rho, \left| \frac{\partial F_5}{\partial E} \right| = |\rho| < \infty, \\
\frac{\partial F_5}{\partial I_s} &= 0, \left| \frac{\partial F_5}{\partial I_s} \right| = |0| < \infty, \\
\frac{\partial F_5}{\partial I_a} &= -(d + \mu + \epsilon + \delta), \left| \frac{\partial F_5}{\partial I_a} \right| = |-(d + \mu + \epsilon + \delta)| < \infty, \\
\frac{\partial F_5}{\partial H} &= 0, \left| \frac{\partial F_5}{\partial H} \right| = |0| < \infty, \\
\frac{\partial F_5}{\partial R} &= 0, \left| \frac{\partial F_5}{\partial R} \right| = |0| < \infty.
\end{aligned}$$

Furthermore, the partial derivatives for F_6 were:

$$\begin{aligned}
\frac{\partial F_6}{\partial S} &= 0, \left| \frac{\partial F_6}{\partial S} \right| = |0| < \infty, \\
\frac{\partial F_6}{\partial W} &= 0, \left| \frac{\partial F_6}{\partial W} \right| = |0| < \infty, \\
\frac{\partial F_6}{\partial E} &= 0, \left| \frac{\partial F_6}{\partial E} \right| = |0| < \infty, \\
\frac{\partial F_6}{\partial I_s} &= \nu, \left| \frac{\partial F_6}{\partial I_s} \right| = |\nu| < \infty, \\
\frac{\partial F_6}{\partial I_a} &= \epsilon, \left| \frac{\partial F_6}{\partial I_a} \right| = |\epsilon| < \infty, \\
\frac{\partial F_6}{\partial H} &= -(d + \mu + \omega), \left| \frac{\partial F_6}{\partial H} \right| = |-(d + \mu + \omega)| < \infty, \\
\frac{\partial F_6}{\partial R} &= 0, \left| \frac{\partial F_6}{\partial R} \right| = |0| < \infty.
\end{aligned}$$

Finally, from F_7 we obtained:

$$\begin{aligned}
\frac{\partial F_7}{\partial S} &= 0, \left| \frac{\partial F_7}{\partial S} \right| = |0| < \infty, \\
\frac{\partial F_7}{\partial W} &= 0, \left| \frac{\partial F_7}{\partial W} \right| = |0| < \infty, \\
\frac{\partial F_7}{\partial E} &= 0, \left| \frac{\partial F_7}{\partial E} \right| = |0| < \infty, \\
\frac{\partial F_7}{\partial I_s} &= \eta, \left| \frac{\partial F_7}{\partial I_s} \right| = |\eta| d < \infty, \\
\frac{\partial F_7}{\partial I_a} &= \delta, \left| \frac{\partial F_7}{\partial I_a} \right| = |\delta| < \infty, \\
\frac{\partial F_7}{\partial H} &= \omega, \left| \frac{\partial F_7}{\partial H} \right| = |\omega| < \infty, \\
\frac{\partial F_7}{\partial R} &= -(\mu + \gamma), \left| \frac{\partial F_7}{\partial R} \right| = |-(\mu + \gamma)| < \infty.
\end{aligned}$$

Therefore, it is shown that all partial derivatives of Equation (3.16) are continuous and bounded, consequently, **Theorem 3** has been used to prove the existence of unique of the differential equations found in Equation (3.1) within the confined region D. The proof is complete. \square

3.3.4 Disease-Free Equilibrium (DFE)

Disease-free equilibrium describes the state in which the region under consideration is free from the disease. The equilibrium points are found by zeroing the right-hand side of all equations in model (3.1) yielding to:

$$\begin{aligned}
\Lambda + \gamma R + (1 - r)W - (\mu + (1 - \theta)\beta_1 I_s)S &= 0, \\
b - \mu W - (1 - r)W - (1 - \xi)\beta_2 r I_s W &= 0, \\
(1 - \theta)\beta_1 I_s S + (1 - \xi)r\beta_2 W I_s - (\alpha + \mu + \rho)E &= 0, \\
\alpha E - (d + \nu + \mu + \eta)I_s &= 0, \\
\rho E - (\mu + d + \delta + \epsilon)I_a &= 0, \\
\nu I_s + \epsilon I_a - (\mu + d + \omega)H &= 0, \\
\eta I_s + \omega H + \delta I_a - (\mu + \gamma)R &= 0.
\end{aligned}$$

When evaluating at $R = I_a = H = E = I_s = 0$, Equation (3.17) is obtained. To compute S^0 and W^0 then, solve for state variable S and W in Equation (3.17).

$$\begin{aligned}
\Lambda + (1 - r)W - \mu S &= 0, \\
b - \mu W - (1 - r)W &= 0.
\end{aligned} \tag{3.17}$$

So

$$S = \frac{b(1 - r)}{\mu(\mu + 1 - r)} + \frac{\Lambda}{\mu},$$

and

$$W = \frac{b}{\mu + 1 - r}.$$

Let F_0 be the DFE point. Therefore, the solution yield together seven steady states such as:

$$F_0 = (S^0, W^0, E^0, I_s^0, I_a^0, H^0, R^0) = \left(\frac{b(1-r)}{\mu(\mu-r+1)} + \frac{\Lambda}{\mu}, \frac{b}{\mu+1-r}, 0, 0, 0, 0, 0 \right).$$

3.3.5 Basic Reproduction Number (R_0)

The basic reproduction number R_0 describes the expected number of secondary infections caused by one infectious individual when introduced completely in the host population (Diekmann *et al.*, 1990; Dietz, 1993). It is a threshold parameter that governs the spread of the disease. Also, R_0 can be called the basic reproduction ratio or basic reproductive rate (Hethcote, 2000). R_0 is the scientific test that is used to estimate the number of cases. It is a threshold quantity that can help in knowing whether the pandemic will invade a population or not. It is helpful in evaluating the

control strategies. The basic reproduction number is a non-dimensional quantity denoted by R_0 . R_0 is computed by using the next generation operator technique as described in Diekmann *et al.* (1990) and improved by Van den Driessche and Watmough (2002). Consider Equation (3.18) in a process of deducing R_0 as:

$$\begin{aligned}\frac{dE}{dt} &= (1 - \xi)r\beta_2WI_s + (1 - \theta)\beta_1I_sS - (\rho + \mu + \alpha)E, \\ \frac{dI_s}{dt} &= \alpha E - (\eta + d + \mu + \nu)I_s, \\ \frac{dI_a}{dt} &= \rho E - (\mu + d + \delta + \epsilon)I_a, \\ \frac{dH}{dt} &= \epsilon I_a + \nu I_s - (d + \omega + \mu)H.\end{aligned}\tag{3.18}$$

To distinguish between new infection from other changes in the population, the system of Equation (3.18) is modified and to be yield:

$$\frac{dx_i}{dt} = F_i(x) - V_i(x),$$

where x_i is a state variable that belongs to the transmitting compartment, F_i the rate of new infections in the compartment i , V_i the transfer of infections from one compartment to another. Also, we need to compute

$$FV^{-1} = [\frac{\partial F_i}{\partial X_j}(E_0)][\frac{\partial V_i}{\partial X_j}(E_0)]^{-1} \text{ with } 1 \leq i, j \leq 4,$$

where E_0 is the disease-free equilibrium point and

$$F_i = \begin{pmatrix} f_1 \\ f_2 \\ f_3 \\ f_4 \end{pmatrix} = \begin{pmatrix} (1 - \theta)\beta_1I_sS + (1 - \xi)r\beta_2WI_s \\ 0 \\ 0 \\ 0 \end{pmatrix}.$$

Partial derivatives of F_i with respect to E, I_s, I_a and H at DFE given as:

$$F = \begin{pmatrix} \frac{\partial F_1}{\partial E}(E_0) & \frac{\partial F_1}{\partial I_s}(E_0) & \frac{\partial F_1}{\partial I_a}(E_0) & \frac{\partial F_1}{\partial H}(E_0) \\ \frac{\partial F_2}{\partial E}(E_0) & \frac{\partial F_2}{\partial I_s}(E_0) & \frac{\partial F_2}{\partial I_a}(E_0) & \frac{\partial F_2}{\partial H}(E_0) \\ \frac{\partial F_3}{\partial E}(E_0) & \frac{\partial F_3}{\partial I_s}(E_0) & \frac{\partial F_3}{\partial I_a}(E_0) & \frac{\partial F_3}{\partial H}(E_0) \\ \frac{\partial F_4}{\partial E}(E_0) & \frac{\partial F_4}{\partial I_s}(E_0) & \frac{\partial F_4}{\partial I_a}(E_0) & \frac{\partial F_4}{\partial H}(E_0) \end{pmatrix},$$

thus gives

$$F = \begin{pmatrix} 0 & \beta_1(1-\theta)\left(\frac{\Lambda(\mu+1-r)+b(1-r)}{\mu(\mu+1-r)}\right) + \frac{(1-\xi)r\beta_2b}{\mu+1-r} & 0 & 0 \\ 0 & 0 & 0 & 0 \\ 0 & 0 & 0 & 0 \\ 0 & 0 & 0 & 0 \end{pmatrix}.$$

On other hand

$$V_i = \begin{pmatrix} v_1 \\ v_2 \\ v_3 \\ v_4 \end{pmatrix} = \begin{pmatrix} (\alpha + \mu + \rho)E \\ -\alpha E + (\eta + d + \mu + \nu)I_s \\ -\rho E + (\mu + d + \delta + \epsilon)I_a \\ -\nu I_s - \epsilon I_a + (\mu + d + \omega)H \end{pmatrix}.$$

partial derivatives of V_i with respect to E, I_s, I_a and H at DFE gives:

$$V = \begin{pmatrix} \frac{\partial V_1}{\partial E}(E_0) & \frac{\partial V_1}{\partial I_s}(E_0) & \frac{\partial V_1}{\partial I_a}(E_0) & \frac{\partial V_1}{\partial H}(E_0) \\ \frac{\partial V_2}{\partial E}(E_0) & \frac{\partial V_2}{\partial I_s}(E_0) & \frac{\partial V_2}{\partial I_a}(E_0) & \frac{\partial V_2}{\partial H}(E_0) \\ \frac{\partial V_3}{\partial E}(E_0) & \frac{\partial V_3}{\partial I_s}(E_0) & \frac{\partial V_3}{\partial I_a}(E_0) & \frac{\partial V_3}{\partial H}(E_0) \\ \frac{\partial V_4}{\partial E}(E_0) & \frac{\partial V_4}{\partial I_s}(E_0) & \frac{\partial V_4}{\partial I_a}(E_0) & \frac{\partial V_4}{\partial H}(E_0) \end{pmatrix}.$$

Thus gives:

$$V = \begin{pmatrix} \alpha + \mu + \rho & 0 & 0 & 0 \\ -\alpha & \nu + \eta + d + \eta & 0 & 0 \\ -\rho & 0 & \mu + \delta + d + \epsilon & 0 \\ 0 & -\nu & -\epsilon & d + \mu + \omega \end{pmatrix}.$$

The inverse of Jacobian matrix V is given by:

$$V^{-1} = \begin{pmatrix} \frac{1}{\rho + \mu + \alpha} & 0 & 0 & 0 \\ \frac{\alpha}{(\rho + \alpha + \mu)(\nu + \eta + d + \mu)} & \frac{1}{\mu + \eta + d + \nu} & 0 & 0 \\ \frac{\rho}{(\rho + \alpha + \mu)(\mu + \epsilon + d + \delta)} & 0 & \frac{1}{\epsilon + \delta + \mu + d} & 0 \\ \frac{\alpha\nu(\epsilon + \delta + d + \mu) + \rho\epsilon(\mu + \eta + d + \nu)}{(\rho + \mu + \alpha)(\omega + \mu + \nu)(\mu + \delta + d + \epsilon)(\mu + \eta + d + \nu)} & \frac{\nu}{(\omega + \mu + d)(\mu + \eta + d + \nu)} & \frac{\epsilon}{(\omega + \mu + d)(\mu + \delta + d + \epsilon)} & \frac{1}{d + \mu + \omega} \end{pmatrix}.$$

We computed the product of the two matrices V^{-1} and F where matrix F should be non-negative while matrix V^{-1} is a non-singular.

$$FV^{-1} = \begin{pmatrix} \alpha \left(\frac{\beta_1(1-\theta)(b(1-r)+\Lambda(1-r+\mu))}{\mu(1-r+\mu)} + \frac{(1-\xi)rb\beta_2}{\mu-r+1} \right) & \frac{\beta_1(1-\theta)(b(1-r)+\Lambda(1-r+\mu))}{\mu(1-r+\mu)} + \frac{(1-\xi)rb\beta_2}{1-r+\mu} & 0 & 0 \\ 0 & 0 & 0 & 0 \\ 0 & 0 & 0 & 0 \\ 0 & 0 & 0 & 0 \end{pmatrix}.$$

Using Wolfram Mathematica 12, four eigenvalues are obtained are:

$$\lambda_1 = 0,$$

$$\lambda_2 = 0,$$

$$\lambda_3 = 0,$$

and

$$\lambda_4 = \frac{\alpha\beta_1(1-\theta)((1-r)(b+\Lambda) + \Lambda\mu) + \alpha\mu(1-\xi)rb\beta_2}{\mu(1-r+\mu)(\rho+\mu+\alpha)(\mu+\eta+d+\nu)}.$$

By applying Van den Driessche and Watmough (2002) definition of R_0 as spectral radius (ρ) of FV^{-1} , so have:

$$R_0 = \rho(FV^{-1}) = \max(\lambda_1, \lambda_2, \lambda_3, \lambda_4).$$

Therefore the most dominant eigenvalue is λ_4 so, the basic reproduction number R_0 is given as:

$$R_0 = \frac{\alpha\beta_1(1-\theta)((1-r)(b+\Lambda) + \Lambda\mu) + \alpha\mu(1-\xi)rb\beta_2}{\mu(1-r+\mu)(\rho+\mu+\alpha)(\mu+\eta+d+\nu)}. \quad (3.19)$$

Equation (3.19) depicted that the numerical value of R_0 depends on the following parameters: recruitment rate Λ , recruitment rate of health workers b , the proportion of health workers becoming susceptible r , transition rate of exposure to asymptomatic infectious ρ , transition rate of exposed to symptomatic α , contact rate β_1 , the coefficient indicating the use of personal protective equipment ξ , the transmission rate of health workers β_2 , the rate at which symptomatic population is admitted in the hospital ν , The rate at which asymptomatic population is hospitalized ϵ , death due to the diseased, natural death μ and the rate of public control measures θ .

In the present study, when $R_0 < 1$, on average, COVID-19 infected individual, less than one new COVID-19 infected individual occurs during the transmission period, and the dissemination rate of COVID-19 decreases. This demonstrates that the disease will eventually disappear and the pandemic will stop. When $R_0 > 1$, on average, each COVID-19 infectious will have more than one new infected individual and the COVID-19 transference rate will increase. This implies that the pandemic will not stop but sustain the existence of the disease. If $R_0 = 1$ this signifies that a single person with sickness takes to an infection on average. In this scenario, the disease will sustain its existence, though it will neither expand to the pandemic nor end.

3.3.6 Local Stability at Disease-Free Equilibrium (DFE)

The local stability is investigated at DFE by computing eigenvalues of the jacobian matrix. The Jacobian matrix refers to a matrix that contains all first-order partial derivatives of a vector-valued function (Mpeshe *et al.*, 2011). A point is locally asymptotically stable if the Jacobian matrix evaluated at the disease-free equilibrium point has negative eigenvalues with real parts. This

study employed the Routh-Hurwitz criterion (Patil, 2021) to investigate the local stability of the disease-free.

Theorem 5: *The disease-free equilibrium J_{DFE} of the proposed COVID-19 model is locally asymptotically stable if $R_0 < 1$, otherwise unstable.*

Proof: To prove this theorem, first the Jacobian matrix of the system (3.1) is computed at DFE. The matrix is obtained through partial differentiation of system (3.1) with respect to S, W, E, I_s, I_a, H and R at DFE. Consider the model Equation (3.1) in the form of:

$$\begin{aligned} f_1 &= \Lambda + \gamma R + (1 - r)W - (\mu + (1 - \theta)\beta_1 I_s)S, \\ f_2 &= b - \mu W - (1 - r)W - (1 - \xi)r\beta_2 W I_s, \\ f_3 &= (1 - \theta)\beta_1 I_s S + (1 - \xi)r\beta_2 W I_s - (\alpha + \mu + \rho)E, \\ f_4 &= \alpha E - (\mu + \nu + d + \eta)I_s, \\ f_5 &= \rho E - (\mu + d + \delta + \epsilon)I_a, \\ f_6 &= \nu I_s + \epsilon I_a - (\mu + d + \omega)H, \\ f_7 &= \eta I_s + \omega H + \delta I_a - (\mu + \gamma)R. \end{aligned}$$

Therefore the Jacobian matrix is given as :

$$J(f_i, i = 1, \dots, 7) = \begin{pmatrix} \frac{\partial f_1}{\partial S} & \frac{\partial f_1}{\partial W} & \frac{\partial f_1}{\partial E} & \frac{\partial f_1}{\partial I_s} & \frac{\partial f_1}{\partial I_a} & \frac{\partial f_1}{\partial H} & \frac{\partial f_1}{\partial R} \\ \frac{\partial f_2}{\partial S} & \frac{\partial f_2}{\partial W} & \frac{\partial f_2}{\partial E} & \frac{\partial f_2}{\partial I_s} & \frac{\partial f_2}{\partial I_a} & \frac{\partial f_2}{\partial H} & \frac{\partial f_2}{\partial R} \\ \frac{\partial f_3}{\partial S} & \frac{\partial f_3}{\partial W} & \frac{\partial f_3}{\partial E} & \frac{\partial f_3}{\partial I_s} & \frac{\partial f_3}{\partial I_a} & \frac{\partial f_3}{\partial H} & \frac{\partial f_3}{\partial R} \\ \frac{\partial f_4}{\partial S} & \frac{\partial f_4}{\partial W} & \frac{\partial f_4}{\partial E} & \frac{\partial f_4}{\partial I_s} & \frac{\partial f_4}{\partial I_a} & \frac{\partial f_4}{\partial H} & \frac{\partial f_4}{\partial R} \\ \frac{\partial f_5}{\partial S} & \frac{\partial f_5}{\partial W} & \frac{\partial f_5}{\partial E} & \frac{\partial f_5}{\partial I_s} & \frac{\partial f_5}{\partial I_a} & \frac{\partial f_5}{\partial H} & \frac{\partial f_5}{\partial R} \\ \frac{\partial f_6}{\partial S} & \frac{\partial f_6}{\partial W} & \frac{\partial f_6}{\partial E} & \frac{\partial f_6}{\partial I_s} & \frac{\partial f_6}{\partial I_a} & \frac{\partial f_6}{\partial H} & \frac{\partial f_6}{\partial R} \\ \frac{\partial f_7}{\partial S} & \frac{\partial f_7}{\partial W} & \frac{\partial f_7}{\partial E} & \frac{\partial f_7}{\partial I_s} & \frac{\partial f_7}{\partial I_a} & \frac{\partial f_7}{\partial H} & \frac{\partial f_7}{\partial R} \end{pmatrix}.$$

$$J_{DFE} = \begin{pmatrix} -\mu & 1 - r & 0 & c_1 & 0 & 0 & \gamma \\ 0 & -(\mu + 1 - r) & 0 & c_3 & 0 & 0 & 0 \\ 0 & 0 & -(\rho + \mu + \alpha) & c_2 & 0 & 0 & 0 \\ 0 & 0 & \alpha & 0 & -c_4 & 0 & 0 \\ 0 & 0 & \rho & 0 & -c_5 & 0 & 0 \\ 0 & 0 & 0 & \nu & \epsilon & -c_6 & 0 \\ 0 & 0 & 0 & \eta & \delta & \omega & -(\mu + \gamma) \end{pmatrix}, \quad (3.20)$$

where

$$c_1 = \beta_1(1 - \theta) \left(\frac{\Lambda}{\mu} + \frac{b(1 - r)}{\mu(\mu + 1 - r)} \right),$$

$$c_2 = \frac{(1-\xi)rb\beta_2}{\mu+1-r} + (1-\theta)\beta_1 \left(\frac{\Lambda}{\mu} + \frac{b(1-r)}{\mu(\mu+1-r)} \right),$$

$$c_3 = \frac{-(1-\xi)rb\beta_2}{1-r+\mu},$$

$$c_4 = (\eta + \mu + d + \nu),$$

$$c_5 = (\delta + d + \mu + \epsilon),$$

$$C_6 = (d + \mu + \omega).$$

It is clear that from the matrix represented by the Equation (3.18), the first, second, third and the fourth eigenvalues are $\lambda_1 = -\mu$, $\lambda_2 = -(\mu + \gamma)$, $\lambda_3 = -(\mu + 1 - r)$, and $\lambda_4 = -(d + \mu + \omega)$.

Therefore, cancellation of respective rows and columns technique reduced a matrix represented by Equation (3.18) to be a 3×3 matrix which is given as:

$$J_{E0} = \begin{pmatrix} -(\rho + \mu + \alpha) & \frac{\beta_1(1-\theta)(b(1-r)+\Lambda(\mu-r+1))}{\mu(\mu-r+1)} + \frac{(1-\xi)rb\beta_2}{1-r+\mu} & 0 \\ \alpha & 0 & -(\mu + \nu + d + \eta) \\ \rho & 0 & -(\mu + \delta + d + \epsilon) \end{pmatrix}.$$

Consider the third-order polynomial of the form:

$$V(X) = X^3 + a_1X^2 + a_2X + a_3,$$

where

$$a_1 = \alpha + d + \delta + 2\mu + \rho + \epsilon.$$

$$a_2 = \frac{-rb\alpha\mu\beta_2 - b\alpha\beta_1(1+r+r\theta-\theta) - \alpha\beta_1\Lambda(1-\theta)(\mu+1-r) + \mu(\mu+\rho+\alpha)(\epsilon+\mu+d+\delta)(1+\mu-r)}{\mu(1+\mu-r)}.$$

So $a_2 > 0$ if

$$rb\alpha\mu\beta_2 + b\alpha\beta_1(1+r+r\theta-\theta) + \alpha\beta_1\Lambda(1-\theta)(\mu+1-r) > \mu(\mu+\rho+\alpha)(\epsilon+\mu+d+\delta)(1+\mu-r).$$

$$a_3 = \frac{(\beta_1(\theta-1)((r-1)(b+\Lambda)-\Lambda\mu) + \mu rb\beta_2)(\alpha(d+\delta+\mu+\epsilon) - \rho(d+\eta+\mu+\nu))}{\mu(\mu-r+1)}.$$

So $a_3 > 0$ if

$$\frac{(\beta_1(\theta-1)((r-1)(b+\Lambda)-\Lambda\mu) + \mu rb\beta_2)(\alpha(d+\delta+\mu+\epsilon) - \rho(d+\eta+\mu+\nu))}{\mu(\mu-r+1)} > 0.$$

It is clear that the value of $a_1 > 0$ and the condition for $a_2 > 0$ and $a_3 > 0$ is provided. The condition for $a_1 a_2 - a_3 > 0$ is investigated. Consider an expression $a_1 a_2 - a_3$ given as:

$$a_1 a_2 - a_3 = (\rho + 2\mu + \delta + d + \alpha)(m_1 + \mu(\mu + \rho + \alpha)(\epsilon + \mu + d + \delta)(1 + \mu - r)) - m_2 m_3.$$

The condition for $a_1 a_2 - a_3 > 0$ is given as:

$$(\rho + 2\mu + \delta + d + \alpha)(m_1 + \mu(\mu + \rho + \alpha)(\epsilon + \mu + d + \delta)(1 + \mu - r)) > m_2 m_3,$$

where

$$m_1 = -(rb\alpha\mu\beta_2 + b\alpha\beta_1(1 + r + r\theta - \theta) + \alpha\beta_1\Lambda(1 - \theta)(\mu + 1 - r)),$$

$$m_2 = \alpha(d + \delta + \mu + \epsilon) - \rho(d + \eta + \mu + \nu),$$

$$m_3 = \beta_1(\theta - 1)((r - 1)(b + \Lambda) - \Lambda\mu) + \mu rb\beta_2.$$

Consequently, the disease-free equilibrium is locally asymptotically stable since the coefficient of characteristic polynomial and aforesaid four eigenvalues are negative. In this account, Routh-Hurwitz criterion are met. \square

3.3.7 Existence and Uniqueness of Endemic Equilibrium

The Endemic equilibrium is denoted by

$$D^E = (S^*, W^*, E^*, I_s^*, I_a^*, H^*, R^*),$$

and it occurs when the disease persist in the community. To obtain this point, equate all equations in model (3.1) to zero. Taking note that initial conditions for the existence of endemic equilibrium are positive then, the following are obtained:

$$\begin{aligned}
S^* &= \frac{\Lambda + (1-r)W^* + \gamma R^*}{\mu + (1-\theta)\beta_1 I_s^*}, \\
W^* &= \frac{b}{1-r + \mu + (1-\xi)\beta_2 I_s^* r}, \\
E^* &= \frac{(1-\theta)\beta_1 I_s^* S^* + (1-\xi)r\beta_2 I_s^* W^*}{\rho + \mu + \alpha}, \\
I_s^* &= \frac{\alpha E^*}{\mu + \eta + d + \nu}, \\
I_a^* &= \frac{\rho E^*}{\mu + \delta + d + \epsilon}, \\
H^* &= \frac{\epsilon I_a^* + \nu I_s^*}{d + \omega + \mu}, \\
R^* &= \frac{\delta I_a^* + \eta I_s^* + \omega H^*}{(\gamma + \mu)}.
\end{aligned}$$

Simplification of all equations at endemic equilibrium results to:

$$r q_1 q_2 (I_s^*)^2 + (\mu q_3 q_4 (1-r) + (\mu + 1 - r) - \alpha \Lambda \beta_1 \beta_2) I_s^* - \mu (\mu + 1 - r) q_3 q_4 (R_0 - 1) = 0.$$

Further simplification leads to:

$$\frac{((\mu + 1 - r) \alpha \Lambda r q_3 + \beta_1 \beta_2 \mu q_3 q_4) (R_0 - 1)}{2 r q_1 q_2},$$

where

$$q_1 = \mu + \eta + d + \nu,$$

$$q_2 = \mu + \delta + d + \epsilon,$$

$$q_3 = \omega + \mu + d,$$

and

$$q_4 = \gamma + \mu.$$

Therefore, the endemic equilibrium point exists and it is only stable when $R_0 > 1$.

3.3.8 Global Stability of Disease-Free Equilibrium

The necessary condition for the disease not to depend on the initial size of the sub-populations is that the disease-free equilibrium point should be asymptotic stable given that $R_0 < 1$. We used the Metzler matrix stability method as stated by Castillo-Chavez *et al.* (2002) to determine the global stability at DFE.

Theorem 6: *The disease-free equilibrium point for COVID-19 model is globally asymptotically stable if $R_0 < 1$ and unstable whenever $R_0 > 1$.*

Proof: To prove this theorem, we need to show that the eigenvalues of the matrix B are negative real part and B_2 is a Metzler matrix. Let's rewrite the model system of Equation (3.1) as:

$$\frac{dy_n}{dt} = B(y_n - y_{DFE}) + B_1 y_i,$$

and

$$\frac{dy_i}{dt} = B_2 y_i,$$

where

y_n is a vector representing the compartments that do not transmit COVID-19,

y_i indicates the COVID-19 transmitting vector components and

y_{DFE} represents row vector at DFE so:

$$y_n = (S, W, R)^T, y_i = (E, I_s, I_a, H)^T.$$

$$y_{DFE} = \left(\frac{\Lambda}{\mu} + \frac{b(1-r)}{\mu(1-r+\mu)}, \frac{b}{1-r+\mu}, 0 \right)^T,$$

and

$$y_n - y_{DFE} = \begin{pmatrix} S - \frac{\Lambda(\mu+1-r)+b(1-r)}{\mu(\mu+1-r)} \\ W - \frac{b}{\mu+1-r} \\ R \end{pmatrix}.$$

Let's identify a matrix B and a Metzler matrix B_2 (i.e the off-diagonal elements of B_2 are non-negative, symbolically denoted by $B_2(y_i) \geq 0, \forall i \neq j$). Equation (3.21) represents equations which transmit and the other which does not transmit the disease.

$$\begin{pmatrix} \Lambda + (1-r)W + \gamma R - (\mu + (1-\theta)\beta_1 I_s)S \\ b - (1-\xi)r\beta_2 W I_s - \mu W - (1-r)W \\ \eta I_s + \omega H + \delta I_a - (\gamma + \mu)R \end{pmatrix} = B \begin{pmatrix} S - \frac{\Lambda(\mu+1-r)+b(1-r)}{\mu(\mu+1-r)} \\ W - \frac{b}{\mu+1-r} \\ R \end{pmatrix} + B_1 \begin{pmatrix} E \\ I_s \\ I_a \\ H \end{pmatrix}, \quad (3.21)$$

and

$$\begin{pmatrix} (1-\theta)\beta_1 I_s S + (1-\xi)r\beta_2 W I_s - (\rho + \mu + \alpha)E \\ \alpha E - (\mu + \nu + d + \eta)I_s \\ \rho E - (\delta + \mu + d + \epsilon)I_a \\ \nu I_s + \epsilon I_a - (\omega + d + \mu)H \end{pmatrix} = B_2 \begin{pmatrix} E \\ I_s \\ I_a \\ H \end{pmatrix}. \quad (3.22)$$

Matrix B in Equation (3.23) is obtained after performing the partial derivatives of (3.21) with

respect to non transmitting state variables S, W, R at DFE.

$$B = \begin{pmatrix} -\mu & 1-r & \gamma \\ 0 & -(1-r+\mu) & 0 \\ 0 & 0 & -(\mu+\gamma) \end{pmatrix}. \quad (3.23)$$

Matrix B_1 in Equation (3.24) is obtained by performing partial differentiation of the Equation (3.21) with respect to the transmitting state variables E, I_s, I_a, H .

$$B_1 = \begin{pmatrix} 0 & -(1-\theta)\beta_1 S & 0 & 0 \\ 0 & -(1-\xi)r\beta_2 W & 0 & 0 \\ 0 & \eta & \delta & \omega \end{pmatrix}, \quad (3.24)$$

Partial derivatives of (3.22) resulted to matrix B_2 as indicated in Equation (3.25).

$$B_2 = \begin{pmatrix} -(\mu+\alpha+\rho) & q_1 & 0 & 0 \\ \alpha & -(\eta+\nu+\mu+d) & 0 & 0 \\ \rho & 0 & -(\delta+d+\mu+\epsilon) & 0 \\ 0 & \nu & \epsilon & -(\mu+\omega+d) \end{pmatrix}, \quad (3.25)$$

where

$$q_1 = (1-\theta)\beta_1 S + (1-\xi)r\beta_2 W.$$

The eigenvalues of matrix B are $-(\gamma+\mu)$, $(1-r+\mu)$ and $-\mu$ as observed in the main diagonal of matrix of Equation (3.23). The three aforesaid eigenvalues are real, distinct, and negative. In addition, B_2 is a Metzler matrix with off-diagonal elements that are non-negative and leading diagonal entries are negative. Therefore, the DFE of system (3.1) is globally asymptotically stable and this completes the proof. \square

3.3.9 Global Stability of Endemic Equilibrium

In this part, the global behavior of the system (3.1) is analyzed. The stability of endemic equilibrium is scrutinized by using the direct Lyapunov method and LaSalle's Invariance Principle. Logarithm Lyapunov function has evinced great success in its application to many epidemiological models with any number of compartments (Korobeinikov & Wake, 2002; McCluskey, 2021).

Theorem 7: *Endemic equilibrium F^* is asymptotically stable when $R_0 > 1$ and unstable when $R_0 < 1$.*

Proof: To prove the theorem the global stability at endemic equilibrium F^* construct a Lyapunov function defined as:

$$\mathcal{V}_0(t) = \sum \mathcal{A}_i (y_i(t) - y_i^* - y_i^* \ln \frac{y_i(t)}{y_i^*}),$$

where \mathcal{A}_i is a non-negative constants to be determined,

$y_i(t)$ presents human individuals in each class varies with time i and

y_i^* presents the level of equilibrium .

$$\begin{aligned} \mathcal{V}_0(t) = & \mathcal{A}_1 \{S(t) - S^* - S^* \ln \frac{S(t)}{S^*}\} + \mathcal{A}_2 \{W(t) - W^* - W^* \ln \frac{W(t)}{W^*}\} + \mathcal{A}_3 \{E(t) - E^* - E^* \ln \frac{E(t)}{E^*}\} \\ & \mathcal{A}_4 \{I_s(t) - I_s^* - I_s^* \ln \frac{I_s(t)}{I_s^*}\} + \mathcal{A}_5 \{I_a(t) - I_a^* - I_a^* \ln \frac{I_a(t)}{I_a^*}\} \\ & + \mathcal{A}_6 \{H(t) - H^* - H^* \ln \frac{H(t)}{H^*}\} + \mathcal{A}_7 \{R(t) - R^* - R^* \ln \frac{R(t)}{R^*}\}, \text{ the constants } \mathcal{A}_1, \mathcal{A}_2, \mathcal{A}_3, \mathcal{A}_4, \mathcal{A}_5, \\ & \mathcal{A}_6 \text{ and } \mathcal{A}_7 \text{ are non negative.} \end{aligned}$$

Now differentiate $\mathcal{V}_0(t)$ one get the following:

$$\frac{d\mathcal{V}_0(t)}{dt} \leq \begin{cases} \mathcal{A}_1(1 - \frac{S^*}{S(t)})\frac{dS}{dt} + \mathcal{A}_2(1 - \frac{W^*}{W(t)})\frac{dW}{dt} \\ + \mathcal{A}_3(1 - \frac{E^*}{E(t)})\frac{dE}{dt} + \mathcal{A}_4(1 - \frac{I_s^*}{I_s(t)})\frac{dI_s}{dt} \\ + \mathcal{A}_5(1 - \frac{I_a^*}{I_a(t)})\frac{dI_a}{dt} + \mathcal{A}_6(1 - \frac{H^*}{H(t)})\frac{dH}{dt} + \mathcal{A}_7(1 - \frac{R^*}{R(t)})\frac{dR}{dt}. \end{cases} \quad (3.26)$$

Substitute (3.1) in (3.26) and we have the following:

$$\frac{d\mathcal{V}_0(t)}{dt} \leq \begin{cases} \mathcal{A}_1(1 - \frac{S^*}{S(t)})(\Lambda + \gamma R + (1 - r)W - (\mu + (1 - \theta)\beta_1 I_s)S) \\ + \mathcal{A}_2(1 - \frac{W^*}{W(t)})(b - \mu W - (1 - r)W - (1 - \xi)r\beta_2 W I_s) \\ + \mathcal{A}_3(1 - \frac{E^*}{E(t)})((1 - \theta)\beta_1 I_s S + (1 - \xi)r\beta_2 W - (\alpha + \mu + \rho)E) \\ + \mathcal{A}_4(1 - \frac{I_s^*}{I_s(t)})(\alpha E - (d + \nu + \mu + \eta)I_s) \\ + \mathcal{A}_5(1 - \frac{I_a^*}{I_a(t)})(\rho E - (d + \mu + \delta + \epsilon)I_a) \\ + \mathcal{A}_6(1 - \frac{H^*}{H(t)})(\nu I_s + \epsilon I_a - (\mu + d + \omega)H) \\ + \mathcal{A}_7(1 - \frac{R^*}{R(t)})(\eta I_s + \omega H + \delta I_a - (\mu + \gamma)R). \end{cases} \quad (3.27)$$

Let set the system of model (3.1) at the endemic equilibrium point, that is:

$$\begin{aligned}
\mu &= \frac{\Lambda}{S^*} + (1-r)\frac{W^*}{S^*} + \gamma\frac{R^*}{S^*} - (1-\theta)\beta_1 I_s^*, \\
1-r+\mu &= \frac{b}{W^*} - (1-\xi)r\beta_2 I_s^*, \\
\rho+\mu+\alpha &= (1-\theta)\frac{\beta_1 I_s^* S^*}{E^*} + \frac{(1-\xi)r\beta_2 W^* I_s^*}{E^*}, \\
\mu+\nu+d+\eta &= \frac{\alpha E^*}{I_s^*}, \\
\delta+\mu+d+\epsilon &= \frac{\rho E^*}{I_a^*}, \\
d+\mu+\omega &= \frac{\nu I_s^*}{H^*} + \frac{\epsilon I_a^*}{H^*}, \\
\gamma+\mu &= \frac{\eta I_s^*}{R^*} + \frac{\omega H^*}{R^*} + \frac{\delta I_a^*}{R^*}.
\end{aligned} \tag{3.28}$$

By substituting (3.28) in (3.27) and solving constant \mathcal{A}_i with $i = 1, 2, \dots, 7$ after simplification we have the following results:

$$\frac{d\mathcal{V}_0(t)}{dt} \leq \left\{ \begin{aligned} &\frac{\Lambda}{S^*} \left(2 - \frac{S(t)}{S^*} - \frac{S^*}{S(t)} \right) + (1-r)\frac{W^*}{S^*} \left(1 - \frac{S}{S^*} + \frac{W}{W^*} - \frac{S^*}{S} \frac{W}{W^*} \right) \\ &+ \frac{\gamma R^*}{S^*} \left(1 - \frac{S}{S^*} + \frac{R}{R^*} - \frac{R}{R^*} \frac{S}{S^*} \right) + (1-\theta)\beta_1 I_s^* \left(\frac{S}{S^*} + \frac{I_s}{I_s^*} - \frac{S}{S^*} \frac{I_s}{I_s^*} - 1 \right) \\ &+ \frac{b}{W^*} \left(2 - \frac{W(t)}{W^*} - \frac{W^*}{W(t)} \right) + (1-\xi)r\beta_2 I_s^* \left(\frac{W}{W^*} - \frac{W}{W^*} \frac{I_s}{I_s^*} + \frac{I_s}{I_s^*} - 1 \right) \\ &+ (1-\theta)\frac{\beta_1 I_s^* S^*}{E^*} \left(1 - \frac{E}{E^*} + \frac{W}{W^*} \frac{I_s}{I_s^*} - \frac{W}{W^*} \frac{I_s}{I_s^*} \frac{E}{E^*} \right) \\ &+ (1-\xi)\frac{r\beta_2 W^* I_s^*}{E^*} \left(1 - \frac{E}{E^*} + \frac{W}{W^*} \frac{I_s}{I_s^*} - \frac{W}{W^*} \frac{I_s}{I_s^*} \frac{E}{E^*} \right) \\ &+ \frac{\alpha E^*}{I_s^*} \left(1 - \frac{I_s}{I_s^*} + \frac{E}{E^*} - \frac{E}{E^*} \frac{I_s}{I_s^*} \right) + \frac{\rho E^*}{I_a^*} \left(1 - \frac{I_a}{I_a^*} + \frac{E}{E^*} - \frac{E}{E^*} \frac{I_a}{I_a^*} \right) \\ &+ \frac{\nu I_s^*}{H^*} \left(1 - \frac{H}{H^*} + \frac{I_s}{I_s^*} - \frac{I_s}{I_s^*} \frac{H}{H^*} \right) + \frac{\epsilon I_a^*}{H^*} \left(1 - \frac{H}{H^*} + \frac{I_a}{I_a^*} - \frac{H}{H^*} \frac{I_a}{I_a^*} \right) \\ &+ \frac{\eta I_s^*}{R^*} \left(1 - \frac{R}{R^*} + \frac{I_s}{I_s^*} - \frac{I_s}{I_s^*} \frac{R}{R^*} \right) + \frac{\omega H^*}{R^*} \left(1 - \frac{R}{R^*} + \frac{H}{H^*} - \frac{H}{H^*} \frac{R}{R^*} \right). \end{aligned} \right. \tag{3.29}$$

Since the arithmetic mean is greater than or equal to geometric mean, from (3.29) the following satisfies:

$$2 - \frac{S(t)}{S^*} - \frac{S^*}{S(t)} \leq 0, \tag{3.30}$$

and

$$2 - \frac{W(t)}{W^*} - \frac{W^*}{W(t)} \leq 0. \tag{3.31}$$

Furthermore, let $\Phi = 1 - z + \ln(z)$ for $z > 1$, if $z = 1$ one can note that $\Phi(z) \leq 0$. Using the

aforesaid properties of $\Phi(z)$ we have that:

$$1 - \frac{S}{S^*} + \frac{W}{W^*} - \frac{S^*}{S} \frac{W}{W^*} = \begin{cases} \Phi\left(\frac{S^*}{S} \frac{W}{W^*}\right) - \ln\left(\frac{S^*}{S} \frac{W}{W^*}\right) + \frac{S}{S^*} + \frac{W}{W^*} \\ \leq \frac{S}{S^*} - \ln \frac{S}{S^*} + \frac{W}{W^*} - \ln \frac{W}{W^*} \leq 0. \end{cases} \quad (3.32)$$

$$1 - \frac{S}{S^*} + \frac{R}{R^*} - \frac{S^*}{S} \frac{R}{R^*} = \begin{cases} \Phi\left(\frac{S^*}{S} \frac{R}{R^*}\right) - \ln\left(\frac{S^*}{S} \frac{R}{R^*}\right) + \frac{S}{S^*} + \frac{R}{R^*} \\ \leq \frac{S}{S^*} - \ln \frac{S}{S^*} + \frac{R}{R^*} - \ln \frac{R}{R^*} \leq 0. \end{cases} \quad (3.33)$$

Similarly we have the following:

$$\frac{S}{S^*} + \frac{I_s}{I_s^*} - \frac{S}{S^*} \frac{I_s}{I_s^*} - 1 = \left\{ \Phi\left(\frac{S}{S^*} \frac{I_s}{I_s^*}\right) + \frac{S}{S^*} + \frac{I_s}{I_s^*} \leq \frac{S}{S^*} - \ln \frac{S}{S^*} + \frac{I_s}{I_s^*} - \ln \frac{I_s}{I_s^*} \leq 0. \right. \quad (3.34)$$

$$\frac{W}{W^*} + \frac{I_s}{I_s^*} - \frac{W}{W^*} \frac{I_s}{I_s^*} - 1 = \left\{ \Phi\left(\frac{W}{W^*} \frac{I_s}{I_s^*}\right) + \frac{W}{W^*} + \frac{I_s}{I_s^*} \leq \frac{W}{W^*} - \ln \frac{W}{W^*} + \frac{I_s}{I_s^*} - \ln \frac{I_s}{I_s^*} \leq 0. \right. \quad (3.35)$$

$$1 - \frac{E}{E^*} + \frac{I_s}{I_s^*} \frac{S}{S^*} - \frac{I_s}{I_s^*} \frac{S}{S^*} \frac{E}{E^*} = \begin{cases} \Phi\left(\frac{I_s}{I_s^*} \frac{S}{S^*} \frac{E}{E^*}\right) - \frac{E}{E^*} + \frac{I_s}{I_s^*} \frac{S}{S^*} \leq \ln \frac{E}{E^*} - \frac{E}{E^*} \\ + \frac{I_s}{I_s^*} \frac{S}{S^*} - \ln \frac{I_s}{I_s^*} \frac{S}{S^*} \leq 0. \end{cases} \quad (3.36)$$

$$1 - \frac{E}{E^*} + \frac{W}{W^*} \frac{I_s}{I_s^*} - \frac{W}{W^*} \frac{I_s}{I_s^*} \frac{E}{E^*} = \begin{cases} \Phi\left(\frac{W}{W^*} \frac{I_s}{I_s^*} \frac{E}{E^*}\right) - \frac{E}{E^*} + \frac{W}{W^*} \frac{I_s}{I_s^*} \leq \ln \frac{E}{E^*} - \frac{E}{E^*} \\ + \frac{W}{W^*} \frac{I_s}{I_s^*} - \ln \frac{W}{W^*} \frac{I_s}{I_s^*} \leq 0. \end{cases} \quad (3.37)$$

Utilizing the same techniques for the remaining terms in (3.29) one can notes

$$1 - \frac{I_s}{I_s^*} + \frac{E}{E^*} - \frac{E}{E^*} \frac{I_s}{I_s^*} \leq \ln \frac{I_s}{I_s^*} - \frac{I_s}{I_s^*} + \frac{E}{E^*} - \ln \frac{E}{E^*} \leq 0. \quad (3.38)$$

$$1 - \frac{I_a}{I_a^*} + \frac{E}{E^*} - \frac{E}{E^*} \frac{I_a}{I_a^*} \leq \ln \frac{I_a}{I_a^*} - \frac{I_a}{I_a^*} + \frac{E}{E^*} - \ln \frac{E}{E^*} \leq 0. \quad (3.39)$$

$$1 - \frac{I_s}{I_s^*} + \frac{H}{H^*} - \frac{H}{H^*} \frac{I_s}{I_s^*} \leq \ln \frac{I_s}{I_s^*} - \frac{I_s}{I_s^*} + \frac{H}{H^*} - \ln \frac{H}{H^*} \leq 0. \quad (3.40)$$

$$1 - \frac{I_a}{I_a^*} + \frac{H}{H^*} - \frac{H}{H^*} \frac{I_a}{I_a^*} \leq \ln \frac{I_a}{I_a^*} - \frac{I_a}{I_a^*} + \frac{H}{H^*} - \ln \frac{H}{H^*} \leq 0. \quad (3.41)$$

$$1 - \frac{I_s}{I_s^*} + \frac{R}{R^*} - \frac{R}{R^*} \frac{I_s}{I_s^*} \leq \ln \frac{I_s}{I_s^*} - \frac{I_s}{I_s^*} + \frac{R}{R^*} - \ln \frac{R}{R^*} \leq 0. \quad (3.42)$$

$$1 - \frac{H}{H^*} + \frac{R}{R^*} - \frac{R}{R^*} \frac{H}{H^*} \leq \ln \frac{H}{H^*} - \frac{H}{H^*} + \frac{R}{R^*} - \ln \frac{R}{R^*} \leq 0. \quad (3.43)$$

Since the arithmetic mean is greater than or equal to geometric mean, it follows that from (3.30) - (3.43) one can note that $\frac{dV_0(t)}{dt} \leq 0$ whenever $R_0 > 1$. Therefore by using Lasalle Invariance principle (LaSalle, 1976), the system (3.1) have global asymptotically stable endemic equilibrium point for all $R_0 > 1$ and this completes the proof.

□

3.4 Summary

The COVID-19 mathematical model was developed and analyzed to understand analytical behavior so as to validate later using numerical results. Qualitative analysis is performed. The qualitative results demonstrated that the model has a positive solution and a region which is biologically feasible. Moreover, we were able to show that the solution of model (3.1) is continuous and bounded. The basic reproductive ratio R_0 was computed by benefiting the next generation matrix method, this threshold quantity determines whether a disease be eradicated or not. Furthermore, the disease-free equilibrium and endemic equilibrium points were obtained and their stability was investigated. The results indicated that the disease-free equilibrium point was locally and globally asymptotic stable whenever $R_0 < 1$. Eventually, the Lyapunov function depicted that the endemic equilibrium point was asymptotically stable if $R_0 > 1$.

CHAPTER FOUR

RESULTS AND DISCUSSION

4.1 Numerical Results

The present study employed simulated data corrupted with Gaussian noise. The fourth-order Runge-Kutta scheme was deployed to simulate the numerical solutions of the model (3.1). Furthermore, the identifiability of model parameters was done using the least square method. The graphical presentations obtained in this chapter assisted in the visualization of the effectiveness of the theoretical solutions. The parameters which are drawn from literature their sources are acknowledged. The parameter values and their units are indicated in Table 3.

4.2 Numerical Simulation for the Model (3.1)

This subsection presents the numerical results to disclose how COVID-19 spread among the community and healthcare workers. For this purpose, $SWEI_s I_a HR$ formulated model is deployed. Further, the present subsection explores the dynamics of the human populations, sensitivity analysis, the impact of varying control parameters value on few compartments, the global stability of the proposed model, and the identifiability of the model parameters. Apart from Runge-Kutta fourth-order scheme used in this dissertation, there are other numerical methods for simulations such as the Adams-Bashforth-Moulton method, Milne method, Eulers' method (Babaei *et al.*, 2019; Yu *et al.*, 2021).

4.2.1 Sensitivity and Uncertainty Analysis

Sensitivity analysis is an essential component of modeling since it can be used to explore the complex interactions of a model. It provides practical information for model builders and users by highlighting the parameters with the highest influence on the model output. Also, sensitivity analysis underlines the parameters of the model that should be accurately measured so as to maximize precision. The reliability of the model prediction depends on sensitivity analysis. The sensitive parameters are investigated through the use forward sensitivity index method as established by Marino *et al.* (2008).

Definition 1: Normalized forward sensitivity index of a variable n that depends on the differentiability on a parameter p is defined as:

$$X_p^n = \frac{\delta n}{\delta p} \times \frac{p}{n},$$

where n represents the value of R_0 of a specific parameter and p represents one of the parameter in which sensitivity on R_0 is sought. The effect of each parameter on the transmission of infection

refers to the index of the parameter. This index implies that the greater the value in its magnitude, the higher sensitive R_0 is to the parameter. Further, the negative (or positive) sign depicts that R_0 decreases (or increases) as n decreases. We evaluated the sensitivity index for all thirteen parameters as found in Table 3 by using the fourth-order Runge-Kutta scheme. From Table 3, it can be observed that the most positive sensitive parameter is α . This implies that increasing (decreasing) of α by 10% will increase (decrease) the value of R_0 by 15.555%. Other parameters which enhance the growth of the value of R_0 are β_1 , ν , Λ , ρ , b , η , β_2 and d . The most negative sensitive parameter is physical distancing θ . If physical distancing is being practiced by 10 % then the value of R_0 will be reduced by 15.640 %. Other negative sensitive parameters include r and ξ . On the other hand, Fig. 4 denotes the positive and negative indices found in Table 3. Also, it can be observed that the most positive sensitive parameter is α and the most negative parameter is θ .

Table 3: Relevant model's parameters and their indices values

Parameter	Value	Value	Indices
Λ	40 day^{-1}	$\mu \times N_0$	0.9079
ξ	0.7	Assumed	-0.0002
β_1	0.5944 day^{-1}	Mugisha <i>et al.</i> (2021)	0.9999
β_2	0.8 day^{-1}	Assumed	0.0001
μ	0.008 day^{-1}	Mugisha <i>et al.</i> (2021)	-0.9156
α	0.06 day^{-1}	Aldila (2020)	1.5555
η	0.62 day^{-1}	Assumed	0.2331
ρ	0.04 day^{-1}	Assumed	0.3703
ν	0.65 day^{-1}	Assumed	0.7574
b	4 day^{-1}	Assumed	0.0921
r	0.4	Assumed	-1.3326
d	0.00011 day^{-1}	Deressa & Duressa (2021)	0.0001
θ	0.8 day^{-1}	Assumed	-1.5640

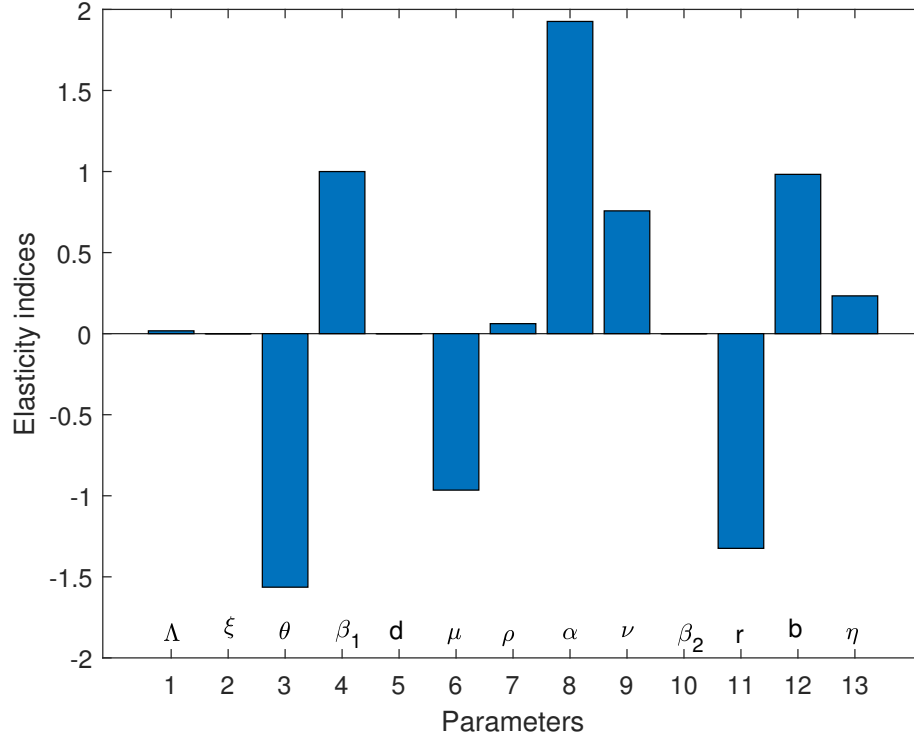


Figure 4: Normalized local sensitivity indices of R_0 for each parameter

Figures 5-16 stipulate the correlation between R_0 versus the parameters found in Table 3. In order to plot Fig. 5, we varied Λ from 0 to 40 using the interval of one while keeping other parameters constant as seen in Table 3. Similar approach resulted into Figs. 6-16.

Figures 5-13 evince a positive correlation between the value of R_0 and their respective parameters on x-axis. Also, Figs. 14-16 depict a negative association between the value of R_0 and their respective parameters.

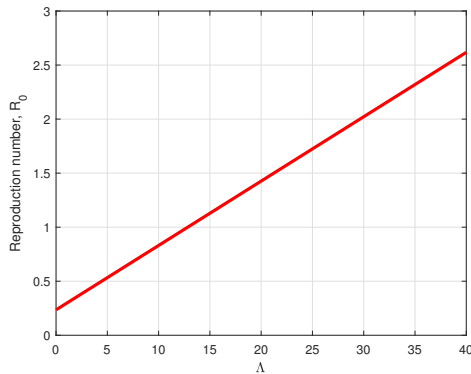


Figure 5: Dependence of R_0 on recruitment rate (Λ)

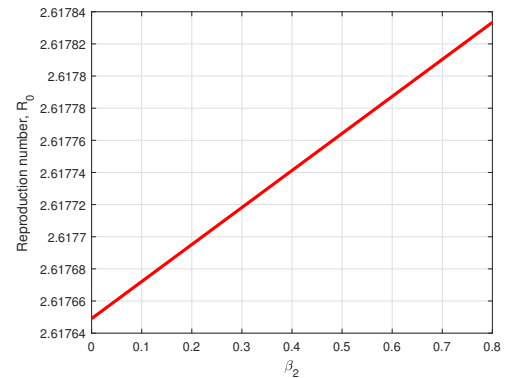


Figure 6: Dependence of R_0 on healthcare workers transmission probability (β_2)

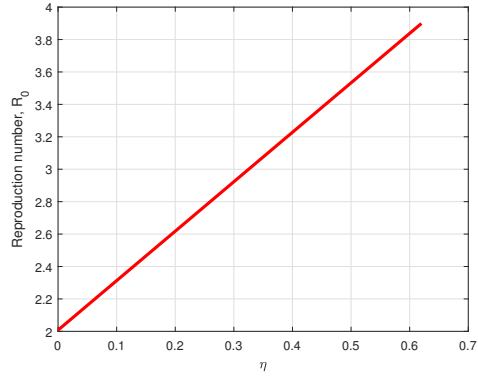


Figure 7: Effect of recovery rate (η) for I_s population on R_0

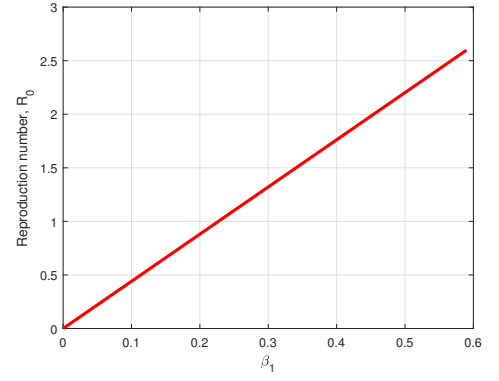


Figure 8: Dependence of R_0 on disease transmission rate (β_1)

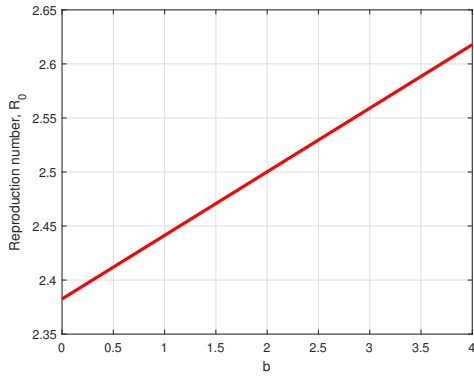


Figure 9: Dependence of R_0 on healthcare workers recruitment rate (b)

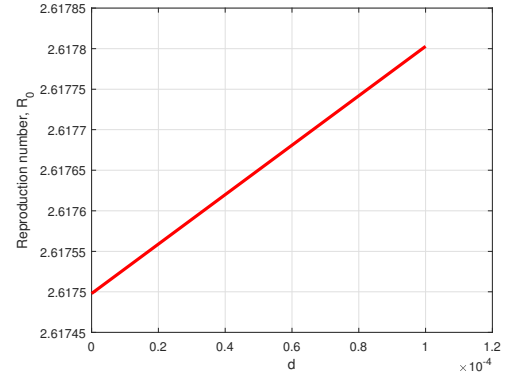


Figure 10: Dependence of R_0 on disease induced death rate (d)

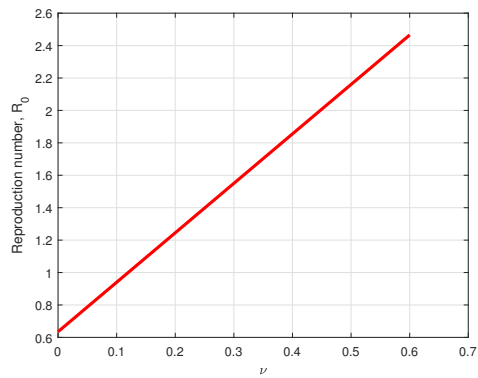


Figure 11: Effect of hospitalizing symptomatic infected population (ν) on R_0

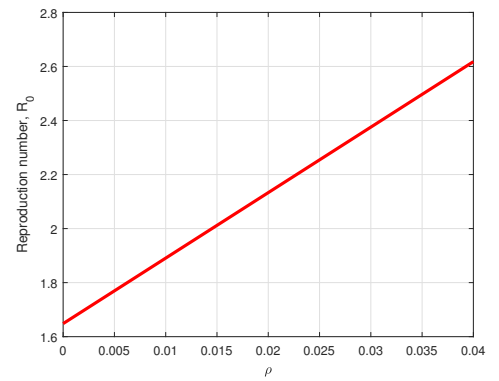


Figure 12: Effect of progression rate (ρ) from E to I_a on R_0

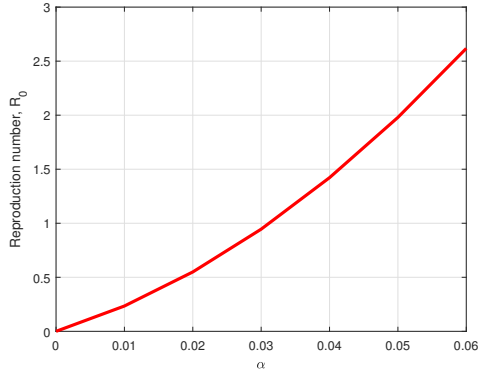


Figure 13: Effect of progression rate (α) from E to I_s on R_0

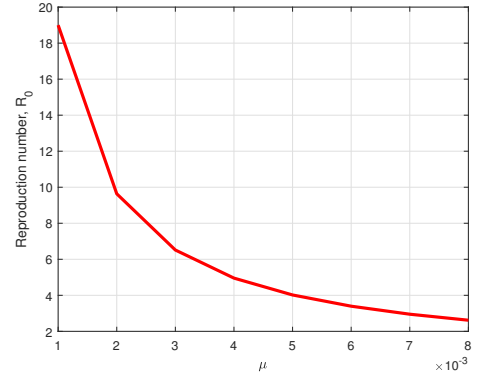


Figure 14: Dependence of R_0 on natural mortality rate (μ)

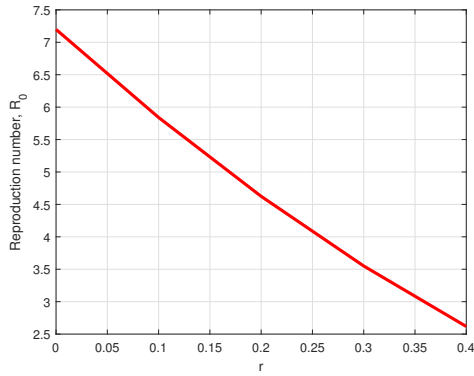


Figure 15: Effect of a proportional of health workers (r) on R_0

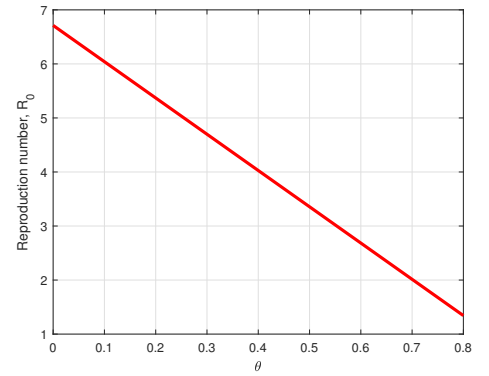


Figure 16: Effect of physical distancing (θ) on R_0

4.2.2 Dynamics of Human Populations

The dynamics of the model system of Equation (3.1) under the initial values of the compartments S, W, E, I_s, I_a, H , and R is investigated. In order to visualize graphical behavior of all seven compartments at the outset of COVID-19, we assumed $S(0) = 1000, W(0) = 300, E(0) = 100, I_s(0) = 16, I_a(0) = 5, H(0) = 4$ and $R(0) = 50$ to be used in simulation. Figure 17 shows the temporal variation of different population classes. Both healthcare workers and susceptible compartments undergo exponential decay as they die naturally and acquire the equilibrium point after one day. The sharp peak is observed in the exposed plot in closer to one day, after that, it decelerates and maintains its' equilibrium point after 3 days. At the start, symptomatic, asymptomatic, and hospitalized sub-populations grow exponentially but decelerate to the equilibrium point after a few days as seen in Fig. 17. At the same time, the recovered plot starts from zero and grows after 6 days it attains its equilibrium point.

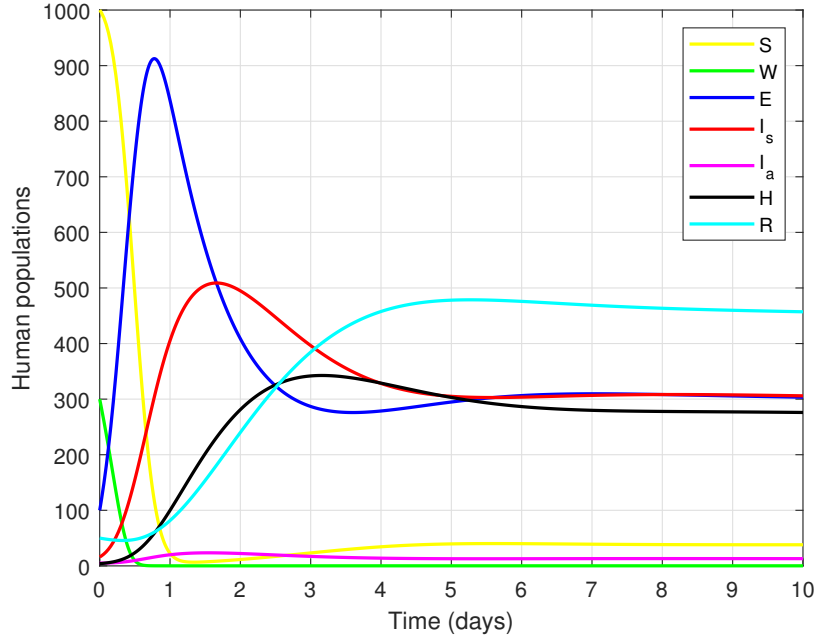


Figure 17: Profile for the dynamics of $SWEI_s I_a HR$ sub-populations

4.2.3 Global Stability at Endemic Equilibrium (EE) for the Proposed Model (3.1)

We scrutinized global stability at the endemic equilibrium point of the model system (3.1). The global stability can be attained whenever the model's state variables coming from distinguished initial values, varied for sometimes, converge to a common point and finally attain a constant horizontal line named endemic equilibrium point. The convergence of the model's trajectories to a common horizontal line signifies the global stability of the model system (3.1). Figure 18 denotes five different trajectories originating from different assumed sub-population of the susceptible compartment such as $S(0) = 1000, S(0) = 900, S(0) = 800, S(0) = 700$ and $S(0) = 600$. All five trajectories converged to a common straight line after 17 days. Also, Fig. 19 reveals five different trajectories of healthcare workers compartment originating from the following sub-population; $W(0) = 500, W(0) = 400, W(0) = 300, W(0) = 200$ and $W(0) = 100$ which converge to a common straight line after around five (5) days. Furthermore, Figs. 20-24 show similar interpretation as those in Figs. 18 and 19.

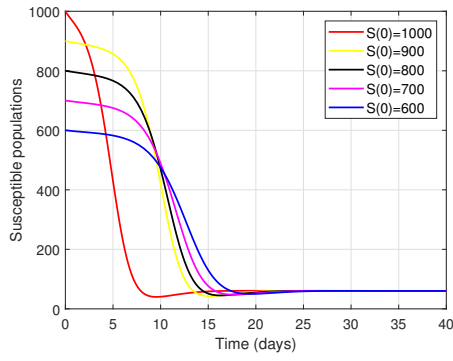


Figure 18: Profile of global stability at EEP for susceptible population

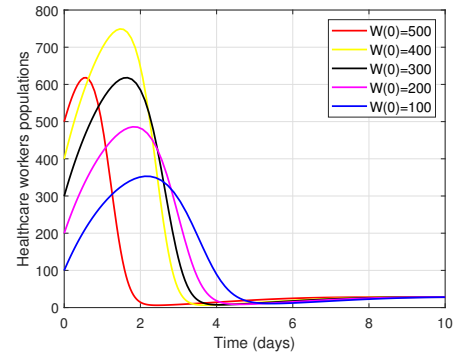


Figure 19: Profile of global stability at EEP for healthcare workers population

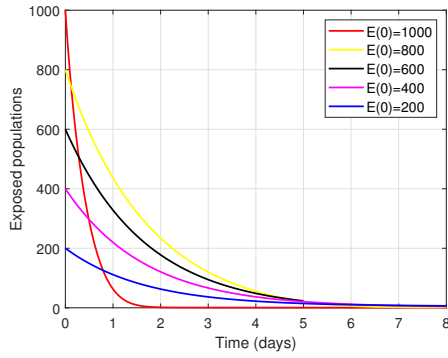


Figure 20: Profile of global stability at EEP for exposed population

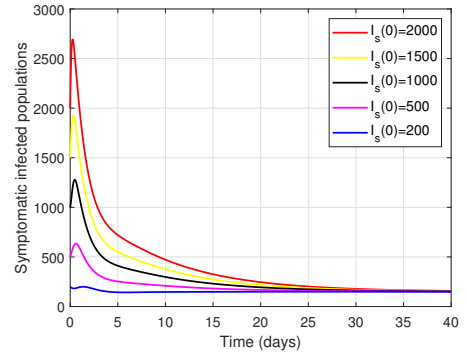


Figure 21: Profile of global stability at EEP for symptomatic infected population

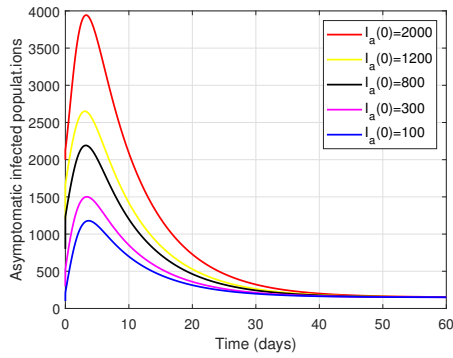


Figure 22: Profile of global stability at EEP for asymptomatic infected population

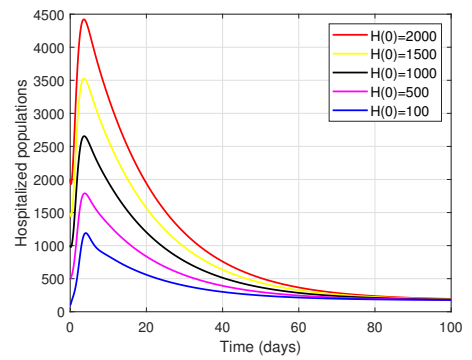


Figure 23: Profile of global stability at EEP for hospitalized population

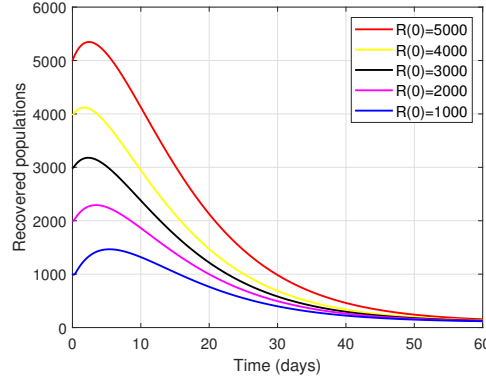


Figure 24: Profile of global stability at EEP for recovered population

4.2.4 Impact of Control Parameters on the COVID-19 Model (3.1)

In this part, we investigated how personal protective equipment (PPE) such as N95 masks, gloves, protective eye-wear, and long-sleeved gowns prevent infection of coronavirus among healthcare workers. The aforesaid PPE is symbolized by ξ . Also, we analyzed how physical distancing θ minimizes the infection of COVID-19 in the community. Physical distancing in this study refers to the cancellation of unnecessary mass gatherings, closure of learning institutions, workplaces, and closure of certain businesses. Whenever the value of θ is not equal to 1 means the strategy of physical distancing is implemented partially. In this study, both ξ and θ are termed as protective measures. Further, we assessed how medication ω on the hospitalized population impacts the spread of the disease. Furthermore, we examined the effect of natural recovery rate (η and δ) for both symptomatic and asymptomatic populations in containing the disease.

First, we observed the impact of maintaining physical distancing in the community. Figure 25 evinces that the number susceptible population raised to 44 individuals when θ is implemented by 0.8. Conversely, Fig. 26 indicates that the number of symptomatic infected decreases to 78 individuals due to implementation of θ at 0.8. On the other hand, Fig. 27 denotes that when θ is implemented by 0.8 the number of patients in the hospital falls to around 175 individuals while Fig. 28 connotes that the recovered human population grow to about 9098 individuals within only 50 days due to the implementation of physical distancing by 0.8.

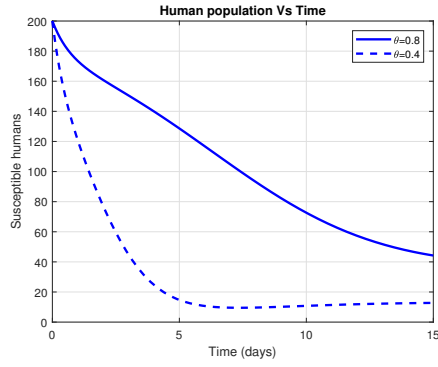


Figure 25: Profile showing the impact of θ on susceptible population

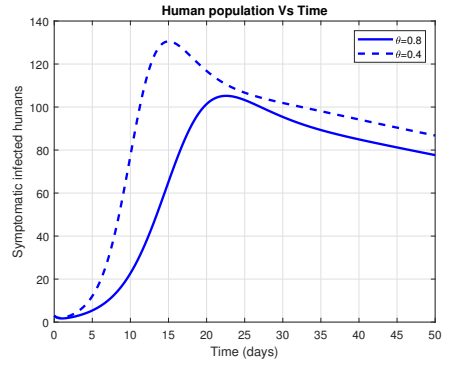


Figure 26: Profile showing the impact of θ on symptomatic population

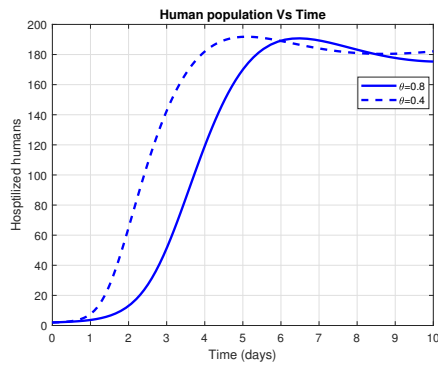


Figure 27: Profile for the impact of θ on hospitalized humans

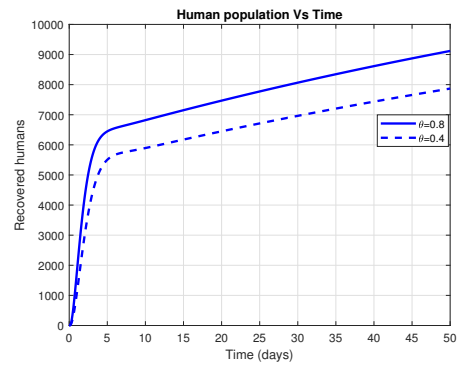


Figure 28: Profile for the impact of θ on recovered humans

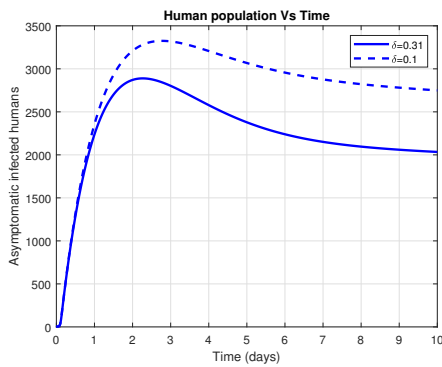


Figure 29: Profile for the impact of treatment (δ) on asymptomatic infected population

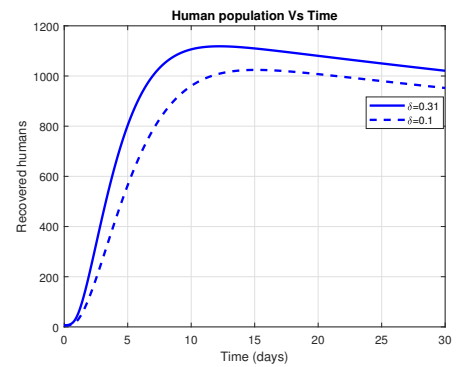


Figure 30: Profile for the impact of treatment (δ) on recovered population

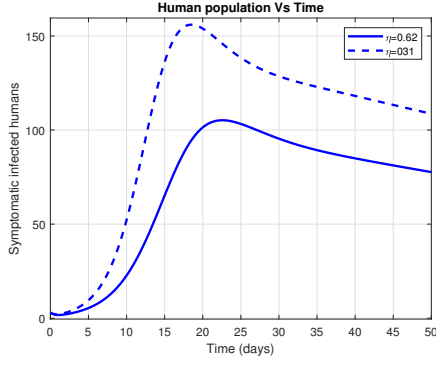


Figure 31: Profile for the impact of treatment (η) on symptomatic infectious

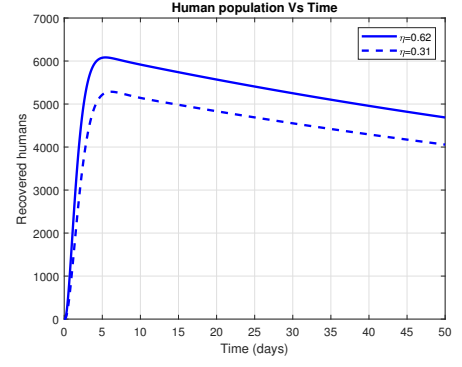


Figure 32: Profile for the impact of treatment (η) on recovered population

Figure 29 reveals that when δ is acquired to a rate of 0.31 by the I_a population the number of asymptomatic infected individuals reduces from the peak (around 2888) to about 2036 patients. At the same time, Fig. 30 demonstrates that the number of the population recovered reached 1022 individuals due to natural recovery (δ) acquired at a rate of 0.31.

On the other hand, Fig. 31 demonstrates that the number of symptomatic infected reduces from its peak of 105 to around 78 infected individuals when the I_s population acquires the natural recovery at a rate of 0.62. Using the aforementioned value of η , Fig. 32 signifies the increase in the number of recovered individuals to around 4697 people.

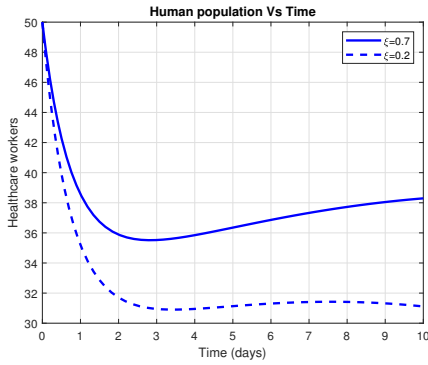


Figure 33: Profile for the impact of (ξ) on healthcare workers population

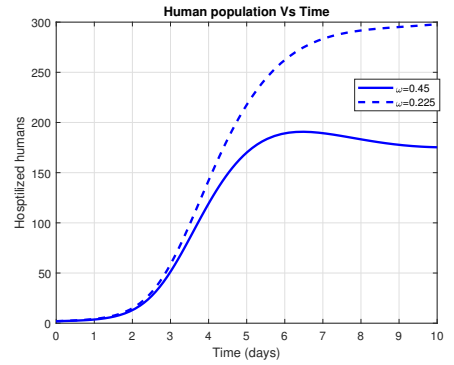


Figure 34: Profile for the impact of (ω) on hospitalized population

Figure 33 reveals that the number of healthcare providers raised to about 38 individuals through the effective use of PPE ($\theta=0.8$). Conversely, Fig. 34 depicts that after treating the isolated group in the hospital the number of patients reduced to about 175 just within 10 days.

Further, deploying parameters value chosen from Table 3, we demonstrated the dynamics transmission behavior of COVID-19 through examining the magnitude of basic reproduction number. Figure 35 indicates that increasing ω and decreasing θ produces the value of R_0 which is larger

than 5. Reversely, when θ is increased by only 60% the value of R_0 reduces to ≈ 0.5 . We conclude that θ can be utilized to minimize the spread of COVID-19. Figure 36 indicates the similar behavior and interpretation on R_0 as the one found in Fig. 35. Further, Fig. 37 depicts that increases in ν contributes to the increase of the value of R_0 . Generally, Figs. 35 and 36 demonstrate contours and mesh grid which help to examine the contribution of each parameter towards the dynamics of R_0 as the changes of these parameters significantly affect the value of basic reproductive ratio R_0 .

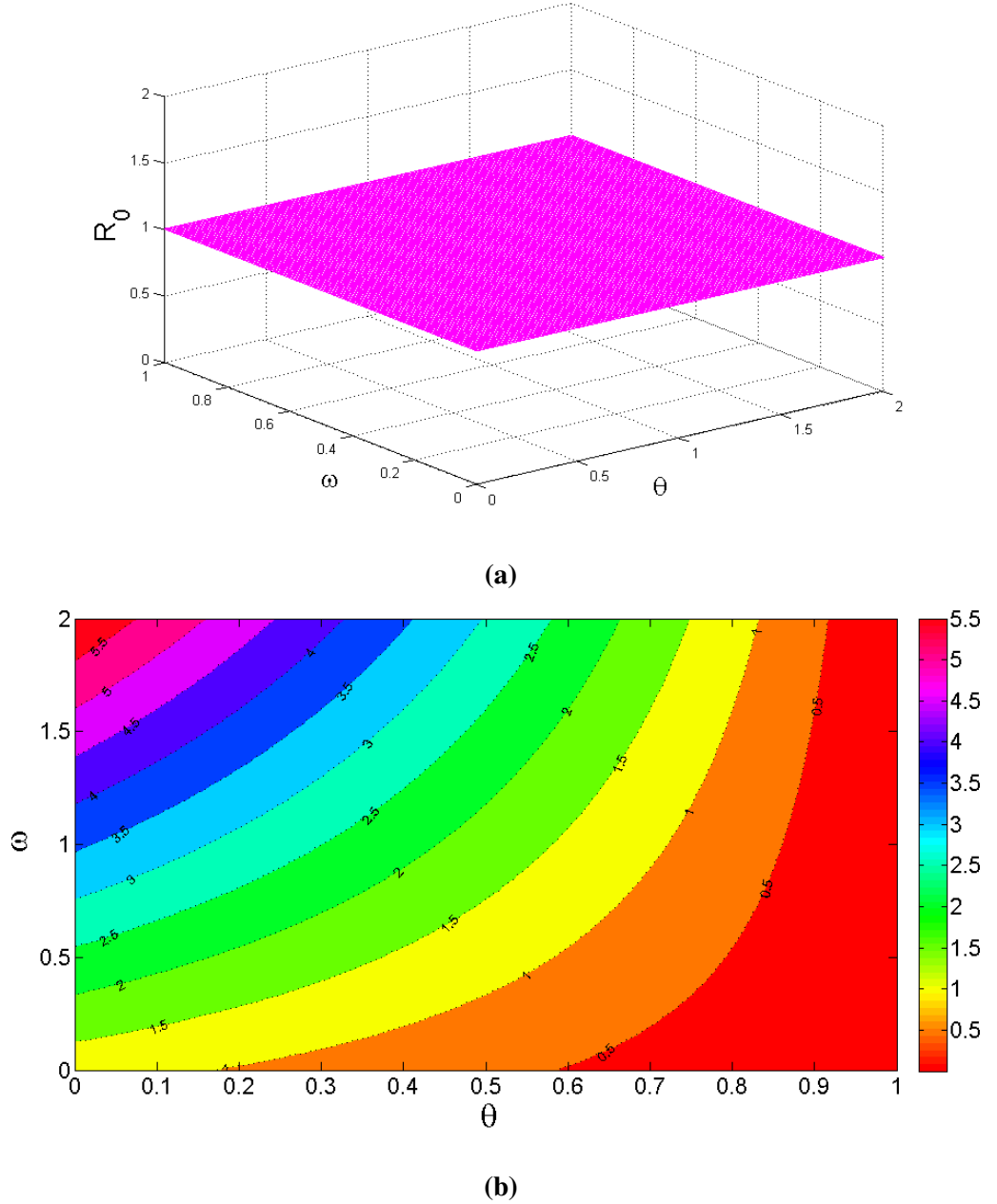
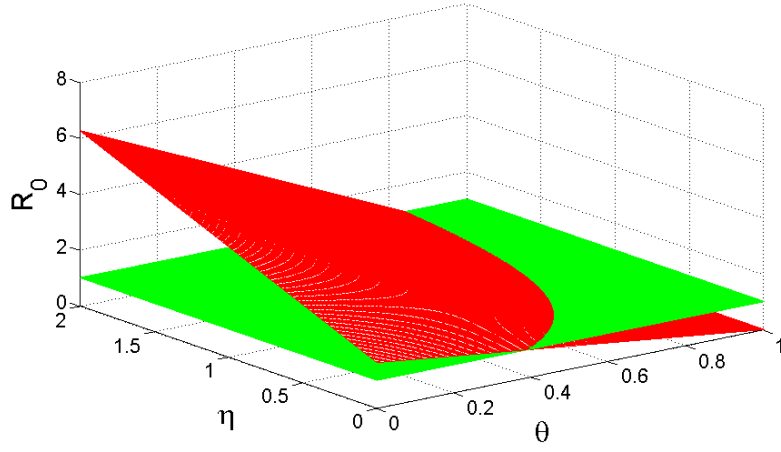
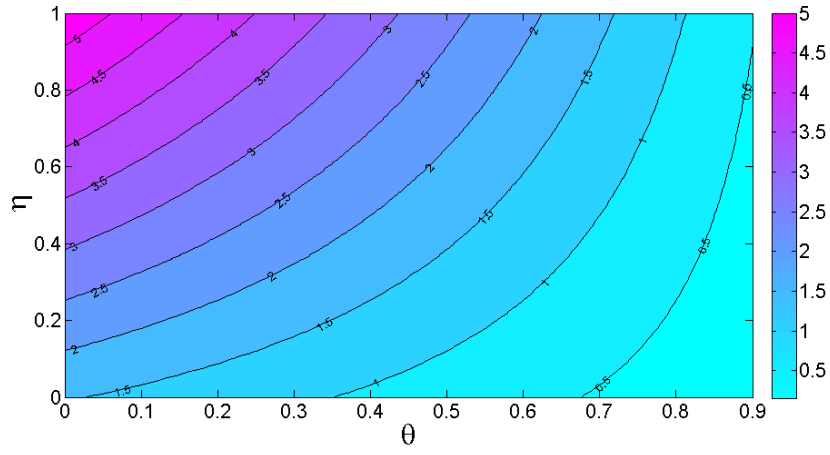


Figure 35: 3D dynamics behavior of R_0 for ω and θ along with contour plot



(a)



(b)

Figure 36: 3D dynamic behavior of R_0 for θ and η along with contour plot

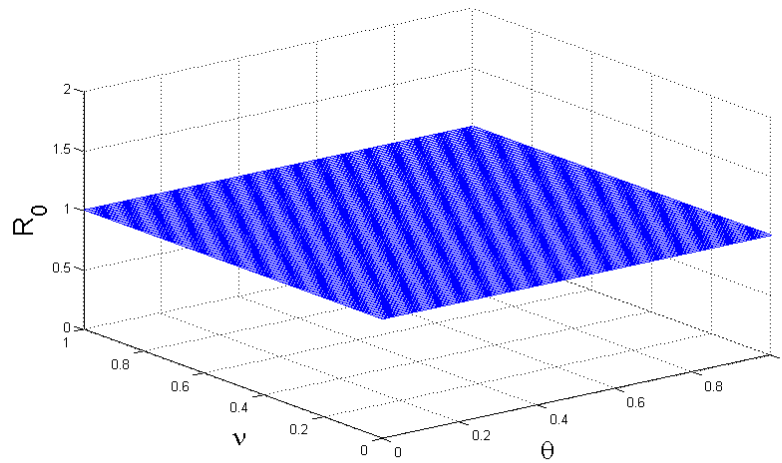


Figure 37: 3D dynamic behavior of R_0 for ν and θ

Also, we determined the value of R_0 using all parameters found in Table 3 and its value was 2.6178. Further, we assessed the effect of varying the level of protection to healthcare workers and physical distancing numerically. Quantifying the value of ξ to be 0.8 and $\theta=0.9$ while maintaining other parameters as seen Table 3, the value of R_0 is 0.6713. In absence of both control measures ($\xi=0$ and $\theta=0$) the value of R_0 raised to 6.7125. When having this information, it can be concluded that COVID-19 can be effectively managed or even eliminated since protective measures are capable of sustaining R_0 to a value below unity.

4.2.5 The Identifiability of Model Parameters

We deployed parameters found in Table 3 to estimate the parameters found in Table 4. The parameters identifiability of the system of Equation (3.1) is investigated through the use of the classical least square methods. In this approach, the idea is to minimize the sum of squared differences between the model and the observations as indicated in Equation (4.1).

$$SS(\theta) = \sum_{i=1}^n (y_i - f(x_i, \theta))^2, \quad (4.1)$$

where y_i indicate observational data values of the model (3.1) which correspond to

$$\{S_i, W_i, E_i, (I_a)_i, (I_s)_i, H_i, R_i\}$$

and $f(x_i, \theta)$, represent predicted values from simulations solution of the seven compartments of model (3.1). Table 4 depicts the initial values of parameters and the model (3.1) optimization. Using the estimated values, the model solution can be compared with the simulated data as shown in Fig. 38. Further, Fig. 38 shows that the simulated data superimpose with the fitted one.

Table 4: Parameter identifiability of the COVID-19 proposed model.

Parameter	Value intensity	Estimates
Λ	40	39.7543
ξ	0.7	0.8779
β_1	0.5944	0.4385
β_2	0.8	0.8038
μ	0.008	0.0093
α	0.06	0.0490
η	0.62	0.2288
ρ	0.04	0.0569
ν	0.65	0.6399
b	4	3.8022
r	0.4	0.3247
d	0.00011	0.0001
θ	0.8	0.6374
ω	0.45	0.4689
ϵ	0.61	0.6277
δ	0.31	0.2551
γ	0.59	0.6145

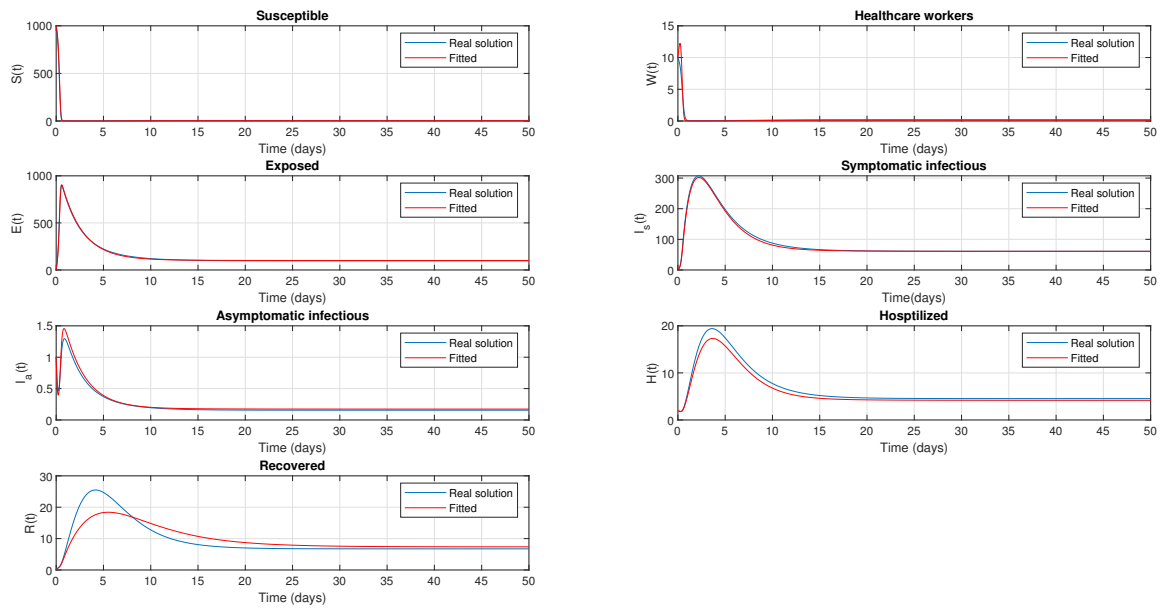


Figure 38: Model fitting

4.3 Discussion

The dynamic transmission of COVID-19 between healthcare workers and the community using a deterministic model named $SWEI_s I_a HR$ was investigated. The parameter ξ and θ quantified the protection level to both healthcare workers and the community when exposed to the disease. Figures 25-28 depicted that physical distancing θ has a greater significance in reducing the spread of COVID-19 within human population. Also, the use of PPE ξ revealed good impact in protecting healthcare workers against the disease, this can be observed in Fig. 33. Since healthcare workers have frequent interaction with patients, its transmission probability is assumed to be higher. The numerical solutions obtained validated analytical results. The stability of model (3.1) numerically is presented in Fig. 17 and Figs. 18-24. The positive association between a parameter and R_0 is shown in Figs. 5-13. These parameters have a great impact on expanding the disease in the public whenever their values are increased. The negative correlation is indicated by Figs. 14-16. These parameters minimize the burden of COVID-19 in the community whenever their values are increased. Further, we assessed the impact of R_0 on some parameters, where we found that in the absence of personal protective equipment ξ and physical distancing in the community θ , the value of R_0 was 6.7125 which leads to an increase in the average number of secondary infection in the community. When θ and ξ were introduced in the model, the basic reproduction number is reduced to 0.6713, indicating the minimization of the endemicity of the disease in the community. The identifiability of model parameters was done using the classical least square method. Generally, the numerical results demonstrated that protection of the public health staff can be achieved through the effective use of personal protective equipment by health care workers and minimization of the spread in the community.

4.4 Summary

In a nutshell, numerical simulation was performed and the results were displayed graphically and discussed. Also, the stability of the model (3.1) is assessed numerically by varying the initial values of the compartments. The results demonstrated the stability of the model. Further, the impact of few parameters such as ξ , θ , ω , η , δ are analyzed. The results evinced that the two parameters ξ and θ played a significant role in curtailing the disease.

CHAPTER FIVE

CONCLUSION AND RECOMMENDATIONS

5.1 Conclusion

In this current work, a deterministic model for the transmission dynamics of COVID-19 between healthcare workers and the community that includes the protective measures with waning immunity is derived and analyzed.

Several assumptions have been considered in the model formulation in order to make the model realistic and biologically meaningful. The main objective of this study was to develop and analyze a mathematical model for COVID-19 transmission dynamics between healthcare workers and the community. In order to achieve the general objective, four specific objectives were proposed: The first objective was to formulate a mathematical model for COVID-19 that includes protective measures. The second objective was to perform stability analyze of the model. The third objective was to study sensitivity analysis of the developed model using a normalized forward sensitivity index. The fourth objective was to carry out the numerical simulation of the model using a MATLAB solver ODE45 Runge-Kutta fourth-order scheme.

First, we proved that there exists a feasible region in which the model is epidemiological and mathematically well-posed. The existence and uniqueness of the solutions are presented using the Lipschitz condition. The basic reproduction number was computed by next-generation matrix approach (Van den Driessche and Watmough, 2002).

Secondly, the stability analysis for disease-free equilibrium is established by linearization method (Roussel, 2005), Hurwitz criterion (Kraus *et al.*, 2002) and Metzler matrix (Castillo-Chavez *et al.*, 2002) and comparison theorem (Diekmann *et al.*, 1990). The stability analysis proved that the model disease-free equilibrium point exists and it is locally and globally symptomatically stable whenever $R_0 < 1$. The stability of endemic equilibria is derived by explicit and logarithmic Lyapunov function (Korobeinikov, 2007) in combination with LaSalle's Invariance Principle (LaSalle, 1976). The model endemic equilibrium point exists and it is globally symptomatically stable only whenever $R_0 > 1$.

Furthermore, numerical simulations were investigated by using the fourth-order Runge-Kutta schemes (Yavuz *et al.*, 2021). On the other hand, parameters identifiability was presented by using the classical least square technique. The numerical results demonstrated that the disease-free and endemic equilibrium points were asymptotically stable as stipulated in Figs. 18-24. Sensitive parameters were identified through the sensitivity analysis method where the most positive sensitive parameter was α while θ influences the model negatively compared to other parameters. The graphs which demonstrate the positive and negative correlation of the parameter and R_0 are illustrated from Figs. 5- 16. Moreover, other remaining figures demonstrated the impact of protective

measures on both healthcare workers and the community.

Conclusively, our findings demonstrated mathematically that public health experts can be protected through effective use of protective measures.

5.2 Recommendations

COVID-19 is a novel coronavirus that can spread rapidly globally in absence of control measures. This study presented the importance of protective measures in curtailing SARS-COV-2. In accordance to the findings of this study, we give the following recommendations:

- (i) Governments should provide adequate personal protective equipment (PPE) to healthcare workers for the sake of protecting and maintaining the health workforce.
- (ii) The general community should voluntarily adhere to the control strategies outlined by the government so as to reduce the spread of COVID-19.
- (iii) Healthcare workers who have not been using the protective measures when working should do so.

5.2.1 Limitation of the Study

The present study is not ultimate in science, there must be some limitations and assumptions which are deviated from actual reality. There were some limitations to this study that must be considered such as:

- (i) Since accessibility of data is challenging, this model did not integrate the data relating to the rate at which people comply with physical distancing and personal protective measures.
- (ii) Disregarding differentiation of individual susceptibility and we assumed that infection vulnerability for the whole population in the native environment was uniform while in real situations older people likely to be attacked by the virus than young people.
- (iii) This compartmental model does not allow us to track the people's performance on the effectiveness of wearing masks maintained of physical distancing and many other control measures.
- (iv) We neglected the effect of unequal population size and assumed that the total population was uniformly distributed.

5.2.2 Future Work

Through reviewing the literature, we have investigated that our study can be improved by carefully incorporating additional information that may influence more understanding of the spread of

COVID-19. This study can be modified for sake of capturing different transmission dynamics of COVID-19. The following are suggestions on the recent study to be conducted in the near future:

- (i) Developing a mathematical model for COVID-19 to assess the impact of vaccines in curtailing the disease.
- (ii) Developing a mathematical model for COVID-19 to assess the impact of environmental factors such as humidity, rainfall, the temperature on the spread of the disease.
- (iii) The study should be extended to a stochastic model which may describe the temporal-spatial evolution of COVID-19 and their control strategies.
- (iv) The study should consider optimal control which takes under consideration vaccination, protective measures, and treatment.
- (v) To include immigration so as to evaluate whether human mobility may enhance the persistence of COVID-19.
- (vi) The study should be modified to Caputo fractional derivatives model for the purpose of capturing more biological phenomena such as crossover behavior and fade memory (Naik *et al.*, 2020; Ali *et al.*, 2021).

REFERENCES

- Abioye, A. I., Peter, O. J., Ogunseye, H. A., Oguntolu, F. A., Oshinubi, K. I. A. A., & Khan, I. (2021). Mathematical model of covid-19 in nigeria with optimal control. *Results in Physics*, 28, 104598. <https://doi.org/10.1016/j.rinp.2021.104598>
- Abrams, S., Wambua, J., Santermans, E., Willem, L., Kuylén, E., Coletti, P., Libin, P., Faes, C., Petrof, O., & Herzog, S. A. (2021). Modelling the early phase of the Belgian COVID-19 epidemic using a stochastic compartmental model and studying its implied future trajectories. *Epidemics*, 35, 100449. <https://doi.org/10.1016/j.epidem.2021.100449>
- Adekola, H. A., Adekunle, I. A., Egberongbe, H. O., Onitilo, S. A., & Abdullahi, I. N. (2020). Mathematical modeling for infectious viral disease: The COVID-19 perspective. *Journal of Public Affairs*, 20(4), e2306. <https://doi.org/10.1002/pa.2306>
- Agaba, G. O. (2020). Modelling the Spread of COVID-19 with Impact of Awareness and Medical Assistance. *Mathematical Theory and Modeling*, 10(4), 21–28.
- Ahmad, W., Abbas, M., Rafiq, M., & Baleanu, D. (2021). Mathematical analysis for the effect of voluntary vaccination on the propagation of Corona virus pandemic. *Results in Physics*, 104917. <https://doi.org/10.1016/j.rinp.2021.104917>
- Aldila, D. (2020). Analyzing the impact of the media campaign and rapid testing for COVID-19 as an optimal control problem in East Java, Indonesia. *Chaos, Solitons & Fractals*, 141, 110364. <https://doi.org/10.1016/j.chaos.2020.110364>
- Aldila, D., Ndi, M. Z., & Samiadi, B. M. (2020). Optimal control on COVID-19 eradication program in Indonesia under the effect of community awareness. *Mathematical Bioscience & Engineering*, 17, 6355–6389. <https://doi.org/10.3934/mbe.2020335>
- Ali, Z., Rabiei, F., Shah, K., & Khodadadi, T. (2021). Qualitative analysis of fractal-fractional order COVID-19 mathematical model with case study of Wuhan. *Alexandria Engineering Journal*, 60(1), 477–489. <https://doi.org/10.1016/j.aej.2020.09.020>
- Antonio-Villa, N. E., Bello-Chavolla, O. Y., Vargas-Vázquez, A., Fermín-Martínez, C. A., Márquez-Salinas, A., Pisanty-Alatorre, J., & Bahena-López, J. P. (2021). Assessing the burden of coronavirus disease 2019 (COVID-19) among healthcare workers in Mexico City: a data-driven call to action. *Clinical Infectious Diseases*, 73(1), e191–e198. <https://doi.org/10.1093/cid/ciaa1487>
- Aquino, E. M. L., Silveira, I. H., Pescarini, J. M., Aquino, R., Souza-Filho, J. A. d., Rocha, A. d. S., Ferreira, A., Victor, A., Teixeira, C., & Machado, D. B. (2020). Social distancing measures to control the COVID-19 pandemic: potential impacts and challenges in Brazil. *Ciencia & Saude Coletiva*, 25, 2423–2446. <https://doi.org/5666>

- Asamoah, J. K. K., Bornaa, C. S., Seidu, B., & Jin, Z. (2020). Mathematical analysis of the effects of controls on transmission dynamics of SARS-CoV-2. *Alexandria Engineering Journal*, 59(6), 5069–5078. <https://doi.org/10.1016/j.aej.2020.09.033>
- Atangana, E., & Atangana, A. (2020). Facemasks simple but powerful weapons to protect against COVID-19 spread: Can they have sides effects? *Results in Physics*, 103425. <https://doi.org/10.1016/j.rinp.2020.103425>
- Baba, I. A., Yusuf, A., Nisar, K. S., Abdel, A. H., & Nofal, T. A. (2021). Mathematical model to assess the imposition of lockdown during COVID-19 pandemic. *Results in Physics*, 20, 103716. <https://doi.org/10.1016/j.rinp.2020.103716>
- Babaei, A., Jafari, H., & Ahmadi, M. (2019). A fractional order HIV/AIDS model based on the effect of screening of unaware infectives. *Mathematical Methods in the Applied Sciences*, 42(7), 2334–2343. <https://doi.org/2>
- Bakar, N. A., & Rosbi, S. (2020). Effect of Coronavirus disease (COVID-19) to tourism industry. *International Journal of Advanced Engineering Research and Science*, 7(4), 189–193. <https://dx.doi.org/10.22161/ijaers.74.23>
- Balsa, C., Lopes, I., Guarda, T., & Rufino, J. (2021). Computational simulation of the COVID-19 epidemic with the SEIR stochastic model. *Computational and Mathematical Organization Theory*, 1–19. <https://doi.org/10.1007/s10588-021-09327-y>
- Bandyopadhyay, S., Baticulon, R. E., Kadhum, M., Alser, M., Ojuka, D. K., Badereddin, Y., Kamath, A., Parepalli, S. A., Brown, G., & Iharchane, S. (2020). Infection and mortality of healthcare workers worldwide from COVID-19: a systematic review. *British Medical Journal of Global Health*, 5(12), e003097. <http://dx.doi.org/10.1136/bmjgh-2020-003097>
- Bastos, S. B., & Cajueiro, D. O. (2020). Modeling and forecasting the early evolution of the Covid-19 pandemic in Brazil. *Scientific Reports*, 10(1), 1–10. <https://doi.org/10.1038/s41598-020-76257-1>
- Brauer, F., Castillo-Chavez, C., & Castillo-Chavez, C. (2012). *Mathematical Models in Population Biology and Epidemiology*, volume 2. Springer.
- Bubar, K. M., Reinholt, K., Kissler, S. M., Lipsitch, M., Cobey, S., Grad, Y. H., & Larremore, D. B. (2021). Model-informed COVID-19 vaccine prioritization strategies by age and serostatus. *Science*, 371(6532), 916–921. <https://doi.org/10.1126/science.abe6959>
- Buhat, C. A. H., Torres, M. C., Olave, Y. H., Gavina, M. K. A., Felix, E. F. O., Gamilla, G. B., Verano, K. V. B., Babierra, A. L., & Rabajante, J. F. (2021). A mathematical model of COVID-19 transmission between frontliners and the general public. *Network Modeling*

- Analysis in Health Informatics and Bioinformatics*, 10(1), 1–12. <https://doi.org/10.1007/s13721-021-00295-6>
- Castillo-Chavez, C., Feng, Z., & Huang, W. (2002). Mathematical on the computation of basic reproduction number and its role in global stability. *The Indian Military Academy Volumes in Mathematics and Its Applications*, 125, 229–250.
- Channapathi, T., & Thatikonda, S. (2020). Stochastic transmission dynamic model for evaluating effectiveness of control measures of COVID-19. *Social Science Research Network*, 3559581. <http://dx.doi.org/10.2139/ssrn.3559581>
- Chatterjee, K., Chatterjee, K., Kumar, A., & Shankar, S. (2020). Healthcare impact of COVID-19 epidemic in India: A stochastic mathematical model. *Medical Journal Armed Forces India*, 76(2), 147–155. <https://doi.org/10.1016/j.mjafi.2020.03.022>
- Chersich, M. F., Gray, G., Fairlie, L., Eichbaum, Q., Mayhew, S., Allwood, B., English, R., Scorgie, F., Luchters, S., & Simpson, G. (2020). COVID-19 in Africa: care and protection for frontline healthcare workers. *Globalization and Health*, 16, 1–6. <https://doi.org/10.1186/s12992-020-00574-3>
- Coronavirus, W. H. O. (2020). URL <https://www.who.int/emergencies/diseases/novel-coronavirus-2019>. *Library Catalog: www.who.int*.
- Da Silveira, M. P., Da Silva, F. K. K., Bizuti, M. R., Starck, É., Rossi, R. C., & Da Silva, D. T. d. R. (2021). Physical exercise as a tool to help the immune system against COVID-19: an integrative review of the current literature. *Clinical and Experimental Medicine*, 21(1), 15–28. <https://doi.org/10.1007/s10238-020-00650-3>
- Danane, J., Allali, K., Hammouch, Z., & Nisar, K. S. (2021). Mathematical analysis and simulation of a stochastic COVID-19 Lévy jump model with isolation strategy. *Results in Physics*, 23, 103994. <https://doi.org/10.1016/j.rinp.2021.103994>
- Deressa, C. T., & Duressa, G. F. (2021). Modeling and optimal control analysis of transmission dynamics of COVID-19: The case of Ethiopia. *Alexandria Engineering Journal*, 60(1), 719–732. <https://doi.org/10.1016/j.aej.2020.10.004>
- Diekmann, O., Heesterbeek, J. A. P., & Metz, J. A. J. (1990). On the definition and the computation of the basic reproduction ratio in models for infectious diseases in heterogeneous populations. *Journal of Mathematical Biology*, 28(4), 365–382. <https://doi.org/10.1007/BF00178324>
- Dietz, K. (1993). The estimation of the basic reproduction number for infectious diseases. *Statistical Methods in Medical Research*, 2(1), 23–41. <https://doi.org/10.1177/096228029300200103>

- Djaoue, S., Kolaye, G. G., Abboubakar, H., Ari, A. A. A., & Damakoa, I. (2020). Mathematical modeling, analysis and numerical simulation of the COVID-19 transmission with mitigation of control strategies used in Cameroon. *Chaos, Solitons & Fractals*, 139, 110281. <https://doi.org/10.1016/j.chaos.2020.110281>
- Dwomoh, D., Iddi, S., Adu, B., Aheto, J. M., Sedzro, K. M., Fobil, J., & Bosomprah, S. (2021). Mathematical modeling of COVID-19 infection dynamics in Ghana: impact evaluation of integrated government and individual level interventions. *Infectious Disease Modelling*, 6, 381–397. <https://doi.org/10.1016/j.idm.2021.01.008>
- Dy, L. F., & Rabajante, J. F. (2020). A COVID-19 infection risk model for frontline health care workers. *Network Modeling Analysis in Health Informatics and Bioinformatics*, 9(1), 1–13. <https://doi.org/10.1007/s13721-020-00258-3>
- Faranda, D., & Alberti, T. (2020). Modeling the second wave of COVID-19 infections in France and Italy via a stochastic SEIR model. *Chaos: An Interdisciplinary Journal of Nonlinear Science*, 30(11), 111101. <https://doi.org/10.1063/5.0015943>
- Fauci, A. S., Touchette, N. A., & Folkers, G. K. (2005). Emerging infectious diseases: a 10-year perspective from the National Institute of Allergy and Infectious Diseases. *International Journal of Risk & Safety in Medicine*, 17(3–4), 157–167.
- Ford, H. (2020). Coronavirus Disease 2019. *Health System*, 19, 100740.
- Garba, S. M., Lubuma, J. M. S., & Tsanou, B. (2020). Modeling the transmission dynamics of the COVID-19 Pandemic in South Africa. *Mathematical Biosciences*, 328, 108441. <https://doi.org/10.1016/j.mbs.2020.108441>
- Gathungu, D. K., Ojiambo, V. N., Kimathi, M. E. M., & Mwalili, S. M. (2020). Modeling the Effects of Nonpharmaceutical Interventions on COVID-19 Spread in Kenya. *Interdisciplinary Perspectives on Infectious Diseases*, 2020. <https://doi.org/10.1155/2020/6231461>
- Ghosh, I., & Martcheva, M. (2021). Modeling the effects of prosocial awareness on COVID-19 dynamics: Case studies on Colombia and India. *Nonlinear Dynamics*, 1–20. <https://doi.org/10.1007/s11071-021-06489-x>
- Girona, T. (2020). Confinement time required to avoid a quick rebound of Covid-19: Predictions from a Monte Carlo stochastic model. *Frontiers in Physics*, 8, 186. <https://doi.org/10.3389/fphy.2020.00186>
- Gostic, K., Gomez, A. C. R., Mummah, R. O., Kucharski, A. J., & Lloyd-Smith, J. O. (2020). Estimated effectiveness of symptom and risk screening to prevent the spread of COVID-19. *Elife*, 9, e55570. <https://doi.org/10.7554/eLife.55570>
- Gozalpour, N., Badfar, E., & Nikoofard, A. (2021). Transmission dynamics of novel coronavirus

- SARS-CoV-2 among healthcare workers, a case study in Iran. *Nonlinear Dynamics*, 1–13. <https://doi.org/10.1007/s11071-021-06778-5>
- Harapan, H., Itoh, N., Yufika, A., Winardi, W., Keam, S., Te, H., Megawati, D., Hayati, Z., Wagner, A. L., & Mudatsir, M. (2020). Coronavirus disease 2019 (COVID-19): A literature review. *Journal of Infection and Public Health*, 13(5), 667–673. <https://doi.org/10.1016/j.jiph.2020.03.019>
- He, S., Peng, Y., & Sun, K. (2020). SEIR modeling of the COVID-19 and its dynamics. *Nonlinear Dynamics*, 101(3), 1667–1680. <https://doi.org/10.1007/s11071-020-05743-y>
- Heinzerling, A., Stuckey, M. J., Scheuer, T., Xu, K., Perkins, K. M., Resseger, H., Magill, S., Verani, J. R., Jain, S., & Acosta, M. (2020). Transmission of COVID-19 to health care personnel during exposures to a hospitalized patient—Solano County, California, February 2020. *Morbidity and Mortality Weekly Report*, 69(15), 472. <https://doi.org/doi:10.15585/mmwr.mm6915e5>
- Hellewell, J., Abbott, S., Gimma, A., Bosse, N. I., Jarvis, C. I., Russell, T. W., Munday, J. D., Kucharski, A. J., Edmunds, W. J., & Sun, F. (2020). Feasibility of controlling COVID-19 outbreaks by isolation of cases and contacts. *The Lancet Global Health*, 8(4), e488–e496. [https://doi.org/10.1016/S2214-109X\(20\)30074-7](https://doi.org/10.1016/S2214-109X(20)30074-7)
- Herron, J. B. T., Hay-David, A. G. C., Gilliam, A. D., & Brennan, P. A. (2020). Personal protective equipment and Covid 19-a risk to healthcare staff? *The British journal of Oral & Maxillofacial Surgery*, 58(5), 500. <https://doi.org/10.1016/j.bjoms.2020.04.015>
- Hethcote, H. W. (2000). The mathematics of infectious diseases. *Society of Indian Automobile Manufacturers Review*, 42(4), 599–653. <https://doi.org/10.1137/S0036144500371907>
- Hui, D. S., Zumla, A., & Tang, J. W. (2021). Lethal zoonotic coronavirus infections of humans—comparative phylogenetics, epidemiology, transmission, and clinical features of coronavirus disease 2019, the Middle East respiratory syndrome and severe acute respiratory syndrome. *Current Opinion in Pulmonary Medicine*, 27(3), 146–154. <https://doi.org/doi:10.1097/MCP.0000000000000774>
- Hussain, S., Zeb, A., Rasheed, A., & Saeed, T. (2020). Stochastic mathematical model for the spread and control of Corona virus. *Advances in Difference Equations*, 2020(1), 1–11. <https://doi.org/10.1186/s13662-020-03029-6>
- Imai, N., Gaythorpe, K. A. M., Abbott, S., Bhatia, S., van, E. S., Prem, K., Liu, Y., & Ferguson, N. M. (2020). Adoption and impact of non-pharmaceutical interventions for COVID-19. *Wellcome Open Research*, 5. <https://doi.org/10.12688/wellcomeopenres.15808.1>
- Ivorra, B., Ferrández, M. R., Vela-Pérez, M., & Ramos, A. M. (2020). Mathematical model-

- ing of the spread of the coronavirus disease 2019 (COVID-19) taking into account the undetected infections. The case of China. *Communications in Nonlinear Science and Numerical Simulation*, 88, 105303. <https://doi.org/10.1016/j.cnsns.2020.105303>
- Kim, R., Nachman, S., Fernandes, R., Meyers, K., Taylor, M., LeBlanc, D., & Singer, A. J. (2020). Comparison of COVID-19 infections among healthcare workers and non-healthcare workers. *PLoS One*, 15(12), e0241956. <https://doi.org/10.1371/journal.pone.0241956>
- Koh, D., Lim, M. K., Chia, S. E., Ko, S. M., Qian, F., Ng, V., Tan, B. H., Wong, K. S., Chew, W. M., & Tang, H. K. (2005). Risk perception and impact of severe acute respiratory syndrome (SARS) on work and personal lives of healthcare Workers in Singapore What can we Learn? *Medical Care*, 676–682. <http://www.jstor.com/stable/3768367>
- Korobeinikov, A. (2007). Global properties of infectious disease models with nonlinear incidence. *Bulletin of Mathematical Biology*, 69(6), 1871–1886. <https://doi.org/10.1007/s11538-007-9196-y>
- Korobeinikov, A., & Wake, G. C. (2002). Lyapunov functions and global stability for SIR, SIRS, and SIS epidemiological models. *Applied Mathematics Letters*, 15(8), 955–960. [https://doi.org/10.1016/S0893-9659\(02\)00069-1](https://doi.org/10.1016/S0893-9659(02)00069-1)
- Kraus, W. E., Houmard, J. A., Duscha, B. D., Knetzger, K. J., Wharton, M. B., McCartney, J. S., Bales, C. W., Henes, S., Samsa, G. P., & Otvos, J. D. (2002). Effects of the amount and intensity of exercise on plasma lipoproteins. *New England Journal of Medicine*, 347(19), 1483–1492. <https://doi.org/10.1056/NEJMoa020194>
- Kucharski, A. J., Klepac, P., Conlan, A. J. K., Kissler, S. M., Tang, M. L., Fry, H., Gog, J. R., Edmunds, W. J., Emery, J. C. A., & Medley, G. (2020). Effectiveness of isolation, testing, contact tracing, and physical distancing on reducing transmission of SARS-CoV-2 in different settings: a mathematical modelling study. *The Lancet Infectious Diseases*, 20(10), 1151–1160. [https://doi.org/10.1016/S1473-3099\(20\)30457-6](https://doi.org/10.1016/S1473-3099(20)30457-6)
- Kumar, P., Erturk, V. S., & Murillo-Arcila, M. (2021). A new fractional mathematical modelling of COVID-19 with the availability of vaccine. *Results in Physics*, 24, 104213. <https://doi.org/10.1016/j.rinp.2021.104213>
- Kursumovic, E., Lennane, S., & Cook, T. M. (2020). Deaths in healthcare workers due to COVID-19: The need for robust data and analysis. *Anaesthesia*. <https://doi.org/doi:10.1111/anae.15116>
- LaSalle, J. P. (1976). Stability theory and invariance principles. In *Dynamical Systems* (pp. 211–222). Elsevier.
- Lin, Q., Zhao, S., Gao, D., Lou, Y., Yang, S., Musa, S. S., Wang, M. H., Cai, Y., Wang, W., & Yang,

- L. (2020). A conceptual model for the coronavirus disease 2019 (COVID-19) outbreak in Wuhan, China with individual reaction and governmental action. *International Journal of Infectious Diseases*, 93, 211–216. <https://doi.org/10.1016/j.ijid.2020.02.058>
- Lopman, B., Liu, C. Y., Le Guillou, A., Handel, A., Lash, T. L., Isakov, A. P., & Jenness, S. M. (2021). A modeling study to inform screening and testing interventions for the control of SARS-CoV-2 on university campuses. *Scientific Reports*, 11(1), 1–11. <https://doi.org/10.1038/s41598-021-85252-z>
- Mahikul, W., Chotsiri, P., Ploddi, K., & Pan-Ngum, W. (2021). Evaluating the Impact of Intervention Strategies on the First Wave and Predicting the Second Wave of COVID-19 in Thailand: A Mathematical Modeling Study. *Biology*, 10(2), 80. <https://doi.org/10.3390/biology10020080>
- Mahmoudi, M. R., Heydari, M. H., Qasem, S. N., Mosavi, A., & Band, S. S. (2021). Principal component analysis to study the relations between the spread rates of COVID-19 in high risks countries. *Alexandria Engineering Journal*, 60(1), 457–464. <https://doi.org/10.1016/j.aej.2020.09>
- Marino, S., Hogue, I. B., Ray, C. J., & Denise, K. E. (2008). A methodology for performing global uncertainty and sensitivity analysis in systems biology. *Journal of Theoretical Biology*, 254(1), 178–196. <https://doi.org/10.1016/j.jtbi.2008.04.011>
- Mbogo, R. W., & Odhiambo, J. W. (2020). COVID-19 outbreak, social distancing and mass testing in Kenya-insights from a mathematical model. *Afrika Matematika*, 1–16.
- Mbogo, R. W., & Odhiambo, J. W. (2021). COVID-19 outbreak, social distancing and mass testing in Kenya-insights from a mathematical model. *Afrika Matematika*, 1–16. <https://doi.org/10.1007/s13370-020-00859-1>
- McCluskey, C. (2021). Lyapunov functions for disease models with immigration of infected hosts. *Discrete & Continuous Dynamical Systems*, 26(8), 4479. <https://doi.org/doi:10.3934/dcdsb.2020296>
- Mishal, A., Saravanan, R., Atchitha, S. S., Santhiya, K., Rithika, M., Menaka, S. S., & Thiruvalluvan, T. (2020). A Review of Corona Virus Disease-2019. *History*, 4(7). <https://dx.doi.org/10.18535/jmscr/v8i7.59>
- Mpeshe, S. C., Haario, H., & Tchuenche, J. M. (2011). A mathematical model of Rift Valley fever with human host. *Acta Biotheoretica*, 59(3), 231–250. <https://doi.org/10.1007/s10441-011-9132-2>
- Mugisha, J. Y. T., Ssebuliba, J., Nakakawa, J. N., Kikawa, C. R., & Ssematimba, A. (2021). Mathematical modeling of COVID-19 transmission dynamics in Uganda: Implications of

- complacency and early easing of lockdown. *PloS One*, 16(2), e0247456. <https://doi.org/10.1371/journal.pone.0247456>
- Mumbu, A. R. J., & Hugo, A. K. (2020). Mathematical modelling on COVID-19 transmission impacts with preventive measures: a case study of Tanzania. *Journal of Biological Dynamics*, 14(1), 748–766. <https://doi.org/10.1080/17513758.2020.1823494>
- Naik, P. A., Yavuz, M., Qureshi, S., Zu, J., & Townley, S. (2020). Modeling and analysis of COVID-19 epidemics with treatment in fractional derivatives using real data from Pakistan. *The European Physical Journal Plus*, 135(10), 1–42. <https://doi.org/10.1140/epjp/s13360-020-00819-5>
- Oka, T., Wei, W., & Zhu, D. (2021). The effect of human mobility restrictions on the COVID-19 transmission network in China. *PloS One*, 16(7), e0254403. <https://doi.org/https://doi.org/10.1371/journal.pone.0254403>
- Olivares, A., & Staffetti, E. (2021). Uncertainty Quantification of a Mathematical Model of COVID-19 Transmission Dynamics with Mass Vaccination Strategy. *Chaos, Solitons & Fractals*, 110895. <https://doi.org/https://doi.org/10.1016/j.chaos.2021.110895>
- Omar, O. A. M., Alnafisah, Y., Elbarkouky, R. A., & Ahmed, H. M. (2021). COVID-19 deterministic and stochastic modelling with optimized daily vaccinations in Saudi Arabia. *Results in Physics*, 28, 104629. <https://doi.org/10.1016/j.rinp.2021.104629>
- Oud, M. A. A., Ali, A., Alrabaiah, H., Ullah, S., Khan, M. A., & Islam, S. (2021). A fractional order mathematical model for COVID-19 dynamics with quarantine, isolation, and environmental viral load. *Advances in Difference Equations*, 2021(1), 1–19. <https://doi.org/10.1186/s13662-021-03265-4>
- Park, S. H. (2020). Personal protective equipment for healthcare workers during the COVID-19 pandemic. *Infection & Chemotherapy*, 52(2), 165. <https://doi.org/doi:10.3947/ic.2020.52.2.165>
- Parolini, N., Dede, L., Antonietti, P. F., Ardenghi, G., Manzoni, A., Miglio, E., Pugliese, A., Verani, M., & Quarteroni, A. (2021). SUIHTER: A new mathematical model for COVID-19. Application to the analysis of the second epidemic outbreak in Italy. *Proceedings of the Royal Society*, 477(2253), 20210027. <https://doi.org/10.1098/rspa.2021.0027>
- Patil, A. (2021). Routh-Hurwitz Criterion for Stability: An Overview and Its Implementation on Characteristic Equation Vectors Using MATLAB. *Emerging Technologies in Data Mining and Information Security*, 319–329. https://doi.org/10.1007/978-981-15-9927-9_32
- Peiris, J. S. M., Lai, S. T., Poon, L. L. M., Guan, Y., Yam, L. Y. C., Lim, W., Nicholls, J., Yee, W. K. S., Yan, W. W., & Cheung, M. T. (2003). Coronavirus as a possible cause of severe

- acute respiratory syndrome. *The Lancet*, 361(9366), 1319–1325. [https://doi.org/10.1016/S0140-6736\(03\)13077-2](https://doi.org/10.1016/S0140-6736(03)13077-2)
- Peter, O. J., Qureshi, S., Yusuf, A., Al-Shomrani, M., & Idowu, A. A. (2021). A New Mathematical Model of COVID-19 Using Real Data from Pakistan. *Results in Physics*, 104098. <https://doi.org/10.1016/j.rinp.2021.104098>
- Poukka, E., Baum, U., Palmu, A. A., Lehtonen, T. O., Salo, H., Nohynek, H., & Leino, T. (2022). Cohort study of Covid-19 vaccine effectiveness among healthcare workers in Finland, December 2020–October 2021. *Vaccine*, 40(5), 701–705. <https://doi.org/10.1016/j.vaccine.2021.12>
- Redhwan, S. S., Abdo, M. S., Shah, K., Abdeljawad, T., Dawood, S., Abdo, H. A., & Shaikh, S. L. (2020). Mathematical modeling for the outbreak of the coronavirus (COVID-19) under fractional nonlocal operator. *Results in Physics*, 19, 103610. <https://doi.org/10.1016/j.rinp.2020.103610>
- Riyapan, P., Shuaib, S. E., & Intarasit, A. (2021). A Mathematical Model of COVID-19 Pandemic: A Case Study of Bangkok, Thailand. *Computational and Mathematical Methods in Medicine*, 2021. <https://doi.org/10.1155/2021/6664483>
- Roussel, M. R. (2005). Stability analysis for ODEs. *Nonlinear Dynamics, lecture notes, University Hall, Canada*.
- Sánchez-Taltavull, D., Castelo-Szekely, V., Candinas, D., Roldán, E., & Beldi, G. (2021). Modelling strategies to organize healthcare workforce during pandemics: application to COVID-19. *Journal of Theoretical Biology*, 523, 110718. <https://doi.org/10.1101/2020.03.29.20047035>
- Scherer, A., & McLean, A. (2002). Mathematical models of vaccination. *British Medical Bulletin*, 62(1), 187–199. <https://doi.org/10.1093/bmb/62.1.187>
- Shahzad, M., Abdel, A. H., Attia, R. A. M., Khoshnaw, S. H. A., Aldila, D., Ali, M., & Sultan, F. (2021). Dynamics models for identifying the key transmission parameters of the COVID-19 disease. *Alexandria Engineering Journal*, 60(1), 757–765. <https://doi.org/10.1093/bmb/62.1.187>
- Shayak, B., Sharma, M. M., Rand, R. H., Singh, A. K., & Misra, A. (2020). Transmission dynamics of COVID-19 and impact on public health policy. *MedRxiv*. <https://doi.org/10.1101/2020.03.29>
- Singh, H., Srivastava, H. M., Hammouch, Z., & Nisar, K. S. (2021). Numerical simulation and stability analysis for the fractional-order dynamics of COVID-19. *Results in Physics*, 20, 103722. <https://doi.org/10.1016/j.rinp.2020.103722>

- Singh, N., Tang, Y., & Ogunseitan, O. A. (2020). Environmentally sustainable management of used personal protective equipment. *Environmental Science & Technology*, 54(14), 8500–8502. <https://doi.org/10.1021/acs.est.0c03022>
- Steardo, L., Steardo Jr, L., Zorec, R., & Verkhatsky, A. (2020). Neuroinfection may contribute to pathophysiology and clinical manifestations of COVID-19. *Acta Physiologica (Oxford, England)*. <https://doi.org/doi:10.1111/apha.13473>
- Tang, Y., & Wang, S. (2020). Mathematic modeling of COVID-19 in the United States. *Emerging Microbes & Infections*, 9(1), 827–829. <https://doi.org/10.1080/22221751.2020.1760146>
- Tatem, A. J., Rogers, D. J., & Hay, S. I. (2006). Global transport networks and infectious disease spread. *Advances in Parasitology*, 62, 293–343. [https://doi.org/10.1016/S0065-308X\(05\)62009-X](https://doi.org/10.1016/S0065-308X(05)62009-X)
- Titus, R. K., Cheruiyot, L. R., & Kipkurgat, C. P. (2020). Mathematical Modeling of Covid-19 Disease Dynamics and Analysis of Intervention Strategies. *Mathematical Modelling and Applications*, 5(3), 176. <https://doi.org/doi:10.11648/j.mma.20200503.16>
- Traoré, A., & Konané, F. V. (2020). Modeling the effects of contact tracing on COVID-19 transmission. *Advances in Difference Equations*, 2020(1), 1–12. <https://doi.org/10.1186/s13662-020-02972-8>
- Tsang, K. W., Ho, P. L., Ooi, G. C., Yee, W. K., Wang, T., Chan-Yeung, M., Lam, W. K., Seto, W. H., Yam, L. Y., & Cheung, T. M. (2003). A cluster of cases of severe acute respiratory syndrome in Hong Kong. *New England Journal of Medicine*, 348(20), 1977–1985. <https://doi.org/10.1056/NEJMoa030666>
- Tuite, A. R., Fisman, D. N., & Greer, A. L. (2020). Mathematical modelling of COVID-19 transmission and mitigation strategies in the population of Ontario, Canada. *Canadian Medical Association Journal*, 192(19), E497–E505. <https://doi.org/10.1503/cmj.200476>
- Ud Din, R., Seadawy, A. R., Shah, K., Ullah, A., & Baleanu, D. (2020). Study of global dynamics of COVID-19 via a new mathematical model. *Results in Physics*, 19, 103468. <https://doi.org/10.1016/j.rinp.2020.103468>
- Van den Driessche, P., & Watmough, J. (2002). Reproduction numbers and sub-threshold endemic equilibria for compartmental models of disease transmission. *Mathematical Biosciences*, 180(1-2), 29–48. <https://doi.org/10.1016/j.rinp.2020.103468>
- Wan, H., Cui, J. A., & Yang, G. J. (2020). Risk estimation and prediction of the transmission of coronavirus disease-2019 (COVID-19) in the mainland of China excluding Hubei province. *Infectious Diseases of Poverty*, 9(1), 1–9. <https://doi.org/10.1186/s40249-020-00683-6>

- Yavuz, M., Coşar, F. Ö., Günay, F., & Özdemir, F. N. (2021). A new mathematical modeling of the COVID-19 pandemic including the vaccination campaign. *Open Journal of Modelling and Simulation*, 9(3), 299–321. <https://doi.org/10.4236/ojmsi.2021.93020>
- Yu, C. J., Wang, Z. X., Xu, Y., Hu, M. X., Chen, K., & Qin, G. (2021). Assessment of basic reproductive number for COVID-19 at global level: A meta-analysis. *Medicine*, 100(18). <https://doi.org/doi:10.1097/MD.00000000000025837>
- Zaki, A. M., Van Boheemen, S., Bestebroer, T. M., Osterhaus, A. D. M. E., & Fouchier, R. A. M. (2012). Isolation of a novel coronavirus from a man with pneumonia in Saudi Arabia. *New England Journal of Medicine*, 367(19), 1814–1820. <https://doi.org/doi:10.1056/NEJMoa1211721>
- Zamir, M., Nadeem, F., Abdeljawad, T., & Hammouch, Z. (2021). Threshold condition and non pharmaceutical interventions's control strategies for elimination of COVID-19. *Results in Physics*, 20, 103698. <https://doi.org/10.1016/j.rinp.2020.103698>
- Zhang, Z., Gul, R., & Zeb, A. (2021). Global sensitivity analysis of COVID-19 mathematical model. *Alexandria Engineering Journal*, 60(1), 565–572. <https://doi.org/10.1016/j.aej.2020.09.035>
- Zhao, Z., Li, X., Liu, F., Zhu, G., Ma, C., & Wang, L. (2020). Prediction of the COVID-19 spread in African countries and implications for prevention and control: A case study in South Africa, Egypt, Algeria, Nigeria, Senegal and Kenya. *Science of the Total Environment*, 729, 138959. <https://doi.org/10.1016/j.scitotenv.2020.138959>

APPENDICES

MATLAB CODE

```
clear
clc

figure(1)
set(gca,'FontSize',12)
set(legend,'FontSize',12)
plot(t,y(:,1),'r','LineWidth',1.5);
xlabel('Time [days]');
ylabel('Susceptible population');
hold on
tspan =0:0.1:20; %Time in days ,
y0=[900,7,4,3,2];
[t,y]=ode45(@LemjiniM,tspan,y0);
```

```
figure(1)
set(gca,'FontSize',12)
set(legend,'FontSize',12)
plot(t,y(:,1),'y','LineWidth',1.5);
xlabel('Time [days]');
ylabel('Susceptible population');
hold on
tspan =0:0.1:20; %Time in days ,
y0=[800,7,4,3,2];
[t,y]=ode45(@LemjiniM,tspan,y0);
```

```
figure(1)
set(gca,'FontSize',12)
set(legend,'FontSize',12)
plot(t,y(:,1),'k','LineWidth',1.5);
xlabel('Time [days]');
ylabel('Susceptible population');
hold on
tspan =0:0.1:20; %Time in days ,
y0=[700,7,4,3,2];
[t,y]=ode45(@LemjiniM,tspan,y0);
```

```

figure(1)
set(gca,'FontSize',12)
set(legend,'FontSize',12)
plot(t,y(:,1),'m','LineWidth',1.5);
xlabel('Time [days]');
ylabel('Susceptible population');
hold on
tspan =0:0.1:20; %Time in days ,
y0=[600,7,4,3,2];
[t,y]=ode45(@LemjiniM,tspan,y0);

```

```

figure(1)
set(gca,'FontSize',12)
set(legend,'FontSize',12)
plot(t,y(:,1),'b','LineWidth',1.5);
xlabel('Time [days]');
ylabel('Susceptible population');
grid on
hold off
legend('S(0)=1000','S(0)=900','S(0)=800','S(0)=700','S(0)=600');
title('Human population Vs Time');

```

%%%

```

tspan =0:30:30; %Time in days ,
y0=[1000,300,40,30,50];
[t,y]=ode45(@LemjiniM,tspan,y0);

```

```

figure(2)
set(gca,'FontSize',12)
set(legend,'FontSize',12)
plot(t,y(:,2),'r','LineWidth',1.5);
xlabel('Time [days]');
ylabel('Exposed population');
hold on
tspan =0:30:30; %Time in days ,
y0=[900,250,30,20,40];

```

```
[t,y]=ode45(@LemjiniM,tspan,y0);

figure(2)
set(gca,'FontSize',12)
set(legend,'FontSize',12)
plot(t,y(:,2),'y','LineWidth',1.5);
xlabel('Time [days]');
ylabel('Exposed population');
hold on
tspan =0:30:30; %Time in days ,
y0=[800,200,30,20,30];
[t,y]=ode45(@LemjiniM,tspan,y0);
```

```
figure(2)
set(gca,'FontSize',12)
set(legend,'FontSize',12)
plot(t,y(:,2),'k','LineWidth',1.5);
xlabel('Time [days]');
ylabel('Exposed population');
hold on
tspan =0:30:30; %Time in days ,
y0=[700,150,24,10,10];
[t,y]=ode45(@LemjiniM,tspan,y0);
```

```
figure(2)
set(gca,'FontSize',12)
set(legend,'FontSize',12)
plot(t,y(:,2),'m','LineWidth',1.5);
xlabel('Time [days]');
ylabel('Exposed population');
hold on
tspan =0:30:30; %Time in days ,
y0=[600,100,14,10,10];
[t,y]=ode45(@LemjiniM,tspan,y0);
```

```
figure(2)
set(gca,'FontSize',12)
set(legend,'FontSize',12)
```

```

plot(t,y(:,2),'b','LineWidth',1.5);
xlabel('Time [days]');
ylabel('Exposed population');
grid on
hold off
legend('E(0)=300','E(0)=250','E(0)=200','E(0)=150','E(0)=100');
title('Human population Vs Time');

```

%%%

```

tspan =0:0.1:30; %Time in days ,
y0=[1000,7,40,0,0];
[t,y]=ode45(@LemjiniM,tspan,y0);

```

```

figure(3)
set(gca,'FontSize',12)
set(legend,'FontSize',12)
plot(t,y(:,3),'r','LineWidth',1.5);
xlabel('Time [days]');
ylabel('Infected population');
hold on
tspan =0:0.1:30; %Time in days ,
y0=[900,7,30,0,0];
[t,y]=ode45(@LemjiniM,tspan,y0);

```

```

figure(3)
set(gca,'FontSize',12)
set(legend,'FontSize',12)
plot(t,y(:,3),'y','LineWidth',1.5);
xlabel('Time [days]');
ylabel('Infected population');
hold on
tspan =0:0.1:30; %Time in days ,
y0=[800,7,20,0,0];
[t,y]=ode45(@LemjiniM,tspan,y0);

```

```

figure(3)
set(gca,'FontSize',12)

```

```

set(legend,'FontSize',12)
plot(t,y(:,3),'k','LineWidth',1.5);
xlabel('Time [days]');
ylabel('Infected population');
hold on
tspan =0:0.1:30; %Time in days ,
y0=[700,7,10,0,0];
[t,y]=ode45(@LemjiniM,tspan,y0);

```

```

figure(3)
set(gca,'FontSize',12)
set(legend,'FontSize',12)
plot(t,y(:,3),'m','LineWidth',1.5);
xlabel('Time [days]');
ylabel('Infected population');
hold on
tspan =0:0.1:30; %Time in days ,
y0=[600,7,5,0,0];
[t,y]=ode45(@LemjiniM,tspan,y0);

```

```

figure(3)
set(gca,'FontSize',12)
set(legend,'FontSize',12)
plot(t,y(:,3),'b','LineWidth',1.5);
xlabel('Time [days]');
ylabel('Infected population');
grid on
hold off
legend('I(0)=40','I(0)=30','I(0)=20','I(0)=10','I(0)=5');
title('Human population Vs Time');

```

%%%

```

tspan =0:50:50; %Time in days ,
y0=[1000,7,4,90,0];
[t,y]=ode45(@LemjiniM,tspan,y0);

```

```

figure(4)
set(gca,'FontSize',12)

```



```

set(legend,'FontSize',12)
plot(t,y(:,4),'r','LineWidth',1.5);
xlabel('Time [days]');
ylabel('Hospitalize population');
hold on
tspan =0:50:50; %Time in days ,
y0=[900,7,4,80,0];
[t,y]=ode45(@LemjiniM,tspan,y0);

```

```

figure(4)
set(gca,'FontSize',12)
set(legend,'FontSize',12)
plot(t,y(:,4),'y','LineWidth',1.5);
xlabel('Time [days]');
ylabel('Hospitalize population');
hold on
tspan =0:50:50; %Time in days ,
y0=[800,7,4,70,0];
[t,y]=ode45(@LemjiniM,tspan,y0);

```

```

figure(4)
set(gca,'FontSize',12)
set(legend,'FontSize',12)
plot(t,y(:,4),'k','LineWidth',1.5);
xlabel('Time [days]');
ylabel('Hospitalize population');
hold on
tspan =0:50:50; %Time in days ,
y0=[700,7,4,60,0];
[t,y]=ode45(@LemjiniM,tspan,y0);

```

```

figure(4)
set(gca,'FontSize',12)
set(legend,'FontSize',12)
plot(t,y(:,4),'m','LineWidth',1.5);
xlabel('Time [days]');
ylabel('Hospitalize population');
hold on

```

```

tspan =0:50:50; %Time in days ,
y0=[600,7,4,50,0];
[t,y]=ode45(@LemjiniM,tspan,y0);

```

```

figure(4)
set(gca,'FontSize',12)
set(legend,'FontSize',12)
plot(t,y(:,4),'b','LineWidth',1.5);
xlabel('Time [days]');
ylabel('Hospitalize population');
grid on
hold off
legend('H(0)=90','H(0)=80','H(0)=70','H(0)=60','H(0)=50');
title('Human population Vs Time');

```

%%%

```

tspan =0:100:100; %Time in days ,
y0=[1000,7,4,0,500];
[t,y]=ode45(@LemjiniM,tspan,y0);

```

```

figure(5)
set(gca,'FontSize',12)
set(legend,'FontSize',12)
plot(t,y(:,5),'r','LineWidth',1.5);
xlabel('Time[days]');
ylabel('Recovered Populations');
hold on
tspan =0:100:100; %Time in days ,
y0=[900,7,4,0,400];
[t,y]=ode45(@LemjiniM,tspan,y0);

```

```

figure(5)
set(gca,'FontSize',12)
set(legend,'FontSize',12)
plot(t,y(:,5),'y','LineWidth',1.5);
xlabel('Time[days]');
ylabel('Recovered Populations');
hold on

```

```

tspan =0:100:100; %Time in days ,
y0=[800,7,4,0,300];
[t,y]=ode45(@LemjiniM,tspan,y0);

```

```

figure(5)
set(gca,'FontSize',12)
set(legend,'FontSize',12)
plot(t,y(:,5),'k','LineWidth',1.5);
xlabel('Time[ days ]');
ylabel('Recovered Populations');
hold on
tspan =0:100:100; %Time in days ,
y0=[700,7,4,0,200];
[t,y]=ode45(@LemjiniM,tspan,y0);

```

```

figure(5)
set(gca,'FontSize',12)
set(legend,'FontSize',12)
plot(t,y(:,5),'m','LineWidth',1.5);
xlabel('Time[ days ]');
ylabel('Recovered Populations');
hold on
tspan =0:100:100; %Time in days ,
y0=[600,7,4,0,100];
[t,y]=ode45(@LemjiniM,tspan,y0);

```

```

figure(5)
set(gca,'FontSize',12)
set(legend,'FontSize',12)
plot(t,y(:,5),'b','LineWidth',1.5);
xlabel('Time[ days ]');
ylabel('Recovered Populations');
grid on
hold off
legend('R(0)=1000','R(0)=900','R(0)=800','R(0)=700','R(0)=600');
% title('Human Population Vs Time');

```

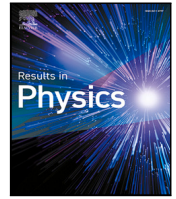
RESEARCH OUTPUT

(a) Publication

- (i) Masandawa, L., Mirau, S. S., & Mbalawata, I. S. (2021). Mathematical modeling of COVID-19 transmission dynamics between healthcare workers and community. *Results in Physics*, 29, 104731. <https://doi.org/10.1016/j.rinp.2021.104731>
- (ii) Masandawa, L., Mirau, S. S., Mbalawata, I. S., Paul, J. N., Kreppel, K., & Msamba, O. M. (2022). Modeling nosocomial infection of COVID-19 transmission dynamics. *Results in Physics*, 37, 105503. <https://doi.org/10.1016/j.rinp.2022.105503>

(b) Poster Presentation

- Mathematical modeling of COVID-19 transmission dynamics between healthcare workers and community.



Mathematical modeling of COVID-19 transmission dynamics between healthcare workers and community

Lemjini Masandawa^{a,*}, Silas Steven Mirau^a, Isambi Sailon Mbalawata^b

^a School of Computational and Communication Science and Engineering, The Nelson Mandela African Institution of Science and Technology, P.O. Box 447, Arusha, Tanzania

^b African Institute for Mathematical Sciences, NEI Global Secretariat, Rue KG590 ST, Kigali, Rwanda

ARTICLE INFO

Keywords:

COVID-19 model
Public control measures
Protective equipment
Parameter estimation
Basic reproduction number

ABSTRACT

Corona-virus disease 2019 (COVID-19) is an infectious disease that has affected different groups of humankind such as farmers, soldiers, drivers, educators, students, healthcare workers and many others. The transmission rate of the disease varies from one group to another depending on the contact rate. Healthcare workers are at a high risk of contracting the disease due to the high contact rate with patients. So far, there exists no mathematical model which combines both public control measures (as a parameter) and healthcare workers (as an independent compartment). Combining these two in a given mathematical model is very important because healthcare workers are protected through effective use of personal protective equipment, and control measures help to minimize the spread of COVID-19 in the community. This paper presents a mathematical model named SWE I_s, I_a, HR ; susceptible individuals (S), healthcare workers (W), exposed (E), symptomatic infectious (I_s), asymptomatic infectious (I_a), hospitalized (H), recovered (R). The value of basic reproduction number R_0 for all parameters in this study is 2.8540. In the absence of personal protective equipment ξ and control measure in the public θ , the value of $R_0 \approx 4.6047$ which implies the presence of the disease. When θ and ξ were introduced in the model, basic reproduction number is reduced to 0.4606, indicating the absence of disease in the community. Numerical solutions are simulated by using Runge–Kutta fourth-order method. Sensitivity analysis is performed to presents the most significant parameter. Furthermore, identifiability of model parameters is done using the least square method. The results indicated that protection of healthcare workers can be achieved through effective use of personal protective equipment by healthcare workers and minimization of transmission of COVID-19 in the general public by the implementation of control measures. Generally, this paper emphasizes the importance of using protective measures.

Introduction

Corona-virus disease 2019 (COVID-19) is an infectious disease that emerged in December 2019 in China caused by a new strain of virus called severe acute respiratory syndrome coronavirus 2 (SARS COV-2) [1–4]. The first case of coronavirus disease originates from the Huanan seafood wholesale market where the live animals are being sold [5]. Coronavirus is classified among the family of coronaviridae, the order of Nidovirale, and the subfamily of Coronavirinae [6]. Alpha-coronavirus, Beta-coronavirus, Delta-coronavirus and Gamma-coronavirus are the four types of coronaviruses that belong to the subfamily orthocoronavirinae [6,7]. Few research findings presented that origin of alpha and beta-coronavirus is from bats and rodents while avian species are the generative sources of gamma and delta-coronavirus [8].

COVID-19 can be spread from one individual to another through inhaling respiratory droplets released from the nose or mouth of an infectious individual when talking, sneezing, or coughing [9]. Also, an individual can acquire this virus through fomite transmission [10]. Older people aged 65 and above are more likely to be hospitalized or die from this disease. There is also a high severity of the disease to the group of people with underlying medical conditions such as hypertension, diabetes, cardiovascular, chronic respiratory disease and cancer [9]. Common clinical symptoms of the disease include tiredness, dry cough and fever [11] while serious symptoms include blood pressure, loss of movement or speech, chest pain and difficulty in breathing.

The basic reproduction number R_0 is the term used in mathematics to indicates how contagious an infectious disease is. It also known

* Corresponding author.

E-mail address: masandawal@nm-aist.ac.tz (L. Masandawa).

<https://doi.org/10.1016/j.rinp.2021.104731>

Received 17 July 2021; Received in revised form 18 August 2021; Accepted 19 August 2021

Available online 6 September 2021

2211-3797/© 2021 The Authors.

Published by Elsevier B.V. This is an open access article under the CC BY-NC-ND license

(<http://creativecommons.org/licenses/by-nc-nd/4.0/>).

as the estimated number of cases. R_0 indicates how many people on average one infected individual can infect in the entire period. If $R_0 > 1$ the disease will persist in the community and when $R_0 < 1$ the disease will die away. The value of R_0 for COVID-19 varies from one region to another for instance, one study conducted for all European countries revealed that the value of R_0 was in a range of 4.22 ± 1.69 with a maximum values of 6.33 and 5.88 in Germany and the Netherlands respectively [12]. Another study of corona-virus indicated that R_0 ranges 2.2–4.7 [13]. Also, one study of corona-virus disease 2019 conducted in 15 Western European countries showed that the value of R_0 is 2.2 [14] while another study of corona-virus conducted in Africa revealed that the value of R_0 is 2.37 [15].

On July 12th, 2021, COVID-19 spread to about 223 countries worldwide in which more than 188 million cases were reported with a total of 4.065 million death globally. Many research groups in different nations in the world have put much effort into developing or producing vaccines [16]. Although some vaccines have been developed, nonpharmaceutical interventions are important in minimizing the outbreak.

Modeling is an essential theoretical tool that helps in understanding, and analysis of effective control and preventive measures of different communicable diseases [16]. Many models of epidemiology divide their population into compartments in which assumptions are made about the nature and time rate of transfer among the human population [17]. These models act as a mathematical framework for studying the complexity of the dynamics of epidemiological processes [9]. A mathematical model is a major tool used to present COVID-19 transmission and its simulation can be used for predictions [16]. Some mathematical models were constructed to analyze the spreads of viruses [18]. During the outbreak of COVID-19, modeling attracted a special attention to many pharmacists, mathematician, chemists, biologists, epidemiologists [1, 2, 19–27]. This can be an effective approach to study, simulate and predict the mechanism and transmission of the disease.

COVID-19 has affected different groups of people such as farmers, soldiers, public drivers, educators, students, healthcare workers and many other groups. The transmission rate of this disease differs from one group to another depending on contact rate. Healthcare workers which is the most important health workforce are at a high risk of contracting the disease due to the high contact rate with patients [28]. Unavailability of diagnostic tests and an insufficient number of protective equipment put the healthcare workers at the highest risk of becoming infected and infecting others. There are some models focused on the risk of COVID-19 on healthcare workers [28, 29] and others dealt with the spread of COVID-19 between the public and frontlines taking into consideration two mutually exclusive population (i.e the public compartment alone and frontlines alone) for instance Buhat et al. [26]. The aforementioned models lack a single compartment to combine both public and healthcare workers. Another mathematical model presented an organization strategies suitable to protect the healthcare workforce through formulating a compartment of health workforce alone without including the general public [30].

Despite the fact that it is hard to separate healthcare workers from the general community, there exists no mathematical model that combines healthcare workers and the general public in a single compartment and focuses on the protection of healthcare workers against COVID-19. Protection of this important health workforce will be possible if the transmission is minimized among the health co-workers. Also, minimizing the spread of infection between the community and healthcare workers will be the other way of protecting healthcare workers. So, there is a need of having a single-compartment mathematical model which takes into account both public control measures (as a parameter) and healthcare workers (as an independent compartment). Combining these two in a given mathematical model helps in protecting healthcare workers through effective use of personal protective equipment and minimize the spread of COVID-19 infection by implementing control measures in the general public. N95 masks (N stand for non resistant

to oil, N95 respirator filters out the airborne particles by 95%), isolation booths, face, and eye shields are the personal protective equipment that signifies the level of protection [28].

This study formulates and analyzes the mathematical model for COVID-19 which takes into account both public control measures (as a parameter) and healthcare workers (as an independent compartment), which is the extension of the work done by Buhat et al. [26], Sánchez-Taltavull et al. [30]. Two important parameters introduced in the model are θ to represent physical distancing, face masks, sanitation, and hygiene which minimizes COVID-19 in the community, and ξ to represent effective use of personal protective equipment by healthcare workers. Furthermore, this study determines how much the transmission rate of healthcare workers influences the model output.

This paper is structured as follows. After the introduction given in Section “Introduction”, a mathematical model of COVID-19 transmission dynamics taking into account both healthcare workers as an independent compartment and public control measures as a parameter is formulated in Section “Model formulation”. The dynamics of the model are analyzed in Section “Model analysis”. The numerical results which include model simulation by using the fourth-order Runge–Kutta method, model fitting and identifiability of model parameter are performed in Section “Numerical simulation”. These results support validating theoretical results. The last section presents conclusions, discussion and the future direction.

Model formulation

This section presents model development, model assumption, model flow diagram and model equations. In model development, a general overview of the deterministic model is provided.

Model development

An infectious disease may spread in a complex manner when having different interacting variables. Mathematical models are among the tool used to analyze and predict the disease spread and its severity. To have a deeper insight on COVID-19 dynamics, this study formulated a biological compartmental model where the human population is divided into seven compartments: susceptible individuals (S), healthcare workers (W), exposed individuals (E), symptomatic infected individuals (I_s), asymptomatic infected individuals (I_a), hospitalized individuals (H) and recovered individuals (R). The total human population $N(t)$ is given by

$$N(t) = S(t) + W(t) + E(t) + I_s(t) + I_a(t) + H(t) + R(t).$$

The natural human natality rate for both susceptible and healthcare workers are Λ and b , respectively. There is a fraction of healthcare workers which move to susceptible class. Susceptible (S) and healthcare workers population (W) get infected from enough contact with infected class I_s at the rate of β_1 and β_2 , respectively and then move to exposed class (E). The progression of the exposed population to symptomatic and asymptomatic infectious is at the rate of α and ρ , respectively. Symptomatic and asymptomatic infectious individuals may be hospitalized at the rate of ν and ϵ , respectively. Infected individuals recover naturally or through local treatment at a rate of η and δ , respectively, but hospitalized individuals recover at a rate of ω . The chance of reinfection after recovery has been considered in this model so, the recovered class can become susceptible at a rate γ . In all classes, individuals can die with a natural mortality rate μ while infected individuals (I_s and I_a) and hospitalized humans decrease as a result of COVID-19 related death at a rate of d . In this model, there are two forces of infection which are $(1-\theta)\beta_1 I_s S$ and $(1-\xi)r\beta_2 W I_s$ where ξ is a fraction of healthcare workers who effectively use personal protective equipment. Also, θ represents a fraction of effective use of face masks, sanitation, hygiene, and maintenance physical distancing. We assumed all aforementioned measures work best in the mass gathering when effectively implemented.

Table 1
Model parameter description.

Parameter	Description
Λ	Natural natality rate of susceptible
b	Recruitment rate of healthcare workers
ξ	proportional use of personal protective equipment
β_1	Disease transmission rate
β_2	Transmission rate of healthcare workers
μ	Natural mortality rate
α	Progression rate from exposed stage to symptomatic infectious stage
ρ	Progression rate from exposed stage to asymptomatic infectious stage
ν	Hospitalization rate of symptomatic infected individuals
ϵ	Hospitalization rate of asymptomatic infectious individuals
ω	Recovery rate of hospitalized population
η	The rate in which symptomatic infectious population recover
δ	The rate in which asymptomatic infectious population recover
d	Disease induced death rate
r	proportional of healthcare workers
γ	Waning rate of disease-induced immunity
θ	The rate of wearing masks, sanitation, hygiene and physical distancing

Model assumptions

Description of infectious diseases through deterministic models need to have some assumptions to be considered based on the characteristics of a specific disease under consideration. In this case, the following are some of the assumptions to be considered in formulating a COVID-19 model (1):

- The members of the population mix homogeneously.
- Transmission is only from human to human.
- Asymptotically infectious individuals are assumed to be less likely to transmit the disease since they cannot cough or sneeze as symptomatic but this is still being debated globally [31].

Model flow diagram and model equations

The model flow diagram illustrated in Fig. 1 lead to the model Eq. (1).

$$\begin{aligned}
 \frac{dS}{dt} &= \Lambda + (1-r)W + \gamma R - (\mu + (1-\theta)\beta_1 I_s)S, \\
 \frac{dW}{dt} &= b - \mu W - (1-r)W - (1-\xi)r\beta_2 W I_s, \\
 \frac{dE}{dt} &= (1-\theta)\beta_1 I_s S + (1-\xi)r\beta_2 W I_s - (\alpha + \mu + \rho)E, \\
 \frac{dI_s}{dt} &= \alpha E - (d + \nu + \mu + \eta)I_s, \\
 \frac{dI_a}{dt} &= \rho E - (\mu + d + \delta + \epsilon)I_a, \\
 \frac{dH}{dt} &= \nu I_s + \epsilon I_a - (\mu + d + \omega)H, \\
 \frac{dR}{dt} &= \eta I_s + \omega H + \delta I_a - (\mu + \gamma)R.
 \end{aligned} \tag{1}$$

The system of Eq. (1) is subjected to the initial conditions: $S(0) = S_0 \geq 0$, $W(0) = W_0 \geq 0$, $I_a(0) = (I_a)_0 \geq 0$, $I_s = (I_s)_0 \geq 0$, $E(0) = E_0 \geq 0$, $H(0) = H_0 \geq 0$, $R(0) = R_0 \geq 0$. The parameters for the system of model (1) are described in Table 1.

Model analysis

This section presents model properties (i.e positivity and invariant), computation of basic reproduction number, existence and uniqueness of the solution. Also, equilibria and their stability results are provided in this section.

Positivity of the solution

A population is biologically meaningful and well defined if all model solutions are non-negative for all $t \geq 0$.

Theorem 1. *If the initial data $[S(0), W(0), E(0), I_s(0), I_a(0), H(0), R(0)] \geq 0$, then the solution for $S(t), W(t), E(t), I_s(t), I_a(t), H(t), R(t)$ of the system of model (1) is non negative $\forall t \geq 0$.*

Proof. To prove this theorem, we used the approach in [32], where we take into account system of model (1). Consider the first equation from model (1),

$$\frac{dS}{dt} = \Lambda + (1-r)W + \gamma R - (\mu + (1-\theta)\beta_1 I_s)S. \tag{2}$$

Omitting the first three terms and introducing inequality in Eq. (2) leads to

$$\frac{dS}{dt} \geq -(\mu + (1-\theta)\beta_1 I_s)S. \tag{3}$$

Apply variable separable technique in Eq. (3) and introduce limit from 0 to t results

$$\int_{S(0)}^{S(t)} \frac{dS}{S} \geq - \int_0^t (\mu + (1-\theta)\beta_1 I_s) dt.$$

Further simplification leads to:

$$S(t) \geq S(0)e^{-(\mu + (1-\theta)\beta_1 I_s)t}, \text{ which implies}$$

$$S(t) \geq 0.$$

This shows that the solution for susceptible population (S) is non-negative $\forall t \geq 0$.

Doing the same approach to the remaining equations in the model (1), it can be simply shown that $W(t) \geq 0$, $E(t) \geq 0$, $I_s(t) \geq 0$, $I_a(t) \geq 0$, $H(t) \geq 0$, $R(t) \geq 0$ for all $t \geq 0$. Therefore $(S(t), W(t), E(t), I_s(t), I_a(t), H(t), R(t))$ of the model Eq. (1) is non negative $\forall t \geq 0$. This completes the proof of Theorem 1 \square

The invariant region

The invariant region describes the domain where all solutions to the model (1) are of biological and mathematical importance. All the model parameters are non-negative for all $t \geq 0$. Also, the solutions with positive initial data remain non-negative with all $t \geq 0$ and are bound.

Theorem 2. *The solution set of $S(t), W(t), E(t), I_s(t), I_a(t), H(t), R(t)$ of the model Equation system (1) is confined in a positive feasible region ϕ .*

Proof. Suppose the feasible region $\phi = (S(t), W(t), E(t), I_s(t), I_a(t), H(t), R(t)) \in \mathbb{R}_+^7$ for $\forall t \geq 0$. At any time t the total human population $N(t)$ will be: $N(t) = S(t) + W(t) + E(t) + I_s(t) + I_a(t) + H(t) + R(t)$. Differentiating with respect to t leads to

$$\frac{dN}{dt} = \frac{dS}{dt} + \frac{dW}{dt} + \frac{dE}{dt} + \frac{dI_s}{dt} + \frac{dI_a}{dt} + \frac{dH}{dt} + \frac{dR}{dt}. \tag{4}$$

Substitute Eq. (1) into Eq. (4), further simplification result into,

$$\frac{dN}{dt} = \Lambda + b - \mu(S + W + E + I_s + I_a + H + R) - (I_s + I_a + H)d. \tag{5}$$

Since $N = S + W + E + I_s + I_a + H + R$, then Eq. (5) is reduced to,

$$\frac{dN}{dt} = \Lambda + b - \mu N - (I_s + I_a + H)d. \tag{6}$$

Assume that there is no disease-induced death for symptomatic, asymptomatic infectious, and hospitalized population due treatment in all three aforementioned classes and introducing inequality, Eq. (6) becomes

$$\frac{dN}{dt} \leq \Lambda + b - \mu N. \tag{7}$$

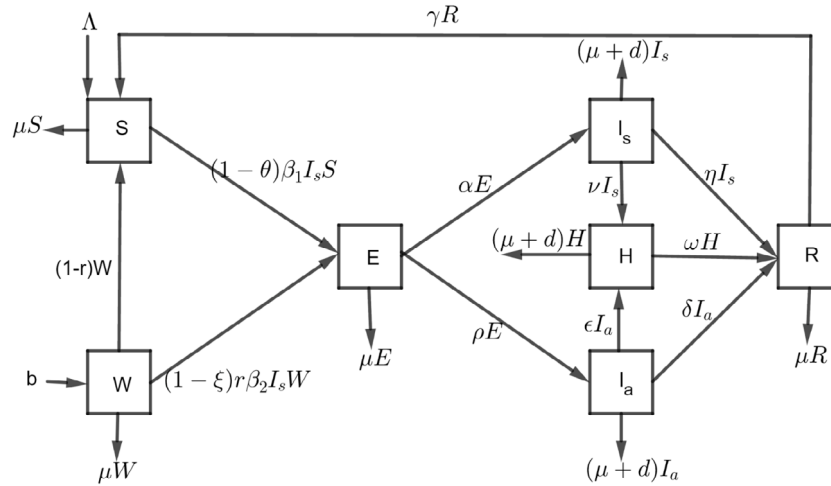


Fig. 1. Schematic diagram of COVID-19.

Separating the variable, introducing integral on both sides for Eq. (7), and then applying limits from 0 to t gives

$$\int_{N(0)}^{N(t)} \frac{dN}{\Lambda + b - \mu N} \leq \int_0^t dt.$$

Further simplification leads to

$$N(t) \leq \frac{\Lambda + b}{\mu} (1 - e^{-\mu t}) + N_0 e^{-\mu t}.$$

When $t \rightarrow 0$, $N(t) \rightarrow N_0$ and when $t \rightarrow \infty$, $N(t) \rightarrow \frac{\Lambda + b}{\mu}$. Finally $\phi = (S, W, E, I_s, I_a, H, R) \in \mathbb{R}_+^7 : 0 \leq N(t) \leq \frac{\Lambda + b}{\mu}$. The domain ϕ is a positive invariant under the flow induced by the system model (1). Therefore all feasible solutions of the model (1) enter the region ϕ , hence the proposed COVID-19 model system (1) is well-posed and is both epidemiologically and mathematically meaningful and we consider to generate the analysis. This implies that, the model system is positive invariant in the region

$$\phi = (S(t), W(t), E(t), I_s(t), I_a(t), H(t), R(t)) \in \mathbb{R}_+^7 : 0 \leq N(t) \leq \frac{\Lambda + b}{\mu},$$

for $[S(0), W(0), E(0), I_s(0), I_a(0), H(0), R(0)] \geq 0 \in \phi$ and this completes the proof. \square

Existence and uniqueness for $SWEI_s I_a HR$ model solution

Consider the ordinary differential equation in the form of

$$\frac{dy}{dt} = f(t, y), \quad y(t_0) = y_0. \quad (8)$$

By using Eq. (8) the interest will be to determine the condition that will lead the solution to be existing and condition to impose in order to have a unique solution.

This study applied the following two theorems to establish the existence and uniqueness of the solution of this model (1).

Theorem 3 (Uniqueness of Solution). As proposed in [33], Let D denote the domain:

$$|t - t_0| \leq a, \|y - y_0\| \leq b, y = (y_1, y_2, \dots, y_n), y_0 = (y_{10}, y_{20}, \dots, y_{n0}). \quad (9)$$

Suppose that $f(t, y)$ satisfies the Lipschitz condition:

$$\|f(t, y_2) - f(t, y_1)\| \leq k \|y_2 - y_1\|, \quad (10)$$

and whenever the pair of (t, y_1) and (t, y_2) belong to the domain D , where k represents a non-negative constant. Then, there exist a constant $\delta > 0$ such

that there exists a unique (exactly one) continuous vector solution $y(t)$ of the system (9) in the interval $|t - t_0| \leq \delta$. It is important to note that condition (10) is satisfied by the requirement that:

$$\left\{ \frac{\partial f_i}{\partial y_j}, i, j = 1, 2, \dots, n, \right.$$

be continuous and bounded in the domain D .

Lemma 1. If $f(t, y)$ has continuous partial derivative $\frac{\partial f_i}{\partial y_j}$ on a bounded closed convex domain \mathbb{R} . The interest is on the domain:

$$1 < \epsilon < \mathbb{R}. \quad (11)$$

So we look for a bounded solution of the form $0 < \mathbb{R} < \infty$ as proposed in the study [33]. In proving Lemma 1 we need to consider Theorem 4.

Theorem 4 (Existence of the Solution). Let D denotes the domain defined in (9) such that Eqs. (10) and (11) hold. Then there exists a solution of a model system of Eq. (1) in our model system, which is bounded in the domain D . Consider the system of Eq. (1);

$$\begin{aligned} F_1 &= \Lambda + \gamma R + (1-r)W - (\mu + (1-\theta)\beta_1 I_s)S, \\ F_2 &= b - \mu W - (1-r)W - (1-\xi)r\beta_2 W I_s, \\ F_3 &= (1-\theta)\beta_1 I_s S + (1-\xi)r\beta_2 W I_s - (\alpha + \mu + \rho)E, \\ F_4 &= \alpha E - (\mu + d + \nu + \eta)I_s, \\ F_5 &= \rho E - (\mu + d + \delta + \epsilon)I_a, \\ F_6 &= \nu I_s + \epsilon I_a - (\mu + d + \omega)H, \\ F_7 &= \eta I_s + \omega H + \delta I_a - (\mu + \gamma)R. \end{aligned} \quad (12)$$

Proof. Consider the first equation of the system of Eq. (12) for the sake of proving this,

$$F_1 = \Lambda + \gamma R + (1-r)W - (\mu + (1-\theta)\beta_1 I_s)S. \quad (13)$$

We need to show that Eq. (13) is continuous and bounded by determining the partial derivatives of F_1 with respect to all state variables (S ,

W, E, I_s, I_a, H, R).

$$\begin{aligned}\frac{\partial F_1}{\partial S} &= -(\mu + (1 - \theta)\beta_1 I_s), \quad \left| \frac{\partial F_1}{\partial S} \right| = |-(\mu + (1 - \theta)\beta_1 I_s)| < \infty, \\ \frac{\partial F_1}{\partial W} &= 1 - r, \quad \left| \frac{\partial F_1}{\partial W} \right| = |1 - r| < \infty, \\ \frac{\partial F_1}{\partial E} &= 0, \quad \left| \frac{\partial F_1}{\partial E} \right| = |0| < \infty, \\ \frac{\partial F_1}{\partial I_s} &= (1 - \theta)\beta_1 S, \quad \left| \frac{\partial F_1}{\partial I_s} \right| = |(1 - \theta)\beta_1 S| < \infty, \\ \frac{\partial F_1}{\partial I_a} &= 0, \quad \left| \frac{\partial F_1}{\partial I_a} \right| = |0| < \infty, \\ \frac{\partial F_1}{\partial H} &= 0, \quad \left| \frac{\partial F_1}{\partial H} \right| = |0| < \infty, \\ \frac{\partial F_1}{\partial R} &= \gamma, \quad \left| \frac{\partial F_1}{\partial R} \right| = |\gamma| < \infty.\end{aligned}$$

All partial derivatives of Eq. (13) verify that the given solution is continuous and bounded. Similarly, taking partial derivatives to the remaining equations in a model system (12) as applied in Eq. (13) will lead to the proof of continuity and boundedness of their solutions. Therefore basing the prove of Eq. (13), we conclude that all partial derivatives of Eq. (12) are continuous and bounded, hence, by Theorem 3, we can say that there exists a unique solution of Eq. (1) in the region D which is the proof of the theorem. \square

Disease free equilibrium solution

The point where there is no disease is referred to as a disease-free equilibrium. We obtain this point by equating the right-hand side of all system of Eq. (1) equal to zero and substituting $E = I = H = R = 0$ in all equations. let F_0 be the disease-free point, therefore $F_0 = (S^0, W^0, E^0, I_s^0, I_a^0, H^0, R^0) = \left(\frac{b(1-r)+A(\mu+r-1)}{\mu(\mu-r+1)}, \frac{b}{\mu+1-r}, 0, 0, 0, 0, 0 \right)$.

Basic reproduction number

The basic reproduction number is defined as the expected number of COVID-19 cases created by a single COVID-19 infected individual in the population during the entire period of infectiousness. In this model, the basic reproduction number is computed using the next generation approach in [34]. The matrix F denotes the generation of new infections while matrix V denotes the disease transfer among compartments evaluated at disease-free equilibrium.

$$F = \begin{pmatrix} 0 & \beta_1(1-\theta)\left(\frac{A(\mu+1-r)+b(1-r)}{\mu(\mu+1-r)}\right) + \frac{(1-\xi)r\beta_2b}{\mu+1-r} & 0 & 0 \\ 0 & 0 & 0 & 0 \\ 0 & 0 & 0 & 0 \\ 0 & 0 & 0 & 0 \end{pmatrix},$$

on other hand,

$$V = \begin{pmatrix} \alpha + \mu + \rho & 0 & 0 & 0 \\ -\alpha & d + \eta + \mu + \nu & 0 & 0 \\ -\rho & 0 & d + \delta + \mu + \epsilon & 0 \\ 0 & -\nu & -\epsilon & d + \mu + \omega \end{pmatrix}.$$

Basic reproduction number is the spectral radius of the next-generation matrix, thus

$$R_0 = \rho(FV^{-1}) = \max(\lambda_1, \lambda_2).$$

$$R_0 = \frac{\alpha\beta_1(\theta-1)((r-1)(b+\lambda)-\lambda\mu) + \alpha\mu(1-\xi)r\beta_2b}{\mu(\mu-r+1)(\alpha+\mu+\rho)(d+\eta+\mu+\nu)}.$$

Local stability of the disease free equilibrium (DFE)

Local stability of the disease-free equilibrium is investigated by using the eigenvalues which are obtained by determining the partial derivatives of the vector-valued function. An equilibrium point is asymptotically stable if the Jacobian matrix evaluated at that point has negative eigenvalues. In this paper, the Routh–Hurwitz criterion in [35] will be used to prove the local stability of the disease-free equilibrium.

Theorem 5. The disease free equilibrium of the model is locally asymptotically stable if $R_0 < 1$ and unstable if $R_0 > 1$.

Proof. In proofing this theorem, linearization of the system of model (1) is done by computing its Jacobian matrix J_{E_0} . The Jacobian matrix is computed at the disease-free equilibrium point by partial derivatives of each equation in the system for state variable S, W, E, I_s, I_a, H and R .

$$J_{DFE} = \begin{pmatrix} -\mu & 1-r & 0 & c_1 & 0 & 0 & \gamma \\ 0 & -(\mu+1-r) & 0 & c_3 & 0 & 0 & 0 \\ 0 & 0 & -(\rho+\mu+\alpha) & c_2 & 0 & 0 & 0 \\ 0 & 0 & \alpha & 0 & -c_4 & 0 & 0 \\ 0 & 0 & \rho & 0 & -c_5 & 0 & 0 \\ 0 & 0 & 0 & \nu & \epsilon & -(d+\mu+\omega) & 0 \\ 0 & 0 & 0 & \eta & \delta & \omega & -(\mu+\gamma) \end{pmatrix}, \quad (14)$$

where

$$\begin{aligned}c_1 &= \beta_1(1-\theta) \frac{A(\mu+1-r)+b(1-r)}{\mu(\mu+1-r)}, \\ c_2 &= \frac{(1-\xi)r\beta_2b}{\mu+1-r} + (1-\theta)\beta_1 \frac{A(\mu+1-r)+(1-r)b}{\mu(\mu+1-r)}, \\ c_3 &= \frac{-(1-\xi)r\beta_2b}{\mu+1-r}, \\ c_4 &= (d+\mu+\eta+\nu), \\ c_5 &= (\mu+d+\delta+\epsilon).\end{aligned}$$

It is clear that from the matrix represented by Eq. (14) the first, second, third and fourth eigenvalues are $\lambda_1 = -\mu$, $\lambda_2 = -(\mu+\gamma)$, $\lambda_3 = -(\mu+r-1)$, and $\lambda_4 = -(d+\mu+\omega)$.

Therefore the matrix (14) reduces to a (3×3) matrix after cancellation of respective rows and columns used to obtain the first, second, third and fourth eigenvalues seen below.

$$J_{E_0} = \begin{pmatrix} -(\alpha+\mu+\rho) & \frac{\beta_1(1-\theta)(b(1-r)+A(\mu-r+1))}{\mu(\mu-r+1)} + \frac{(1-\xi)r\beta_2b}{\mu-r+1} & 0 \\ \alpha & 0 & -(d+\eta+\mu+\nu) \\ \rho & 0 & -(d+\delta+\mu+\epsilon) \end{pmatrix}.$$

The characteristic polynomial is of the form

$$Z(\lambda) = \lambda^3 + a_1\lambda^2 + a_2\lambda + a_3,$$

where, $a_1 = \alpha + d + \delta + 2\mu + \rho + \epsilon$,

$$a_2 = \frac{\alpha\beta_1(b(\theta(r-1)+r+1)+(\theta-1)A(-\mu+r-1)+\mu(-\mu+r-1)(\alpha+\mu+\rho)(d+\delta+\mu+\epsilon)+\alpha\mu(1-\xi)r\beta_2b)}{\mu(\mu-r+1)}.$$

So $a_2 > 0$ if

$$\frac{\alpha b \beta_1 \theta (1-r)}{\mu(\mu-r+1)} + (\alpha + \mu + \rho)(d + \delta + \mu + \epsilon) > \frac{\alpha \beta_1 (1-\theta) A(\mu-r+1) + (1-\xi) \alpha \mu r \beta_2 b}{\mu(\mu-r+1)},$$

$$a_3 = \frac{(R_0(\alpha+\mu+\rho)(d+\eta+\mu+\nu))(\alpha(d+\delta+\mu+\epsilon)-\rho(d+\eta+\mu+\nu))}{\alpha}.$$

So $a_3 > 0$ if $\frac{\alpha(d+\delta+\mu+\epsilon)(R_0(\alpha+\mu+\rho)(d+\eta+\mu+\nu))}{\alpha}$

$$> \frac{\rho(d+\eta+\mu+\nu)(R_0(\alpha+\mu+\rho)(d+\eta+\mu+\nu))}{\alpha}.$$

We have got $a_1 > 0$, $a_2 > 0$ and $a_3 > 0$ so just need to find the condition for $a_1 a_2 - a_3 > 0$.

Consider the value of $a_1 a_2 - a_3$,

$$\begin{aligned}a_1 a_2 - a_3 &= (m_1 - m_2)(\alpha + d + \delta + 2\mu + \rho + \epsilon) \\ &\quad - \alpha R_0(\alpha + \mu + \rho)(d + \delta + \mu + \epsilon)(d + \eta + \mu + \nu) + m_3.\end{aligned}$$

The condition for $a_1 a_2 - a_3$ to be greater than zero is:

$$\begin{aligned}m_1(\alpha + d + \delta + 2\mu + \rho + \epsilon) + m_3 &> m_1 m_2(\alpha + d + \delta + 2\mu + \rho + \epsilon) \\ &\quad + \alpha R_0(\alpha + \mu + \rho)(d + \delta + \mu + \epsilon)(d + \eta + \mu + \nu),\end{aligned}$$

where

$$m_1 = \frac{\alpha b \beta_1 \theta (1-r)}{\mu(\mu-r+1)} + (\alpha + \mu + \rho)(d + \delta + \mu + \epsilon),$$

$$m_2 = \frac{\alpha \beta_1 (1-\theta) A (\mu-r+1) + (1-\xi) \alpha \mu r b \beta_2}{\mu(\mu-r+1)},$$

$$m_3 = \frac{\rho(d + \eta + \mu + \nu) (R_0(\alpha + \mu + \rho)(d + \eta + \mu + \nu))}{\alpha}.$$

According to the Routh–Hurwitz criterion, the necessary and sufficient condition for the stability of any system is that all the factors of the characteristic polynomial of a system must be negative. Since the eigenvalues are negative and conditions for the Routh–Hurwitz criteria are met, therefore the disease is asymptotically stable. \square

Existence of endemic equilibrium point

The endemic equilibrium point is a steady-state solution in which the disease exists in the population. This solution is obtained when we take all derivatives of Eq. (1) to be equal to zero and let its solution being represented by $D^E = (S^*, W^*, E^*, I_s^*, I_a^*, H^*, R^*)$.

For the existence of the endemic equilibrium conditions $S^* > 0, W^* > 0, E^* > 0, I_s^* > 0, I_a^* > 0, H^* > 0, R^* > 0$ must be satisfied.

$$\begin{aligned} I_s^* &= \frac{\alpha E^*}{d + \eta + \mu + \nu}, & I_a^* &= \frac{E^* \rho}{d + \delta + \mu + \epsilon}, \\ W^* &= \frac{b}{\mu + (1-\xi)\beta_2 I_s^* r - r + 1}, & H^* &= \frac{\nu I_s^* + I_a^* \epsilon}{d + \mu + \omega}, \\ R^* &= \frac{H^* \omega + \eta I_s^* + \delta I_a^*}{(\mu + \gamma)}, & E^* &= \frac{(1-\xi)\beta_2 I_s^* r W^* - \beta_1 \theta I_s^* S^* + \beta_1 I_s^* S^*}{\alpha + \mu + \rho}, \\ S^* &= \frac{\Lambda - r W^* + \gamma R^* + W^*}{\mu - \beta_1 \theta I_s^* + \beta_1 I_s^*}. \end{aligned}$$

In this case, the solution exists and it is unique. From these conditions, we conclude that the endemic equilibrium solution is stable if and only if $R_0 > 1$ exhibits persistence of COVID-19 transmission in the population.

Global stability of disease free equilibrium

This study analyzes the global stability of the disease-free equilibrium point of model (1) by using an approach presented in [36]. The model can be written in the following format:

$$\frac{dy_n}{dt} = B(y_n - y_{DFE}) + B_1 y_i,$$

and

$$\frac{dy_i}{dt} = B_2 y_i.$$

From the two equations above y_n and y_i are vectors of no transmitting and transmitting compartments respectively, and y_{DFE} is the vector at the disease-free equilibrium of the same length as y_n where $y_n = (S, W, R)^T$, $y_i = (E, I_s, I_a, H)^T$.

$$y_{DFE} = \left(\frac{\Lambda(\mu + 1 - r) + b(1 - r)}{\mu(\mu + 1 - r)}, \frac{b}{\mu + 1 - r}, 0 \right)^T, \text{ and}$$

$$y_n - y_{DFE} = \begin{pmatrix} S - \frac{\Lambda(\mu+1-r)+b(1-r)}{\mu(\mu+1-r)} \\ W - \frac{b}{\mu+1-r} \\ R \end{pmatrix}.$$

For global stability of DFE we need to show that matrix B has a real negative eigenvalues and B_2 is a Metzler matrix (i.e the off-diagonal elements of B_2 are non-negative, symbolically denoted by $B_2(y_{ij}) \geq 0, \forall i \neq j$). From model (1) we can obtain equations with and without transmission which can be written as follows:

$$\begin{pmatrix} \Lambda + (1-r)W + \gamma R - (\mu + (1-\theta)\beta_1 I_s)S \\ b - \mu W - (1-r)W - (1-\xi)r\beta_2 W I_s \\ \eta I_s + \omega H + \delta I_a - (\mu + \gamma)R \end{pmatrix}$$

$$= B \begin{pmatrix} S - \frac{\Lambda(\mu+1-r)+b(1-r)}{\mu(\mu+1-r)} \\ W - \frac{b}{\mu+1-r} \\ R \end{pmatrix} + B_1 \begin{pmatrix} E \\ I_s \\ I_a \\ H \end{pmatrix},$$

and,

$$\begin{pmatrix} (1-\theta)\beta_1 I_s S + (1-\xi)r\beta_2 W I_s - (\alpha + \mu + \rho)E \\ \alpha E - (d + \nu + \mu + \eta)I_s \\ \rho E - (\mu + d + \delta + \epsilon)I_a \\ \nu I_s + \epsilon I_a - (\mu + d + \omega)H \end{pmatrix} = B_2 \begin{pmatrix} E \\ I_s \\ I_a \\ H \end{pmatrix}.$$

For compatibility of matrix B is 3×3 , B_1 should be 3×4 and B_2 will be 4×4 . Using non-transmitting elements from the Jacobian matrix of the system of the model Eq. (1) result to,

$$B = \begin{pmatrix} -\mu & 1-r & \gamma \\ 0 & -(\mu+1-r) & 0 \\ 0 & 0 & -(\mu+\gamma) \end{pmatrix},$$

$$B_1 = \begin{pmatrix} 0 & -(1-\theta)\beta_1 S & 0 & 0 \\ 0 & -(1-\xi)r\beta_2 W & 0 & 0 \\ 0 & \eta & \delta & \omega \end{pmatrix},$$

$$B_2 = \begin{pmatrix} -(\mu + \alpha + \rho) & (1-\theta)\beta_1 S + (1-\xi)r\beta_2 W & 0 & 0 \\ \alpha & -(\eta + \nu + \mu + d) & 0 & 0 \\ \rho & 0 & -(d + \delta + \mu + \epsilon) & 0 \\ 0 & \nu & \epsilon & -(\mu + \omega + d) \end{pmatrix}.$$

The study found that B is a matrix whose eigenvalues are located on the main diagonal. Therefore the eigenvalues of the given matrix B (i.e $-\mu$, $(1-r+\mu)$ and $-(\mu+\gamma)$) are real, distinct and negative. Additionally, B_2 is a Metzler matrix since its off-diagonal elements are positive and the leading diagonal entries are negative. Therefore, the DFE of our system is globally asymptotically stable, thus we have established the following important theorem.

Theorem 6. The disease free equilibrium point is globally asymptotically stable if $R_0 < 1$ and unstable if $R_0 > 1$.

Global stability of endemic equilibrium

This study used the logarithmic Lyapunov function to analyze the stability of endemic equilibrium as used in [37]. This logarithmic function will be in this form $P = \sum a_i (y_i - y_i^* \ln(y_i))$. Where a_i is a positive chosen constants, y_i is population of compartment i and y_i^* is the equilibrium level.

$P(S, W, E, I_s, I_a, H, R) = A_1(S - S^* \ln S) + A_2(W - W^* \ln W) + A_3(E - E^* \ln E) + A_4(I_s - I_s^* \ln I_s) + A_5(I_a - I_a^* \ln I_a) + A_6(H - H^* \ln H) + A_7(R - R^* \ln R)$. The constants $A_1, A_2, A_3, A_4, A_5, A_6$ and A_7 are non negative and the function P is chosen in such away that it is a continuous and differentiable in space ∇ .

$$\frac{dP}{dt} = \begin{pmatrix} A_1(1 - \frac{S^*}{S}) \frac{dS}{dt} + A_2(1 - \frac{W^*}{W}) \frac{dW}{dt} \\ + A_3(1 - \frac{E^*}{E}) \frac{dE}{dt} + A_4(1 - \frac{I_s^*}{I_s}) \frac{dI_s}{dt} \\ + A_5(1 - \frac{I_a^*}{I_a}) \frac{dI_a}{dt} + A_6(1 - \frac{H^*}{H}) \frac{dH}{dt} \\ + A_7(1 - \frac{R^*}{R}) \frac{dR}{dt} \end{pmatrix}. \quad (15)$$

At endemic equilibrium point,

$$\begin{aligned} A &= (\mu + (1-\theta)\beta_1 I_s) S^* \\ &\quad - \gamma R^* - (1-r)W^*, \quad b = \mu W^* + (1-r)W^* + (1-\xi)r\beta_2 W^* I_s^*, \\ (v+d+\mu+\eta) &= \frac{\alpha E^*}{I_s^*}, \quad (\delta+d+\mu+\epsilon) = \frac{\rho E^*}{I_a^*}, \\ d+\mu+\omega &= \frac{v I_s^* + \epsilon I_a^*}{H^*}, \quad (\mu+\gamma) = \frac{\eta I_s^* + \omega H^* + \delta I_a^*}{R^*}, \\ (\alpha+\mu+\rho) &= \frac{(1-\theta)\beta_1 I_s^* S^* + (1-\xi)r\beta_2 W^* I_s^*}{E^*}. \end{aligned}$$

It is possible to re-write Eq. (15) using the definition of the parameters value as indicated at endemic equilibrium point above which results to

$$\frac{dP}{dt} = \begin{cases} A_1(1 - \frac{S^*}{S})(\mu + (1-\theta)\beta_1 I_s) S^* \\ - \gamma R^* - (1-r)W^* + (1-r)W + \gamma R \\ - (\mu + (1-\theta)\beta_1 I_s) S \\ + A_2(1 - \frac{W^*}{W})(\mu W^* + (1-r)W^* + (1-\xi)r\beta_2 W^* I_s^* \\ - \mu W - (1-r)W - (1-\xi)r\beta_2 W I_s) \\ + A_3(1 - \frac{E^*}{E})(1-\theta)\beta_1 I_s S^* + (1-\xi)r\beta_2 W I_s^* \\ - \frac{(1-\theta)\beta_1 I_s^* S^* + (1-\xi)r\beta_2 W^* I_s^*}{E^*} E \\ + A_4(1 - \frac{I_s^*}{I_s})(\alpha E - \frac{\rho E^*}{I_a^*} I_s) \\ + A_5(1 - \frac{I_a^*}{I_a})(\rho E - \frac{\rho E^*}{I_a^*} I_a) \\ + A_6(1 - \frac{H^*}{H})(v I_s + \epsilon I_a - \frac{v I_s^* + \epsilon I_a^*}{H^*} H) \\ + A_7(1 - \frac{R^*}{R})(\eta I_s + \omega H + \delta I_a - \frac{\eta I_s^* + \omega H^* + \delta I_a^*}{R^*} R). \end{cases} \quad (16)$$

Further simplification of Eq. (16) gives

$$\frac{dP}{dt} = -\mu A_1 \frac{(S - S^*)^2}{S} - b A_2 \frac{(W - W^*)^2}{W} + F(E, I_s, I_a, H, R), \quad (17)$$

where F is the balance of the right term of Eq. (17). According to the approach in [38,39], the function F is negative when $(E, I_s, I_a, H, R) \geq 0$, thus $\frac{dP}{dt} \leq 0$ or zero if $E = E^*, H = H^*, R = R^*, I_s = I_s^*, I_a = I_a^*$. By LaSalle's invariant principle [40] implies that in the interior of F the endemic equilibrium point F^* is globally asymptotically stable when $R_0 > 1$. This results is summarized in the following the theorem.

Theorem 7. Endemic equilibrium F^* is asymptotically stable when $R_0 > 1$ and unstable when $R_0 < 1$.

Numerical simulation

Model simulations are carried out using the values of the parameters obtained from different existing literatures. Other parameters which are not found in the literature were assumed basing on a reasonable proportionality. This section covers sensitivity and uncertainty analysis, dynamics population simulation, stability analysis of the model, the effect of varying some parameters to study the model dynamics and identifiability of model parameters. Numerical simulation in this study is done by using Runge–Kutta fourth-order method, however there are other numerical methods for simulations of non-linear differential equations such as Milne method, Eulers' method, Adams–Bashforth–Moulton method [15,20,41].

Sensitivity and uncertainty analysis

The sensitivity analysis describes how the model's parameters influence basic reproduction number R_0 . We performed a sensitivity analysis of R_0 for the model's parameters using the method established in [42]. Normalized forward sensitivity index of R_0 , depends on the

Table 2

Parameter and Indices Value of the model.

Parameter	Value	Source	Indices
Λ	0.009	[43]	0.01740
ξ	0.7	Assumed	-0.0003
β_1	0.5944	[31]	0.9999
β_2	0.8	Assumed	0.0001
μ	0.008	[31]	-0.9652
α	0.6	[44]	1.9258
η	0.2	Assumed	0.2330
ρ	0.04	Assumed	0.0617
ν	0.65	Assumed	0.7475
b	0.8	Assumed	0.9826
r	0.4	Assumed	-1.3244
d	0.00011	[45]	0.0001
θ	0.61	Assumed	-1.5639

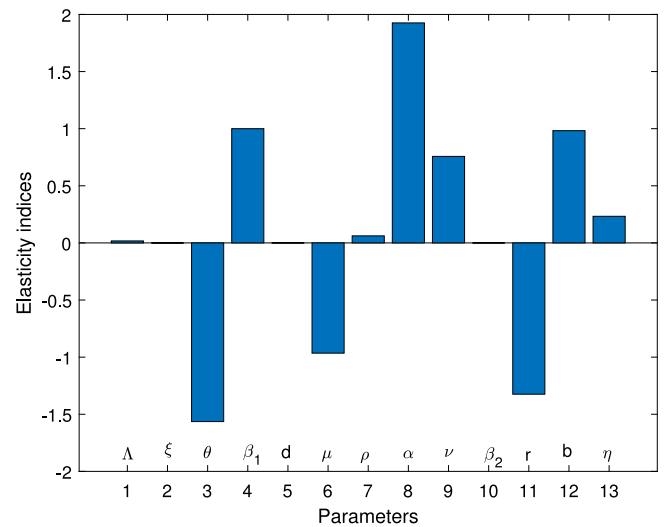


Fig. 2. Elasticity indices for significance of parameters in R_0 .

differentiability of R_0 with respect to a given parameter, say M, and can be computed as:

$$X_M^{R_0} = \frac{\delta R_0}{\delta M} \frac{M}{R_0}.$$

The value of basic reproduction number R_0 obtained using all parameters found in Table 2 is 2.8540. Also, when $\theta=0$ and $\xi=0$, $R_0=4.6047$. When $\theta=0.8$ and $\xi=0.9$, $R_0=0.4606$. Under this note, the implementation of public control measures in the community will minimize the spread of COVID-19. Also, the effective use of personal protective equipment by the healthcare workers reduced the transmission among the healthcare workers. This implies the two aforementioned parameters are very important in suppressing the spread of COVID-19.

Table 2 shows the parameters value and indices for the model system (1). The most positive index is α . This implies that increasing (decreasing) of α by 10% will increase (decrease) the value of R_0 by 19.258%. So, this parameter contributes positively to the model output R_0 . The most negative sensitive parameter is θ . This indicates that the more the population practices these measures θ keeping other parameters constant, the more the reduction of the spread of the disease. For example when the population practices θ by 10% then the value of R_0 will be reduced by 15.639%. Numerical indices and their signs indicated in Table 3 are also, shown in Fig. 2. Fig. 2 illustrates the parameters which can easily influence negatively or positively the spread of COVID-19. Fig. 3 depicts that control measures θ has a negative correlation with R_0 while Fig. 4 indicates that β_2 has a positive

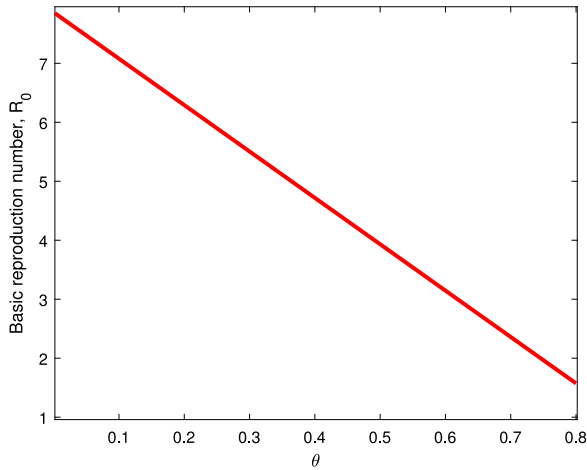


Fig. 3. Effect θ on R_0 .

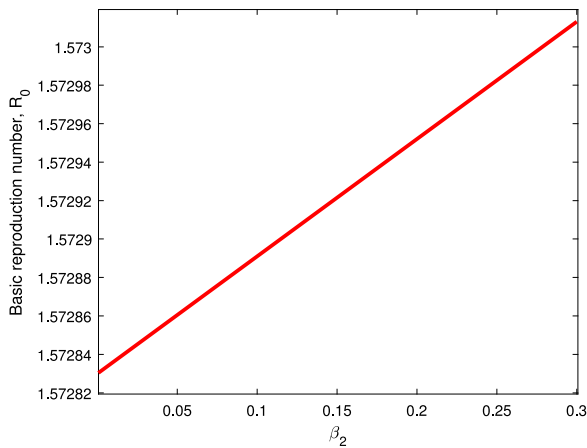


Fig. 4. Effect of β_2 on R_0 .

correlation with R_0 . This implies that θ contribute negatively to the pandemic while β_2 contribute positively to COVID-19.

Dynamics of populations simulation

Studying the dynamics of compartments, model (1) is simulated using the Runge–Kutta method of the fourth-order. Fig. 5 indicates seven different plots to represent various human populations. The susceptible population and healthcare workers' population decelerate exponentially to acquire endemic equilibrium levels as they die naturally or death due to a disease. Exposed, symptomatic, asymptomatic, hospitalized and recovered sub-population describes a parabola shape as it increases exponentially to attain its maximum point before decelerating exponentially to a specific endemic level.

Simulation on stability of endemic equilibrium point (EEP)

Numerical simulations for stability analysis are performed to validate analytical results. The equilibrium point is said to be globally asymptotically stable if the trajectories of the model state variables originating from different initial values vary for some time, converge to a common point and eventually maintain a constant horizontal level called an endemic equilibrium point. For this case, the trajectories are represented by red, yellow, magenta, black and blue solid plots that converge towards the equilibrium point as the time approaches infinity. Consider compartment S, suppose the initial value is (100, 90, 80, 70

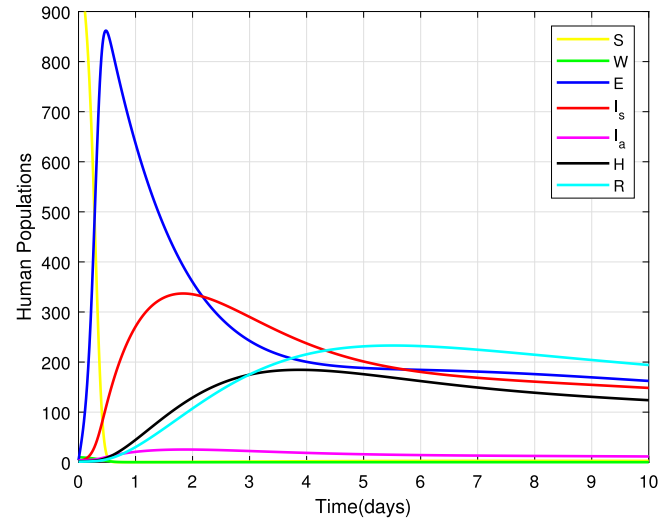


Fig. 5. Dynamics of SWEI_sI_aHR sub-populations.

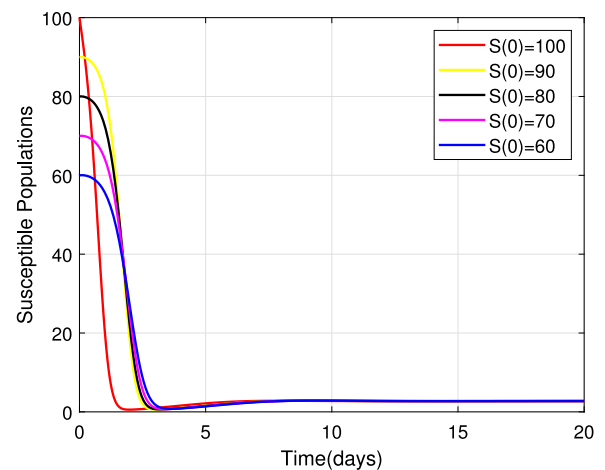


Fig. 6. Stability of the EEP for susceptible population.

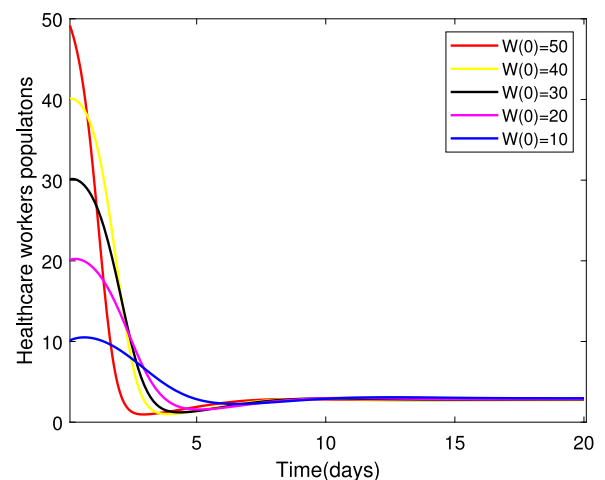


Fig. 7. Stability of the EEP for healthcare workers population.

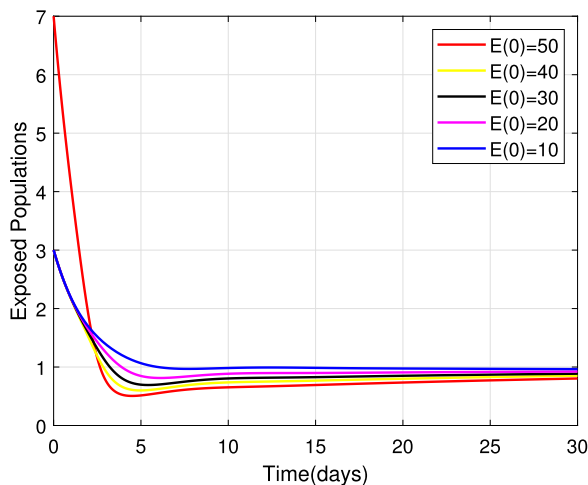


Fig. 8. Stability of the EEP for exposed population.

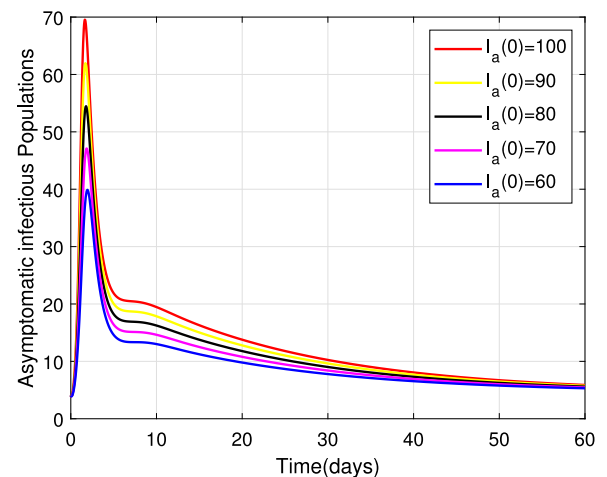


Fig. 10. Stability of the EEP for asymptomatic infectious population.

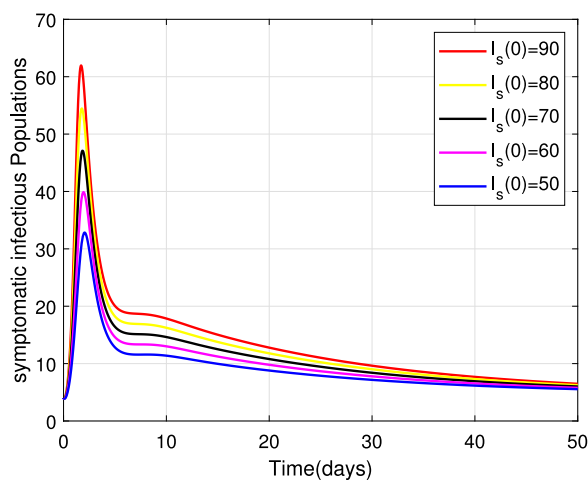


Fig. 9. Stability of the EEP for symptomatic infectious population.

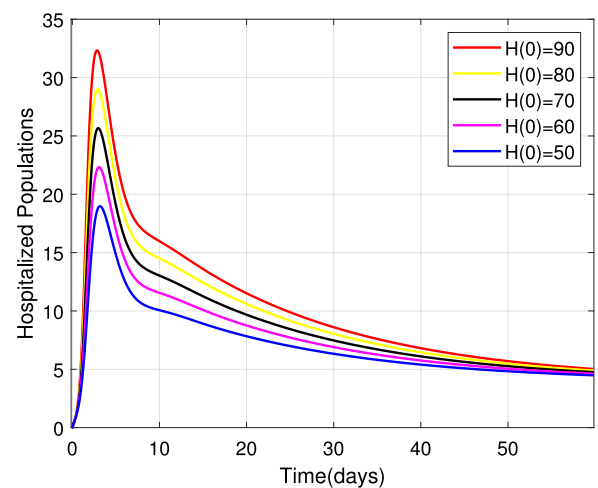


Fig. 11. Stability of the EEP for hospitalized population.

and 60). Simulating model (1), we get different trajectories for S to vary at the beginning but after approaching 8 all four stabilizes. This can be observed in Fig. 6. The same interpretations can be made from other compartments as seen in Figs. 7–12.

Effect of some parameters on the model

In this section, we have explored the behavior of each state variable of the proposed COVID-19 model (1). Also, profiles for state variables are graphically obtained through variation of some important parameters found in Table 2. Furthermore, mesh grid and contour plots are indicated to capture the behavior of R_0 with respect to some parameters

Considering the trends of Fig. 13 it can be noticed that the susceptible population increased to more than 9 people within only 15 days after implementation of control measures by 80%. Fig. 14 reveals that when implementing θ by 0.8, symptomatic infectious population reduces to below 135 patients within only 10 days. Fig. 15 shows that the number of admitted people to the hospital reduces to 130 patients after 10 days while Fig. 16 indicates that recovered increase to around 235 individuals when social distance, hygiene, and sanitation is implemented.

Figs. 17 and 19 reveals that both asymptomatic and symptomatic infectious reduces to around 23 and 135 patients respectively, within

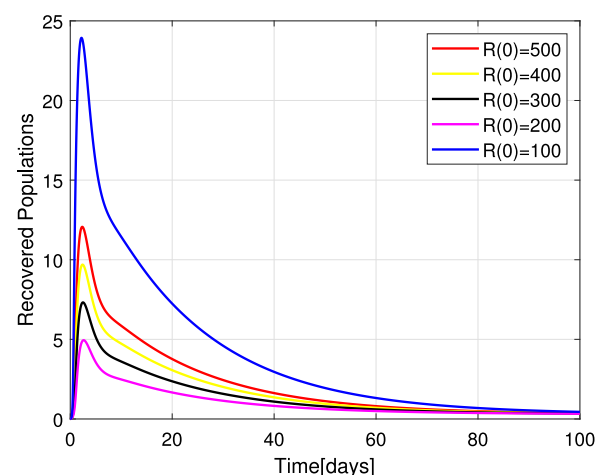


Fig. 12. Stability of the EEP for recovered population.

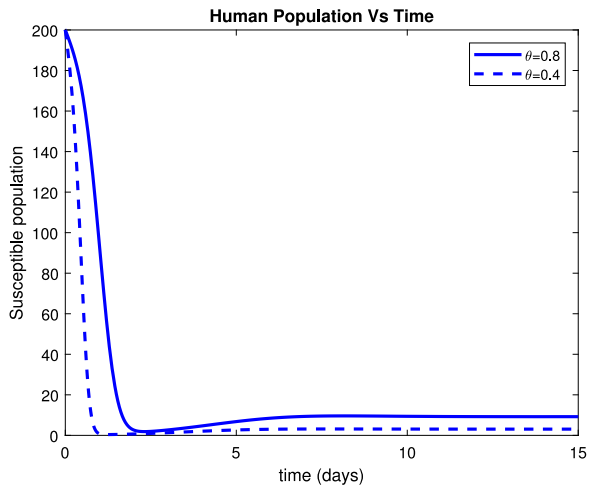


Fig. 13. Effect of θ on susceptible population.

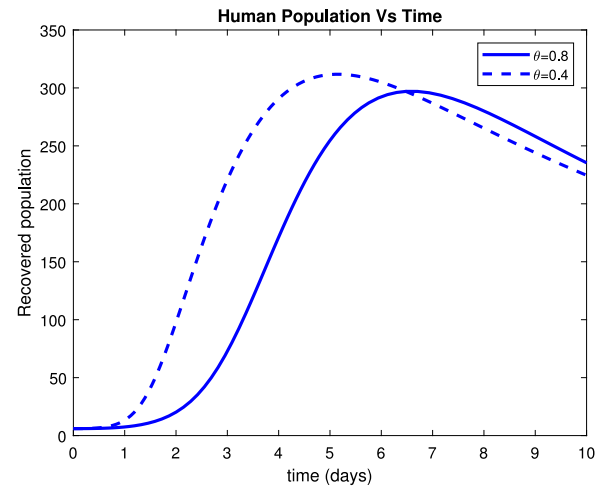


Fig. 16. Effect of θ on recovered humans.

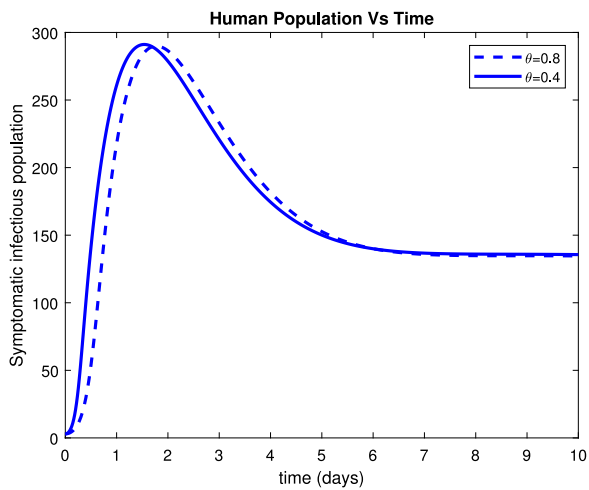


Fig. 14. Effect of θ on symptomatic population.

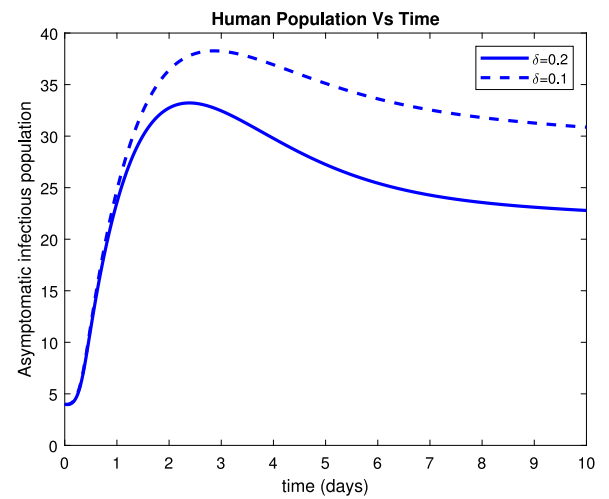


Fig. 17. Effect of treatment (δ) on asymptomatic infectious population.

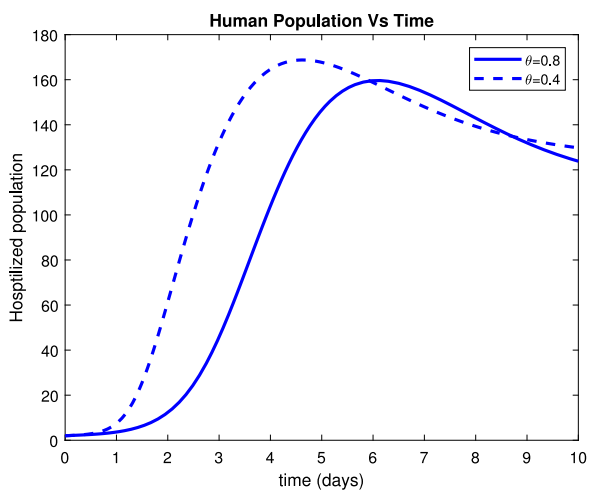


Fig. 15. Effect of θ on hospitalized humans.

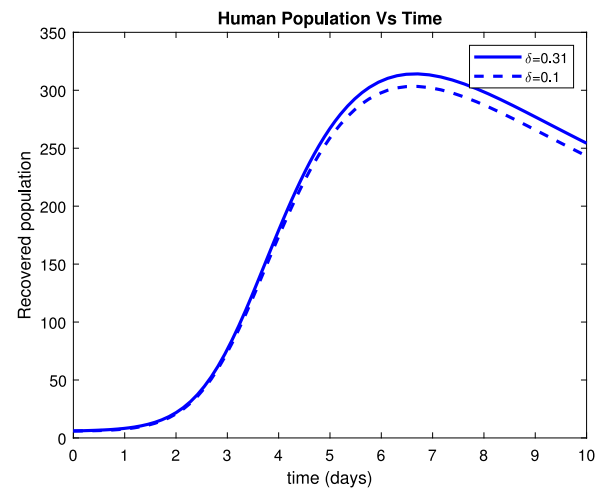


Fig. 18. Effect of treatment (δ) on recovered population.

10 days after getting treatment. Fig. 18 shows that about 254 individuals recovered due to treatment within 10 days while Fig. 20 indicates that about 235 patients recovered due to treatment within 10 days.

Fig. 21 depicts that the number of healthcare workers started rising after effective use of personal protective equipment. Fig. 22 shows that hospitalized individuals decrease to about 128 patients within 10 days

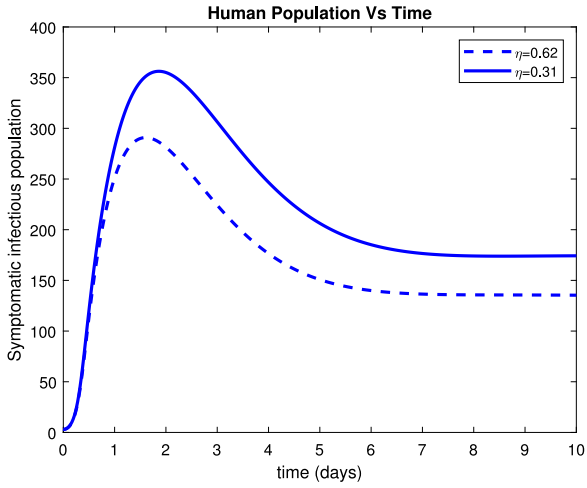


Fig. 19. Effect of treatment (η) on symptomatic infectious.

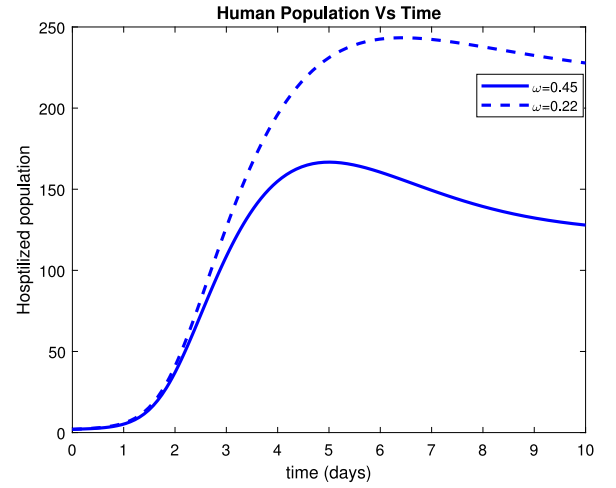


Fig. 22. Effect of treatment (ω) on hospitalized population.

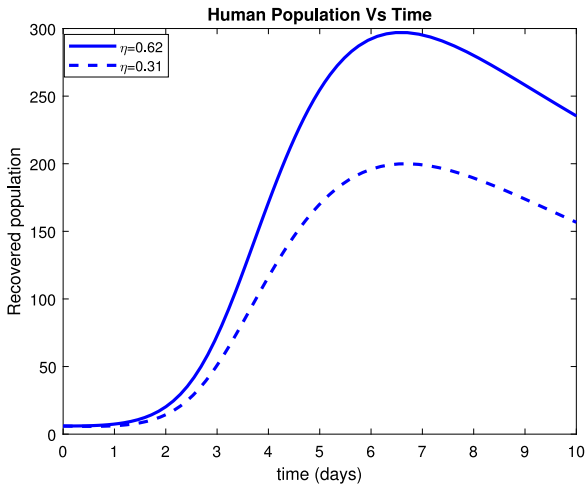


Fig. 20. Effect of treatment (η) on recovered population.

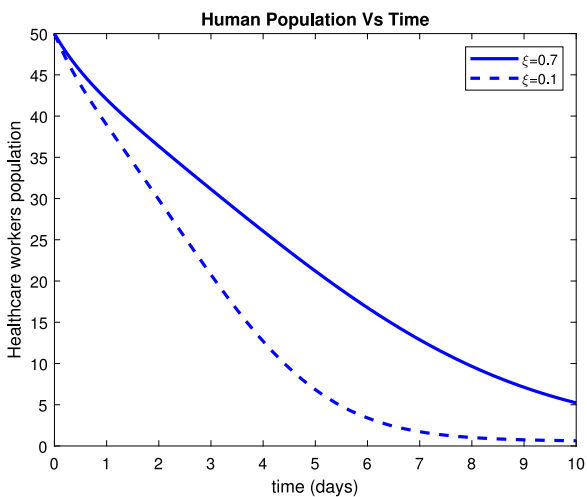


Fig. 21. Effect of personal protective equipment (ξ) on healthcare workers population.

after treatment. Also, the profile of R_0 versus some combination of parameters selected randomly from Table 2 via contour plots and mesh grids are shown in Figs. 23 and 24.

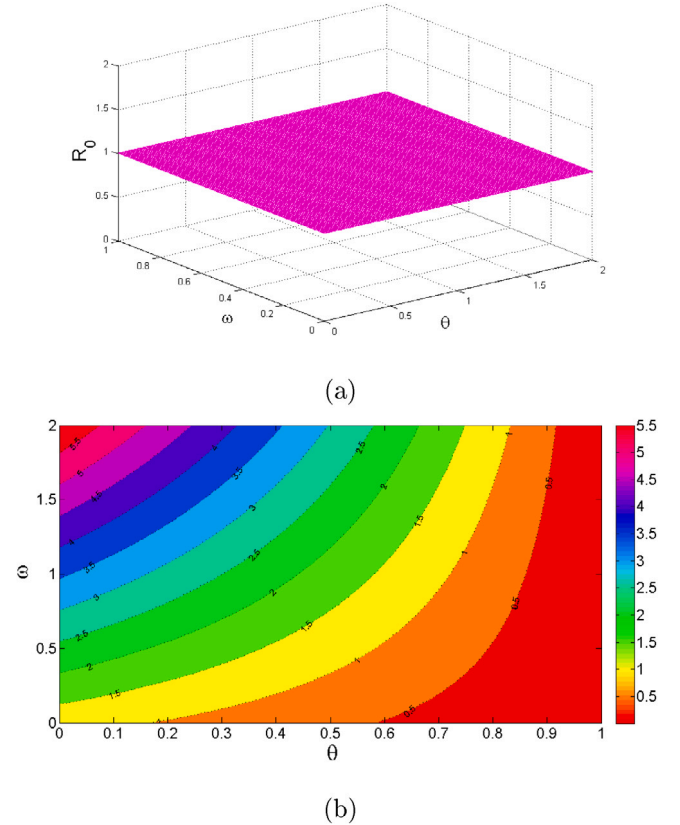
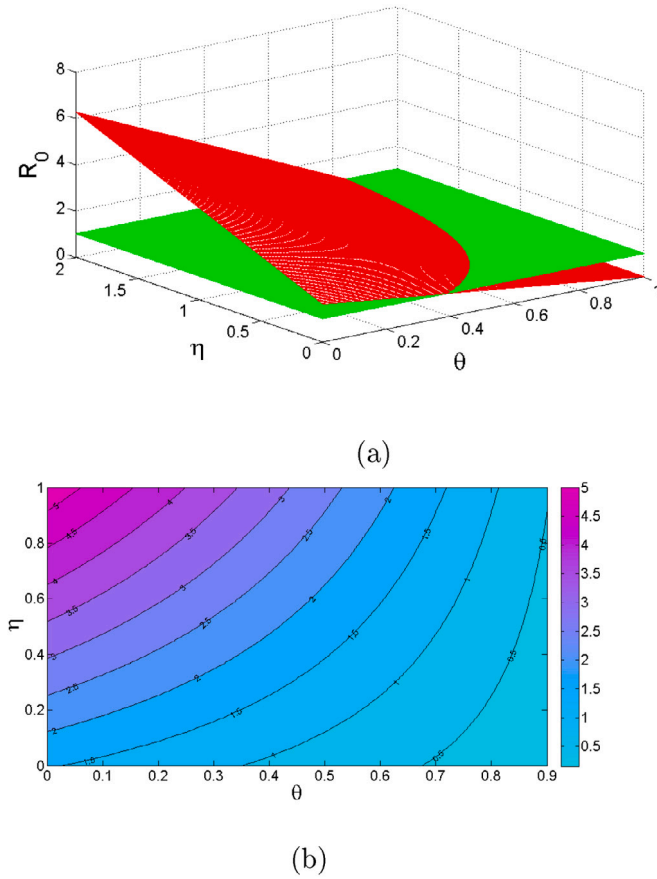


Fig. 23. Dynamic behavior of R_0 for varying ω and θ on $H(t)$.

Numerical results reveals that $R_0 = 4.6047$ which implies $R_0 > 1$ in absence of protective measures. Since $R_0 > 1$ this is a validation of analytical results of disease-free equilibrium which is an unstable and endemic point that is asymptotically stable. Also $R_0 = 0.4606$ in the presence of control measures in the general public and effective use of personal protective equipment by healthcare workers. Since $R_0 < 1$ this implies that disease-free equilibrium is asymptotically stable. This proves the importance of having control measures as well as personal protective equipment in controlling COVID-19 among the population since $R_0 < 1$.

Fig. 24. Dynamic behavior of R_0 for varying η and θ on $I_s(t)$.

Identifiability of model parameters

This subsection is devoted to the identifiability of the Parameters of the COVID-19 model (1). Some of the model (1) parameters assessed the effectiveness of the control measures in minimizing the

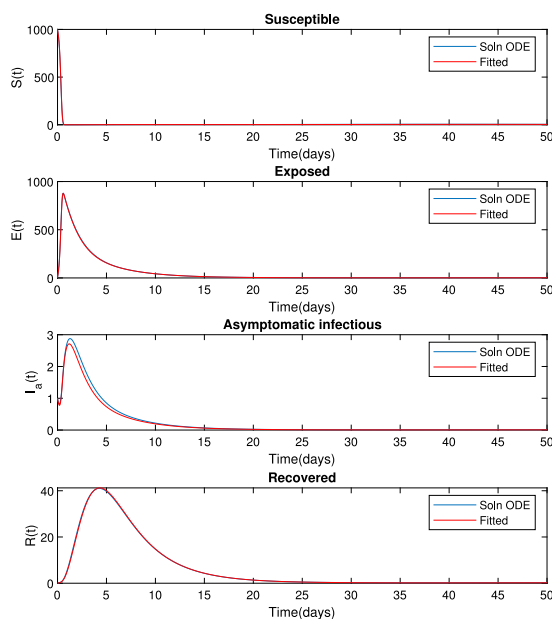


Fig. 25. Curve fitting.

Table 3

Parameter identifiability.

Parameter	Value	Estimate
Λ	0.009	0.0093
ξ	0.7	0.7269
β_1	0.5944	0.6130
β_2	0.8	0.8854
μ	0.008	0.0082
α	0.6	0.6368
η	0.2	0.0823
ρ	0.04	0.0671
ν	0.65	0.4800
b	0.8	0.9593
r	0.4	0.3474
d	0.00011	0.0001
θ	0.61	0.6160
ω	0.45	0.4459
ϵ	0.62	0.6325
δ	0.31	0.1500
γ	0.59	0.3955

transmission of COVID-19 in the entire community while others focused on protecting the healthcare workers for the sake of maintaining the workforce. Parameter estimation is conducted by using the least-squares method, where the idea here is to minimize the sum of squared differences between the observations and the model:

$$SS(\theta) = \sum_{i=1}^n (y_i - f(x_i, \theta))^2, \quad (18)$$

where y_i is observed data of all model (1) which correspond to $[S_i, W_i, E_i, (I_a)_i, (I_s)_i, H_i, R_i]$ and $f(x_i, \theta)$ is the model solution of all compartments of model (1). Table 3 indicates initial values of parameters and the model (1) optimization. Using the estimated values, the model solution can be compared with the simulated data as shown in Fig. 25. From this figure, it is observed that the simulated and fitted superimpose.

Conclusion and discussion

This paper introduced a mathematical model which consists of a system of seven non-linear ordinary differential equations. The aim of the model is to study the transmission of COVID-19 dynamics taking

into account both public control measures (as a parameter) and healthcare workers (as an independent compartment). It was important to have these two parameters because we have illustrated mathematically that healthcare workers are protected through effective use of personal protective equipment and control measures are used to minimize the spread of COVID-19 in the public.

Mathematical analyses including positivity of a solution, boundedness, computation of equilibria, calculation of the basic reproduction ratio, and stability analysis of the equilibria were carried out. Numerical simulations were performed by an effective MATLAB solver ODE45 Runge–Kutta fourth-order schemes [32] and the results indicated that in the absence of both θ and ξ , $R_0 = 4.6047$. However, when the two parameters are introduced to the model, the value of R_0 is reduced to 0.4606. This signifies the importance of the two parameters congruently when incorporated in the model for the sake of breaking the transmission of the disease.

Conclusively, the results indicated that protection of healthcare workers can be achieved through effective use of personal protective equipment by healthcare workers and minimization of transmission of COVID-19 in the general public by the implementation of control measures. Although many healthcare workers have been using protective equipment, this work emphasizes its impacts mathematically and strongly recommend others who have not been using them to do so.

The proposed model of this paper can be further improved by considering a Fractional-order analog as well as a stochastic model in order to capture more transmission dynamics of COVID-19 [7,23].

Funding

Not applicable.

CRediT authorship contribution statement

Lemjini Masandawa: Data curation, Writing – original draft, Methodology, Writing – review & editing, Conceptualization. **Silas Steven Mirau:** Visualization, Investigation, Supervision, Validation, Editing, Formal analysis, Project administration, Resource. **Isambi Sailon Mbalawata:** Conceptualization, Software, Preparation, Supervision, Editing, Project administration.

Declaration of competing interest

The authors declare that they have no known competing financial interests or personal relationships that could have appeared to influence the work reported in this paper.

Availability of data and material

All the data used in this manuscript can be found on different cited literature.

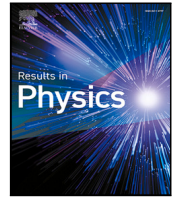
Acknowledgments

The authors acknowledge with thanks the support from AIMS. Also, authors would like to thank the reviewers and editors of this paper for their careful attention to detail and constructive feedback that improved the presentation of the paper greatly

References

- [1] Ogana W, Juma VO, Bulimo WD. A SIRD model applied to COVID-19 dynamics and intervention strategies during the first wave in Kenya, MedRxiv. 2021.
- [2] Ivorra B, Ferrández MR, Vela-Pérez M, Ramos A. Mathematical modeling of the spread of the coronavirus disease 2019 (COVID-19) taking into account the undetected infections. The case of China. Commun Nonlinear Sci Numer Simul 2020;88:105303.
- [3] Oud MAA, Ali A, Alrabaiah H, Ullah S, Khan MA, Islam S. A fractional order mathematical model for COVID-19 dynamics with quarantine, isolation, and environmental viral load. Adv Difference Equ 2021;2021(1):1–19.
- [4] Mahmoudi MR, Heydari MH, Qasem SN, Mosavi A, Band SS. Principal component analysis to study the relations between the spread rates of COVID-19 in high risks countries. Alex Eng J 2021;60(1):457–64.
- [5] Sardar T, Nadim SS, Rana S, Chattopadhyay J. Assessment of lockdown effect in some states and overall India: A predictive mathematical study on COVID-19 outbreak. Chaos Solitons Fractals 2020;139:110078.
- [6] Hui DS, Zumla A, Tang JW. Lethal zoonotic coronavirus infections of humans—comparative phylogenetics, epidemiology, transmission, and clinical features of coronavirus disease 2019, The Middle East respiratory syndrome and severe acute respiratory syndrome. Curr Opin Pulm Med 2021;27(3):146–54.
- [7] Naik PA, Yavuz M, Qureshi S, Zu J, Townley S. Modeling and analysis of COVID-19 epidemics with treatment in fractional derivatives using real data from Pakistan. Eur Phys J Plus 2020;135(10):1–42.
- [8] Bozkurt F, Yousef A, Baleanu D, Alzabut J. A mathematical model of the evolution and spread of pathogenic coronaviruses from natural host to human host. Chaos Solitons Fractals 2020;138:109931.
- [9] Peter OJ, Qureshi S, Yusuf A, Al-Shomrani M, Idowu AA. A new mathematical model of COVID-19 using real data from Pakistan. Results Phys 2021;104098.
- [10] Mbogo RW, Odhiambo JW. COVID-19 outbreak, social distancing and mass testing in Kenya—insights from a mathematical model. Afrika Mat 2021;1–16.
- [11] Gostic K, Gomez AC, Mummah RO, Kucharski AJ, Lloyd-Smith JO. Estimated effectiveness of symptom and risk screening to prevent the spread of COVID-19. Elife 2020;9:e55570.
- [12] Linka K, Peirlinck M, Kuhl E. The reproduction number of COVID-19 and its correlation with public health interventions. Comput Mech 2020;66(4):1035–50.
- [13] Gill BS, Jayaraj VJ, Singh S, Mohd Ghazali S, Cheong YL, Md Iderus NH, et al. Modelling the effectiveness of epidemic control measures in preventing the transmission of COVID-19 in Malaysia. Int J Environ Res Public Health 2020;17(15):5509.
- [14] Locatelli I, Trätschel B, Rousson V. Estimating the basic reproduction number for COVID-19 in Western Europe. Plos One 2021;16(3):e0248731.
- [15] Yu C-J, Wang Z-X, Xu Y, Hu M-X, Chen K, Qin G. Assessment of basic reproductive number for COVID-19 at global level: A meta-analysis. Medicine 2021;100(18).
- [16] Shahzad M, Abdel-Aty A-H, Attia RA, Khoshnaw SH, Aldila D, Ali M, et al. Dynamics models for identifying the key transmission parameters of the COVID-19 disease. Alex Eng J 2021;60(1):757–65.
- [17] Olivares A, Staffetti E. Uncertainty quantification of a mathematical model of COVID-19 transmission dynamics with mass vaccination strategy. Chaos Solitons Fractals 2021;110895.
- [18] Bocharov G, Volpert V, Ludewig B, Meyerhans A. In: Mathematical immunology of virus infections, vol. 245, Springer; 2018.
- [19] Neto OP, Kennedy DM, Reis JC, Wang Y, Brizzi ACB, Zambrano GJ, et al. Mathematical model of COVID-19 intervention scenarios for São Paulo—Brazil. Nature Commun 2021;12(1):1–13.
- [20] Baba IA, Yusuf A, Nisar KS, Abdel-Aty A-H, Nofal TA. Mathematical model to assess the imposition of lockdown during COVID-19 pandemic. Results Phys 2021;20:103716.
- [21] Abdullah SA, Owyed S, Abdel-Aty A-H, Mahmoud EE, Shah K, Alrabaiah H. Mathematical analysis of COVID-19 via new mathematical model. Chaos Solitons Fractals 2021;143:110585.
- [22] Ahmed I, Modu GU, Yusuf A, Kumam P, Yusuf I. A mathematical model of coronavirus disease (COVID-19) containing asymptomatic and symptomatic classes. Results Phys 2021;21:103776.
- [23] Ali Z, Rabiei F, Shah K, Khodadadi T. Qualitative analysis of fractal-fractional order COVID-19 mathematical model with case study of wuhan. Alex Eng J 2021;60(1):477–89.
- [24] Moore S, Hill EM, Tildesley MJ, Dyson L, Keeling MJ. Vaccination and non-pharmaceutical interventions for COVID-19: a mathematical modelling study. Lancet Infect Dis 2021.
- [25] Contreras S, Priesemann V. Risking further COVID-19 waves despite vaccination. Lancet Infect Dis 2021.
- [26] Buhat CAH, Torres MC, Olave YH, Gavina MKA, Felix EFO, Gamilla GB, et al. A mathematical model of COVID-19 transmission between frontliners and the general public. Netw Model Anal Health Inform Bioinform 2021;10(1):1–12.
- [27] Adak D, Majumder A, Bairagi N. Mathematical perspective of Covid-19 pandemic: Disease extinction criteria in deterministic and stochastic models. Chaos Solitons Fractals 2021;142:110381.
- [28] Dy LF, Rabajante JF. A COVID-19 infection risk model for frontline health care workers. Netw Model Anal Health Inform Bioinform 2020;9(1):1–13.
- [29] Chatterjee K, Chatterjee K, Kumar A, Shankar S. Healthcare impact of COVID-19 epidemic in India: A stochastic mathematical model. Med J Armed Forces India 2020;76(2):147–55.
- [30] Sánchez-Taltavull D, Castelo-Szekely V, Candinas D, Roldán E, Beldi G. Modelling strategies to organize healthcare workforce during pandemics: application to COVID-19. J Theoret Biol 2021;523:110718.

- [31] Mugisha JY, Ssebuliba J, Nakakawa JN, Kikawa CR, Ssematimba A. Mathematical modeling of COVID-19 transmission dynamics in Uganda: Implications of complacency and early easing of lockdown. *PLoS One* 2021;16(2):e0247456.
- [32] Yavuz M, Coşar FO, Günay F, Özdemir FN. A new mathematical modeling of the COVID-19 pandemic including the vaccination campaign. *Open J Model Simul* 2021;9(3):299–321.
- [33] Zhang Z, Gul R, Zeb A. Global sensitivity analysis of COVID-19 mathematical model. *Alex Eng J* 2021;60(1):565–72.
- [34] Van den Driessche P, Watmough J. Reproduction numbers and sub-threshold endemic equilibria for compartmental models of disease transmission. *Math Biosci* 2002;180(1–2):29–48.
- [35] Patil A. Routh-hurwitz criterion for stability: An overview and its implementation on characteristic equation vectors using MATLAB. *Emerg Technol Data Min Inf Secur* 2021;319–29.
- [36] Castillo-Chavez C, Feng Z, Huang W, et al. On the computation of R_0 and its role in global stability. *IMA Vol Math Appl* 2002;125:229–50.
- [37] Korobeinikov A, Wake GC. Lyapunov Functions and global stability for SIR, SIRS, and SIS epidemiological models. *Appl Math Lett* 2002;15(8):955–60.
- [38] Korobeinikov A. Global properties of infectious disease models with nonlinear incidence. *Bull Math Biol* 2007;69(6):1871–86.
- [39] McCluskey CC. Lyapunov functions for tuberculosis models with fast and slow progression. *Math Biosci Eng* 2006;3(4):603.
- [40] LaSalle JP. Stability theory and invariance principles. In: *Dynamical systems*. Elsevier; 1976, p. 211–22.
- [41] Babaei A, Jafari H, Ahmadi M. A fractional order HIV/AIDS model based on the effect of screening of unaware infectives. *Math Methods Appl Sci* 2019;42(7):2334–43.
- [42] Carvalho D, Barbastefano R, Pastore D, Lippi MC. A novel predictive mathematical model for COVID-19 pandemic with quarantine, contagion dynamics, and environmentally mediated transmission. *medrxiv*. 2020.
- [43] Mbabazi FK, Gavamukulya Y, Awichi R, Olupot-Olupot P, Rwahwire S, Biira S, et al. A mathematical model approach for prevention and intervention measures of the COVID–19 pandemic in Uganda. 2020.
- [44] Aldila D. Analyzing the impact of the media campaign and rapid testing for COVID-19 as an optimal control problem in East Java, Indonesia. *Chaos Solitons Fractals* 2020;141:110364.
- [45] Deressa CT, Duressa GF. Modeling and optimal control analysis of transmission dynamics of COVID-19: The case of Ethiopia. *Alex Eng J* 2021;60(1):719–32.



Modeling nosocomial infection of COVID-19 transmission dynamics

Lemjini Masandawa^{b,*}, Silas Steven Mirau^b, Isambi Sailon Mbalawata^a,
James Nicodemus Paul^b, Katharina Kreppel^b, Oscar M. Msamba^c

^a African Institute for Mathematical Sciences, NEI Global Secretariat, Rue KG590 ST, Kigali, Rwanda

^b School of Computational and Communication Science and Engineering, The Nelson Mandela African Institution of Science and Technology, P.O. Box 447, Arusha, Tanzania

^c Arusha Technical College, P.O. Box 296, Arusha, Tanzania

ARTICLE INFO

Keywords:

Proposed COVID-19 model
Personal protective equipment
PRCC
Basic reproduction number
Hospital-acquired infection

ABSTRACT

COVID-19 epidemic has posed an unprecedented threat to global public health. The disease has alarmed the healthcare system with the harm of nosocomial infection. Nosocomial spread of COVID-19 has been discovered and reported globally in different healthcare facilities. Asymptomatic patients and super-spreaders are sought to be among the source of these infections. Thus, this study contributes to the subject by formulating a *SEIHR* mathematical model to gain the insight into nosocomial infection for COVID-19 transmission dynamics. The role of personal protective equipment θ is studied in the proposed model. Benefiting the next generation matrix method, R_0 was computed. Routh–Hurwitz criterion and stable Metzler matrix theory revealed that COVID-19-free equilibrium point is locally and globally asymptotically stable whenever $R_0 < 1$. Lyapunov function depicted that the endemic equilibrium point is globally asymptotically stable when $R_0 > 1$. Further, the dynamics behavior of R_0 was explored when varying θ . In the absence of θ , the value of R_0 was 8.4584 which implies the expansion of the disease. When θ is introduced in the model, R_0 was 0.4229, indicating the decrease of the disease in the community. Numerical solutions were simulated by using Runge–Kutta fourth-order method. Global sensitivity analysis is performed to present the most significant parameter. The numerical results illustrated mathematically that personal protective equipment can minimize nosocomial infections of COVID-19.

Introduction

Recently, more attention has been given to the research of epidemic diseases like H1N1, malaria, Ebola, HIV, HBV, and many others [1]. The ability of bacteria, viruses, and parasites which are causative agents of these infectious diseases to keep changing over time posed challenges in controlling them. Currently the newest of the epidemic diseases disturbing the whole world is called COVID-19 [1]. COVID-19 is a respiratory illness that spread to many parts of the world within a short period after its evolution in China in late December in the year 2019 [2, 3]. It is the newest kind of virus caused by SARS COV-2 [4]. COVID-19 can affect either the lower respiratory tract (lungs and windpipes) or the upper respiratory tract (throat, sinuses, and nose). It started as unusual pneumonia of unknown etiology in Wuhan City in central China. On 7 January, 2020 it was discovered that the cause of the new outbreak of pneumonia is called the novel coronavirus (2019-nCoV) and later, on 11 February, 2020 the disease is named as Coronavirus Disease 2019 (COVID-19) [5]. Some studies suggested that the potential intermediary source of the novel infection is pangolins [3,6]. In spite

of the fact that the Chinese government imposed a strong lockdown, yet the disease spread very quickly throughout China and many other parts of the world through travelers from Wuhan. WHO announced it as pandemic on 11 March, 2020.

COVID-19 is transmitted from one person to another via breathing in the large respiration system's droplets coming from the mucous membrane (eye, mouth, and nose) of an infected person when sneezing, coughing, talking, or exhaling [7]. These respiratory droplets are too heavy to hang in the air so, the force of gravity influences and travel not more than one meter before quickly falling on the floor or surface thus, a social distance of 2 meters is a precaution. Further, the disease can be acquired through fomite transmission [8]. Predominantly transmission occurs through inhaling respiratory droplets from an infected person in close contact.

Zamir et al. [9] in their research presented that about 75% of COVID-19 victims do not show symptoms but recover naturally from the disease, only 20% can develop symptoms. The infected person will take 2–14 days to manifest full symptoms of the disease [10].

* Corresponding author.

E-mail address: masandawa@gmail.com (L. Masandawa).

<https://doi.org/10.1016/j.rinp.2022.105503>

Received 19 January 2022; Received in revised form 3 March 2022; Accepted 8 April 2022

Available online 21 April 2022

2211-3797/© 2022 The Author(s). Published by Elsevier B.V. This is an open access article under the CC BY-NC-ND license (<http://creativecommons.org/licenses/by-nc-nd/4.0/>).

About 80% of infected individuals recover without any treatment [10]. Mid-infected individuals recover within two weeks while critical cases recover within 3 to 6 weeks. The mortality and recovery rate of the disease is 7% and 93%, respectively [11].

The disease is much severe to the age group of 65 and above compared to young people. The human population having a long-term illness that weakens the body immunity such as cancer, diabetes, hypertension, and cardiovascular have the highest chance of getting much sickness [7]. Common symptoms for the disease include tiredness, sleep disorders, throat infection, nausea, vomiting, diarrhea, severe headache, muscles ache, runny nose, dry cough, red eyes, fatigue, sneezing, losing smell, and test [10,12]. The very serious clinical symptoms include breathing problems, persistent pain in the chest, blood pressure, kidney failure, and lack of voluntary movement [13].

Basic reproduction number R_0 is the threshold parameter which can be used to govern the spread of a specific disease. It helps in knowing how many in average one sick person can infect. In regards to COVID-19, one study revealed that R_0 to be 6.33 which is the highest value in German during the early outbreak of the disease [14]. One of the study done in Africa evinced the value of R_0 to be 2.37 [15].

Theories and practices of mathematical models have a paramount importance in describing infectious diseases. Formulation and analysis of these models can assist to gain an insight about the mechanism for the spread as well as the characteristic of the disease. Mathematical models can provide an information which can be useful in suggesting an effective strategy for prediction and prevention of the disease in the population. To date, there are plenty of mathematical models for describing the transmission dynamics of COVID-19 [5,13,14,16–23].

Apart from the global impact of economic and social disruption caused by the novel coronavirus, it has alarmed the healthcare system with the harm of healthcare-associated infection (HAI) [24]. These infections are acquired from the hospital setting. These infections are spread by various means, including between co-healthcare workers, between public healthcare workers and patients, and between sick individuals themselves [25]. Medical staff can acquire or transmit disease indirectly when attending infected individuals or susceptible patients. Also, the spread of infections in hospitals from infected to healthy personal is through directly sharing of the same rooms and environments.

Different governments around the world have been discovering hospital-acquired infections for COVID-19 in their healthcare facilities and report. One research conducted in one of the hospital in Germany revealed a total of 48 COVID-19 confirmed cases associated with HAI, in which 28 were healthcare professionals (HCPs), and 7 were accompanying their family members to the hospital, and 13 were patients in the hospitals [24]. Out of aforementioned cases, 4 infected persons had a 15 minutes close interaction with medical staffs without wearing personal protective equipment (PPE). In addition, seven other HCPs became infected after provision of medication to COVID-19 sick individuals without wearing PPE [24]. The other study depicted that the prevalence of nosocomial infections for COVID-19 was between 12.5%–15% in the united kingdom and up to 44% in China [26].

One of the research conducted by Lecy-Schoenherr [27] revealed that, HAI can be prevented through proper wearing of PPE, appropriate hand hygiene, proper monitoring of sick persons, and regular disinfecting environments. Since the outset of the pandemic the resources such as goggles, masks, apron, gloves, and gowns collectively termed PPE have been in a limited supply [25,28]. There are few research done on nosocomial transmission of SARS-COV-2. Martos et al. [26] did modeling on the transmission dynamics of COVID-19 inside hospital bays, a research conducted in UK. Authors in their paper, they focused only the hospitalized patients. Du et al. [24] in their review paper, reported nosocomial infections of SARS-COV-2 as new challenge to the healthcare professionals. In their work they suggested different strategies such as education, hygiene and environmental surveillance as means to prevent nosocomial infection. Oke et al. [29] formulated

a SEIHRD mathematical model to examine the impact of saturated treatment in Nigeria. In their study they concluded that minimization of infectivity rate alone cannot stop COVID-19 but can only be controlled when the disease's protocols are observed. Currently, little is known about the impact of PPE on COVID-19 nosocomial transmission dynamics.

Motivated by the above reason, the study at hand proposes a compartmental model to analyze the impact of PPE on nosocomial infection of the novel coronavirus transmission dynamics.

After introduction in the first part, the rest of the articles is designed as follows. The proposed model for COVID-19 nosocomial infection is presented in a section named “Mathematical Model Development and Description”. In another part by the name “Analysis of the Proposed COVID-19 Model” of the paper, theoretical analysis is investigated. A section of “Numerical Simulation” presents the numerical simulations. Conclusions, and the future direction is presented in the last section.

Mathematical model development and description

Deterministic compartment models divided the population into groups which are defined by the possible disease states that could be there at a specific time. This is a basis for the foundation of mathematical epidemiology since it helps in building models. In the proposed deterministic model the available population is categorized into five classes such as: Susceptible individuals (S), Exposed individuals (E), Infected individuals (I), Hospitalized individuals (H) and Recovered individuals (R). Therefore

$$N(t) = S(t) + E(t) + I(t) + H(t) + R(t),$$

where $N(t)$ indicate the whole population. The flowchart of the model is depicted in Fig. 1. When building this deterministic model, the available population is assumed to mix freely. Also, we assumed since the chance that a random contact by an infective is with a susceptible, who can then transmit infection is $\frac{S}{N}$, therefore the rate of new infection is given as $\left(\frac{S}{N}\right)(\beta_1 I + \beta_2 H)N = (\beta_1 I + \beta_2 H)S$. The susceptible class is increased by birth at a rate of Λ and recovered individuals who soon lost their immunity at the rate of γ . A susceptible compartment may catch the infection after enough contact with I and H . In some circumstances, individuals who accompany their patients to health facilities may acquire the disease through their interaction with patients and sharing the same environments. Further, Medical staff can acquire or transmit disease indirectly when attending to infected individuals or susceptible patients. So, hospitalized individuals and public health workers are assumed to participate in disease transmission but at a lower rate compared to free-leaving infectious individuals. β_1 and β_2 present the coefficients of the disease transmission relative to both infected and hospitalized class, respectively. The proportion of individuals who wear PPE within the community is denoted as θ where $0 \leq \theta \leq 1$. Contact tracing and isolation of individuals into the hospital is done at the rate of ϵ . Self-isolated individuals enter into the compartment I at the transformation rate of α . Hospitalized individuals are assumed to be infectious but with a low infectivity rate compared to $I(t)$. Among hospitalized groups and active patients the death occurs at the rate of d . The infected individuals are admitted to the hospital when they suffer from advanced symptoms of COVID-19 such as shorten in a breath at the rate of ν , otherwise join the group of individuals who have recovered at the rate of δ after their bodies gaining natural immunity. Hospitalized cases are discharged from the hospital and join the recovered group with the rate of ω . Finally, the parameter μ represents death due to the novel coronavirus rate for all individuals in all five compartments.

In formulating the proposed model for this paper the following hypothesis are made:

- i. All individuals are born susceptible.

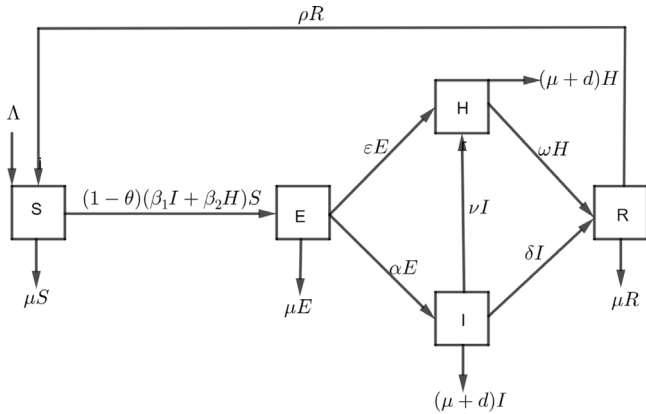


Fig. 1. Schematic diagram of COVID-19.

Table 1

Model variable description.

Variables	Description
$N(t)$	Total population at given time t
$S(t)$	Susceptible population at time t
$E(t)$	Exposed population at a given time t
$I(t)$	Infected population at time t
$H(t)$	Hospitalized population at time t
$R(t)$	Removed population at time t

Table 2

Parameters of the proposed model.

Parameter	Description
Λ	Recruitment rate
β_1	Contact rate
β_2	Contact rate of hospitalized group
μ	Removal rate
α	Rate at which exposed individuals become infected
ε	Rate at which exposed individuals are isolated in hospitals
ν	The rate where infected individuals are being hospitalized
ω	Recovery rate of hospitalized population
δ	The rate at which infected individuals recover
ρ	Rate of leaving the recovered class
d	The disease induced death rate
θ	The rate wearing PPE

- ii. Vertical transmission are ignored.
- iii. Initially every person in the population is considered susceptible.

Schematic diagram found in Fig. 1 can be used to derive Eq. (1).

The meaning of state variables for Eq. (1) are found in Table 1.

Deploying the given assumptions and variables, Eq. (1) is formulated having positive initial conditions

$$\begin{aligned}
 \frac{dS}{dt} &= \Lambda + \rho R - (\mu + (1-\theta)(\beta_1 I + \beta_2 H))S, \\
 \frac{dE}{dt} &= ((1-\theta)(\beta_1 I + \beta_2 H)S - (\alpha + \mu + \varepsilon)E), \\
 \frac{dI}{dt} &= \alpha E - (\delta + \nu + d + \mu)I, \\
 \frac{dH}{dt} &= \varepsilon E + \nu I - (d + \mu + \omega)H, \\
 \frac{dR}{dt} &= \delta I + \omega H - (\mu + \rho)R.
 \end{aligned} \tag{1}$$

Table 2 depicts the meaning of all parameters used in Eq. (1).

Analysis of the proposed COVID-19 model

This section covers positiveness of the solution, biological invariant region, equilibria solution, basic reproduction number, local and global stability of the proposed model (1).

Positiveness of the model of the solution

In this sub-section we have proved that the proposed model (1) solutions are positive for all $t \geq 0$.

Theorem 1. Assume that the model solution (1) starts Ω and remain in Ω for all time $t \geq 0$ and

$$\Omega = \{S(t), E(t), I(t), H(t), R(t)\} \in \mathbb{R}_+^5 \geq 0.$$

Proof. In proving this theorem, let us deploy an approach used by [30], Let define $\Psi(t) = \{x(t) = 0 \text{ and } (S(t), E(t), I(t), H(t), R(t)) \in \mathbb{R}_+^5 \geq 0\} \forall x \in \{S(t), E(t), I(t), H(t), R(t)\}$. Therefore, from Eq. (1), we have:

$$\begin{aligned}
 \frac{dS}{dt} | \Phi(S) &= \Lambda + \rho R \geq 0, \\
 \frac{dE}{dt} | \Phi(E) &= ((1-\theta)(\beta_1 I + \beta_2 H)S) \geq 0, \\
 \frac{dI}{dt} | \Phi(I) &= \alpha E \geq 0, \\
 \frac{dH}{dt} | \Phi(H) &= \varepsilon E + \nu I \geq 0, \\
 \frac{dR}{dt} | \Phi(R) &= \delta I + \omega H \geq 0.
 \end{aligned}$$

Using the approach by [30] helped in completing the proof. \square

Biological feasible region

The proposed model of COVID-19 nosocomial infection is realistic when all states variable are bounded in a feasible region Γ if initial conditions are positive for all $t \geq 0$.

Theorem 2. Let the solutions for Eq. (1) with positive initial condition are stated in the feasible region Γ where

$$\Gamma = \{S(t), E(t), I(t), H(t), R(t)\} \in \mathbb{R}_+^5$$

for all positive t .

Proof. To evaluate this, first consider the whole population which is given as:

$$N(t) = S(t) + E(t) + I(t) + H(t) + R(t).$$

Differentiating with respect to t leads to:

$$\frac{dN}{dt} = \frac{dS}{dt} + \frac{dE}{dt} + \frac{dI}{dt} + \frac{dH}{dt} + \frac{dR}{dt}. \tag{2}$$

Substitute Eq. (1) into Eq. (2), further simplification result into:

$$\frac{dN}{dt} = \Lambda - \mu(S + E + I + H + R) - (I + H)d. \tag{3}$$

Substituting N to the sum of all five states variables in Eq. (3) leads to:

$$\frac{dN}{dt} = \Lambda - \mu N - (I + H)d. \tag{4}$$

In absence of death due to novel coronavirus ($d = 0$) Eq. (4) reduces to:

$$\frac{dN}{dt} \leq \Lambda - \mu N. \tag{5}$$

Integrating both sides Eq. (5) with its initial condition gives:

$$\int_{N(0)}^{N(t)} \frac{dN}{\Lambda - \mu N} \leq \int_0^t dt.$$

Which simplifies into:

$$N(t) \leq N_0 e^{-\mu t} + \frac{\Lambda}{\mu} (1 - e^{-\mu t}).$$

As $t \rightarrow \infty$ the population size, $N(t) \rightarrow \frac{\Lambda}{\mu}$ which implies that $0 \leq N \leq \frac{\Lambda}{\mu}$, so the feasible region is given by $\Gamma = \{S, E, I, H, R\} \in \mathbb{R}_+^5 : 0 \leq N(t) \leq \frac{\Lambda}{\mu}$. Hence, the proposed model is well posed mathematically and this completes the proof. \square

Equilibrium analysis of model (1)

In any dynamical system, the state at which the system does not vary with time is called equilibrium point. Whenever the system starts from equilibrium it will never change for all time. There are two equilibria which are disease-free and endemic. Let E_0 be the disease-free point and it is given as:

$$E_0 = (S^0, E^0, I^0, H^0, R^0) = \left(\frac{\Lambda}{\mu}, 0, 0, 0, 0\right).$$

Further, an endemic equilibrium point (F^*) is given by:

$$\begin{aligned} I^* &= \frac{\epsilon E^*}{d + \delta + \mu + \nu} > 0, \\ H^* &= \frac{\alpha E^* + \nu I^*}{d + \mu + \omega} > 0, \\ E^* &= \frac{(1 - \theta)S^* (\beta_2 H^* + \beta_1 I^*)}{\alpha + \mu + \epsilon} > 0, \\ R^* &= \frac{\omega H^* + \delta I^*}{\mu + \rho} > 0, \\ S^* &= \frac{\Lambda + \rho R^*}{-\beta_2 \theta H^* + \beta_2 H^* + \mu - \beta_1 \theta I^* + \beta_1 I^*} > 0. \end{aligned}$$

After obtaining S^*, E^*, I^*, H^* and R^* we have to formulate a quadratic function in the format

$$F(E^*) = A(E^*)^2 + BE^* + C = 0,$$

where by in our case the value of A and B are as follows:

$$A = \frac{p_1 + p_2 p_3}{p_4}, \quad (6)$$

where

$$p_1 = d^2(\mu + \rho)(\alpha + \mu + \epsilon) + d(\alpha(\mu + \rho)(\delta + 2\mu + \nu) + \alpha\mu\omega + \delta\mu(\mu + \rho + \epsilon) + (\mu + \rho)(\mu + \epsilon)(2\mu + \nu + \omega)).$$

$$p_2 = \mu(\alpha(\delta + \mu + \nu)(\mu + \rho + \omega) + \delta(\mu + \omega)(\mu + \rho + \epsilon) + \rho\omega(\mu + \nu + \epsilon) + (\mu + \nu)(\mu + \rho)(\mu + \epsilon) + \omega(\mu + \nu)(\mu + \epsilon)).$$

$$p_3 = \beta_2(\nu(\alpha + \epsilon) + \alpha(\delta + d + \mu)) + \beta_1\epsilon(\omega + \mu + d),$$

and

$$p_4 = -\frac{\theta - 1}{(d + \mu + \omega)^2(\mu + \rho)(\nu + \delta + \mu + d)^2}.$$

$$B = \mu(\alpha + \mu + \epsilon) + \frac{(\theta - 1)A(\beta_2(\nu(\epsilon + \alpha) + \alpha(\delta + \mu + d)) + \beta_1\epsilon(d + \mu + \omega))}{(d + \mu + \omega)(d + \delta + \mu + \nu)}. \quad (7)$$

We have used quadratic formula to obtain the value of E^* as follows

$$E^* = -B + \frac{\sqrt{B^2 - 4AC}}{2A},$$

where A and B are given in Eqs. (6) and (7), respectively while C is equal to zero in this case.

$$E^* = \frac{\mu(\alpha + \mu + \epsilon) \left(\frac{(\theta - 1)A(\beta_1(-\epsilon)(d + \mu + \omega) - \beta_2(\nu(\alpha + \epsilon) + \alpha(d + \delta + \mu)))}{\mu(\alpha + \mu + \epsilon)(d + \mu + \omega)(d + \delta + \mu + \nu)} - 1 \right)}{\frac{\mu r_2((1 - \theta)A(\alpha + \mu + \epsilon)(\beta_2(\nu(\alpha + \epsilon) + \alpha(d + \delta + \mu)) + \beta_1\epsilon(d + \mu + \omega)))}{\Lambda(\mu(\alpha + \mu + \epsilon)(d + \mu + \omega)(d + \delta + \mu + \nu))} + r_1}. \quad (8)$$

By substituting

$$R_0 = -\frac{(\theta - 1)A(\epsilon + \alpha + \mu)(\beta_2(\nu(\alpha + \epsilon) + \alpha(d + \delta + \mu)) + \beta_1\epsilon(d + \mu + \omega))}{\mu(\alpha + \mu + \epsilon)(d + \mu + \omega)(d + \delta + \mu + \nu)},$$

in Eq. (8) lead to:

$$E^* = \frac{\Lambda\mu(\alpha + \epsilon + \mu)(R_0 - 1)}{\Lambda r_1 + \mu r_2 R_0},$$

where r_1 and r_2 are given in Box I.

Hence, we can conclude that the endemic point exist if and only if $R_0 > 1$.

Threshold parameter R_0

It is scientific test used to estimate the number of cases. It is commonly know as basic reproduction number. R_0 governs the spread of diseases. The next generation matrix is benefited in calculating the value of R_0 [31]. Consider Eq. (9) in a process of deducing R_0 as:

$$\begin{aligned} \frac{dE}{dt} &= ((1 - \theta)S(\beta_1 I + \beta_2 H) - (\alpha + \mu + \epsilon)E), \\ \frac{dI}{dt} &= \epsilon E - (\delta + \nu + d + \mu)I, \\ \frac{dH}{dt} &= \alpha E + \nu I - (d + \mu + \omega)H. \end{aligned} \quad (9)$$

To distinguish between new infection from other changes in the population, the system of Eq. (9) is modified and to be yield:

$$\frac{dx_i}{dt} = F_i(x) - V_i(x),$$

where x_i is a state variable that belongs to the transmitting compartment, F_i the rate of new infections in the compartment i , V_i the transfer of infections from one compartment to another.

$$F_i = \begin{pmatrix} f_1 \\ f_2 \\ f_3 \end{pmatrix} = \begin{pmatrix} (1 - \theta)\frac{\Lambda}{\mu}(\beta_1 I + \beta_2 H) \\ 0 \\ 0 \end{pmatrix}.$$

Partial derivatives of F_i with respect to E, I and H at DFE E_0 .

$$F = \begin{pmatrix} \frac{dF_1}{dE}(E_0) & \frac{dF_1}{dI}(E_0) & \frac{dF_1}{dH}(E_0) \\ \frac{dF_2}{dE}(E_0) & \frac{dF_2}{dI}(E_0) & \frac{dF_2}{dH}(E_0) \\ \frac{dF_3}{dE}(E_0) & \frac{dF_3}{dI}(E_0) & \frac{dF_3}{dH}(E_0) \end{pmatrix},$$

and

$$V = \begin{pmatrix} 0 & \beta_1(1 - \theta)\frac{\Lambda}{\mu} & \beta_2(1 - \theta)\frac{\Lambda}{\mu} \\ 0 & 0 & 0 \\ 0 & 0 & 0 \end{pmatrix}.$$

Considering V_i yields:

$$V_i = \begin{pmatrix} (\alpha + \mu + \epsilon)E \\ -\epsilon E + (\mu + d + \nu + \delta)I \\ (\omega + \mu + d)H - \alpha E - \nu I \end{pmatrix},$$

Partial derivatives with respect to E, I, H results to:

$$V = \begin{pmatrix} \alpha + \epsilon + \mu & 0 & 0 \\ -\epsilon & \mu + \nu + d + \delta & 0 \\ -\alpha & -\nu & d + \mu + \omega \end{pmatrix}.$$

The inverse of V is given as:

$$V^{-1} = \begin{pmatrix} \frac{1}{\alpha + \epsilon + \mu} & 0 & 0 \\ \frac{\epsilon}{(\alpha + \epsilon + \mu)(d + \delta + \mu + \nu)} & \frac{1}{d + \delta + \nu + \mu} & 0 \\ \frac{\alpha\delta + \alpha\mu + \alpha\nu + \alpha d + \epsilon\nu}{(\alpha + \epsilon + \mu)(d + \mu + \omega)(d + \delta + \mu + \nu)} & \frac{\nu}{(d + \mu + \omega)(d + \delta + \mu + \nu)} & \frac{1}{d + \mu + \omega} \end{pmatrix}.$$

The product of two Jacobian matrices (F and V^{-1}) gives:

$$FV^{-1} = \begin{pmatrix} \frac{\beta_2(1 - \theta)\Lambda(\alpha\nu + d\epsilon + \delta\epsilon + \epsilon\mu + \epsilon\nu)}{\mu(\alpha + \epsilon + \mu)(d + \mu + \omega)(d + \delta + \mu + \nu)} + \frac{\beta_1(1 - \theta)\Lambda\alpha}{\mu(\alpha + \epsilon + \mu)(d + \delta + \mu + \nu)} & \omega_1 & \frac{\beta_2(1 - \theta)\Lambda}{\mu(d + \mu + \omega)} \\ 0 & 0 & 0 \\ 0 & 0 & 0 \end{pmatrix},$$

where

$$\omega_1 = \frac{\beta_2(1 - \theta)\Lambda\nu}{\mu(d + \mu + \omega)(d + \delta + \mu + \nu)} + \frac{\beta_1(1 - \theta)\Lambda}{\mu(d + \delta + \mu + \nu)}.$$

Eigenvalues are given by:

$$\left\{ 0, 0, \frac{(1 - \theta)\Lambda(\beta_2(\alpha\nu + \epsilon(d + \delta + \mu + \nu)) + \alpha\beta_1(d + \mu + \omega))}{\mu(\alpha + \epsilon + \mu)(d + \mu + \omega)(d + \delta + \mu + \nu)} \right\}.$$

So

$$R_0 = \rho(FV^{-1}) = \max(\lambda_1, \lambda_2, \lambda_3).$$

$$r_1 = \frac{d^2(1-\theta)(\rho+\mu)(\epsilon+\mu\alpha) + d(\alpha(\mu+\rho)(\delta+2\mu+\nu) + \alpha\mu\omega + \delta\mu(\mu+\rho+\epsilon) + (\mu+\rho)(\mu+\epsilon)(2\mu+\nu+\omega))}{(\mu+\rho)(d+\mu+\omega)^2(d+\delta+\mu+\nu)^2},$$

and

$$r_2 = \frac{\mu(\alpha(\delta+\mu+\nu)(\mu+\rho+\omega) + \delta(\mu+\omega)(\mu+\rho+\epsilon) + \rho\omega(\mu+\nu+\epsilon) + (\mu+\nu)(\mu+\rho)(\mu+\epsilon) + \omega(\mu+\nu)(\mu+\epsilon))}{(\mu+\rho)(d+\mu+\omega)(d+\delta+\mu+\nu)}.$$

Box I.

$$a_2 = \frac{\alpha\beta_2(1-\theta)\Lambda + \beta_1(1-\theta)\Lambda\epsilon + \mu(\alpha(\delta+2\mu+\nu+\omega) + d^2 + d(2\alpha+\delta+4\mu+\nu+\omega+2\epsilon) + 2\delta\mu + \delta\omega + \delta\epsilon + 2\mu\nu + 2\mu\omega + 3\mu + \nu\omega + 2\mu\epsilon + \nu\epsilon + \omega\epsilon)}{\mu}.$$

Box II.

Therefore

$$R_0 = \frac{(1-\theta)\Lambda(\beta_2(\alpha\nu + \epsilon(d+\delta+\mu+\nu)) + \alpha\beta_1(d+\mu+\omega))}{\mu(\alpha+\epsilon+\mu)(d+\mu+\omega)(d+\delta+\mu+\nu)}.$$

Stability analysis of the model

In this sub-section the proposed model is analyzed at disease-free (both local and global) and endemic. Metzler matrix and Lyapunov function are deployed in proving local and global stability, respectively.

Local behavior of the model

Local behavior of the model is achieved whenever all eigenvalues of the Jacobian matrix of the proposed model (1) at disease-free have non-positive real parts. Let demonstrate this by utilizing the ideas as in [32].

Theorem 3. COVID-19 free equilibrium, $E_0 = (S^0, E^0, I^0, H^0, R^0) = (\frac{\Lambda}{\mu}, 0, 0, 0, 0)$ is locally asymptotically stable if and only if $R_0 < 1$.

Proof. Partial differentiation of Eq. (1) at E_0 results to a matrix of the form:

$$J_{DFE} = \begin{pmatrix} -\mu & 0 & \frac{\beta_1(\theta-1)\Lambda}{\mu} & \frac{\beta_2(\theta-1)\Lambda}{\mu} & \rho \\ 0 & -\alpha-\mu-\epsilon & \frac{\beta_1(\theta-1)\Lambda}{\mu} & \frac{\beta_2(\theta-1)\Lambda}{\mu} & 0 \\ 0 & \epsilon & -d-\delta-\mu-\nu & 0 & 0 \\ 0 & \alpha & \nu & -d-\mu-\omega & 0 \\ 0 & 0 & \delta & \omega & -\mu-\rho \end{pmatrix}. \quad (10)$$

From Eq. (10), we have two eigenvalues which are $\lambda_1 = -\mu$ and $\lambda_2 = -\mu - \rho$.

$$J_{DFE} = \begin{pmatrix} -\alpha-\mu-\epsilon & \frac{\beta_1(\theta-1)\Lambda}{\mu} & \frac{\beta_2(\theta-1)\Lambda}{\mu} \\ \epsilon & -d-\delta-\mu-\nu & 0 \\ \alpha & \nu & -d-\mu-\omega \end{pmatrix}. \quad (11)$$

Eq. (11) leads to the characteristic equation given as:

$$Z(\lambda) = \lambda^3 + a_1\lambda^2 + a_2\lambda + a_3, \quad (12)$$

where

$$a_1 = \alpha + 2d + \delta + 3\mu + \nu + \omega + \epsilon.$$

a_2 is given in Box II.

$$a_3 = (\alpha + \epsilon + \mu)(d + \mu + \omega)(d + \delta + \mu + \nu)(d + 2\mu + \nu + \omega)(1 - R_0).$$

By utilizing Routh–Hurwitz criteria, the negative real root of Fig. 12 is only obtained if and only if $a_1 > 0$, $a_3 > 0$ and $a_1a_2 > a_3$. In our case, a_1 is non negative since it is a summation of positive variables, but in order for a_3 to be positive, $1 - R_0$ must be non-negative which implies $R_0 < 1$. Consequently, the disease-free equilibrium point is locally asymptotically stable whenever $R_0 < 1$, otherwise unstable. \square

Global behavior of the model at E_0

The global behavior of the proposed model (1) is investigated using an approach presented in [33]. In showing that the eradication of COVID-19 in the human population does not dependent on the initial size of infected cases, it is very important to prove that disease-free equilibrium is globally asymptotically stable whenever $R_0 < 1$ [34].

Theorem 4. Whenever $R_0 < 1$, the proposed COVID-19 model posses the disease-free equilibrium point which is globally asymptotically stable.

Proof. Let us constructing Lyapunov function of the model (1) by considering the equation of the form:

$$P(t) = S - S^0 \ln S + E + I + H + R.$$

Taking derivatives both side yield

$$\frac{P(t)}{dt} = \left(1 - \frac{S^0}{S}\right) \frac{dS}{dt} + \frac{dE}{dt} + \frac{dI}{dt} + \frac{dH}{dt} + \frac{dR}{dt}. \quad (13)$$

Combining Eq. (1) with Eq. (13) at E_0 leads to:

$$\frac{P(t)}{dt} = \left(1 - \frac{S^0}{S}\right) (\Lambda - \mu S),$$

at point E_0 , $S^0 = \frac{\Lambda}{\mu}$, $\Lambda = \mu S^0$, hence

$$\frac{P(t)}{dt} = \left(1 - \frac{S^0}{S}\right) (\mu S^0 - \mu S),$$

further simplification result to:

$$\frac{P(t)}{dt} = \frac{-\mu(S - S^0)^2}{S}.$$

Therefore $\frac{P(t)}{dt} \leq 0$. Also, it can be observed that the largest invariant set of the model (1) is obtained whenever $S = S^0$. Hence by LaSalle Invariance Principle [35] at E_0 the model (1) is globally asymptotically stable for $R_0 < 1$ and this completes the proof. \square

*Global behavior at F^**

In order to investigate the global behavior of the model (1), consider the Lyapunov function V as used in [36] which is defined as: $V(S, E, I, H, R) = A_1(S - S^* \ln S) + A_2(E - E^* \ln E) + A_3(I - I^* \ln I) +$

$A_4(H - H^* \ln H) + A_5(R - R^* \ln R)$. The constants A_1, A_2, A_3, A_4 , and A_5 are non negative.

$$\frac{dV}{dt} = \begin{cases} A_1(1 - \frac{S^*}{S})\frac{dS}{dt} + A_2(1 - \frac{E^*}{E})\frac{dE}{dt} \\ + A_3(1 - \frac{I^*}{I})\frac{dI}{dt} + A_4(1 - \frac{H^*}{H})\frac{dH}{dt} \\ + A_5(1 - \frac{R^*}{R})\frac{dR}{dt}. \end{cases} \quad (14)$$

Substituting Eq. (1) into Eq. (14) yields:

$$\frac{dV}{dt} = \begin{cases} A_1(1 - \frac{S^*}{S})\lambda + \rho R - (\mu + (1 - \theta)(\beta_1 I + \beta_2 H)S) \\ + A_2(1 - \frac{E^*}{E})((1 - \theta)(\beta_1 I + \beta_2 H)S - (\alpha + \varepsilon + \mu)E) \\ + A_3(1 - \frac{I^*}{I})(\alpha E - (\delta + \nu + \mu + d)I) \\ + A_4(1 - \frac{H^*}{H})(\varepsilon E + \nu I - (d + \mu + \omega)H) \\ + A_5(1 - \frac{R^*}{R})(\delta I + \omega H - (\mu + \rho)R). \end{cases} \quad (15)$$

By substituting the value of the following parameters in Eq. (14) yield to Fig. 15.

$$\begin{aligned} \lambda &= \mu S^* + (1 - \theta)(\beta_1 I^* + \beta_2 H^*)S^* - \rho R^*, \\ \nu + d + \mu + \delta &= \frac{\alpha E^*}{I^*}, \\ d + \mu + \omega &= \frac{\nu I^* + \alpha E^*}{H^*}, \\ \mu + \rho &= \frac{\delta I^* + \omega H^*}{R^*}, \\ \alpha + \mu + \varepsilon &= \frac{(1 - \theta)(\beta_1 I^* + \beta_2 H^*)S^*}{E^*}. \end{aligned}$$

$$\frac{dV}{dt} = \begin{cases} A_1(1 - \frac{S^*}{S})(\mu + (1 - \theta)(\beta_1 I^* + \beta_2 H^*)S^*) - \gamma R^* \\ + \rho R - (\mu + (1 - \theta)(\beta_1 I + \beta_2 H)S) \\ + A_2(1 - \frac{E^*}{E})((1 - \theta)(\beta_1 I + \beta_2 H)S - \frac{(1 - \theta)(\beta_1 I^* + \beta_2 H^*)S^*}{E^*} E) \\ + A_3(1 - \frac{I^*}{I})(\alpha E - (\frac{\alpha E^*}{I^*})I) \\ + A_4(1 - \frac{H^*}{H})(\varepsilon E + \nu I - \frac{\nu I^* + \alpha E^*}{H^*} H) \\ + A_5(1 - \frac{R^*}{R})(\delta I + \omega H - \frac{\delta I^* + \omega H^*}{R^*} R). \end{cases} \quad (16)$$

Solving for constant A_i with $i = 1, 2, \dots, 5$ after simplification we have the following results:

$$\frac{dV}{dt} = \begin{cases} (1 - \theta)\beta_2 H^* S^* (2 - \frac{S^*}{S} + \frac{H}{H^*} - \frac{E}{E^*} - \frac{HSE^*}{H^* S^* E}) \\ + (1 - \theta)\beta_1 I^* S^* (2 - \frac{S^*}{S} + \frac{I}{I^*} - \frac{E}{E^*} - \frac{ISE^*}{I^* S^* E}) \\ + \mu S^* (2 - \frac{S^*}{S} - \frac{S}{S^*}) + \rho R^* (1 - \frac{S^*}{S} - \frac{R}{R^*} + \frac{RS^*}{R^* S}) \\ + \alpha E^* (1 + \frac{E}{E^*} - \frac{I}{I^*} - \frac{EI^*}{E^* I}) \\ + \varepsilon E^* (1 + \frac{E}{E^*} - \frac{H}{H^*} - \frac{EH^*}{E^* H}) \\ + \nu I^* (1 + \frac{I}{I^*} - \frac{H}{H^*} - \frac{IH^*}{I^* H}) \\ + \omega H^* (1 - \frac{R}{R^*} + \frac{H}{H^*} - \frac{HR^*}{H^* R}) \\ + \delta I^* (1 - \frac{R}{R^*} + \frac{I}{I^*} - \frac{IR^*}{I^* R}) \end{cases} \quad (17)$$

Since the arithmetic mean exceeds the geometric mean, the following inequalities hold:

$$\begin{aligned} (2 - \frac{S^*}{S} + \frac{H}{H^*} - \frac{E}{E^*} - \frac{HSE^*}{H^* S^* E}) &\leq 0, \\ (2 - \frac{S^*}{S} + \frac{I}{I^*} - \frac{E}{E^*} - \frac{ISE^*}{I^* S^* E}) &\leq 0, \\ (2 - \frac{S^*}{S} - \frac{S}{S^*}) &\leq 0, \\ (1 - \frac{S^*}{S} - \frac{R}{R^*} + \frac{RS^*}{R^* S}) &\leq 0, \\ (1 + \frac{E}{E^*} - \frac{I}{I^*} - \frac{EI^*}{E^* I}) &\leq 0, \\ (1 + \frac{E}{E^*} - \frac{H}{H^*} - \frac{EH^*}{E^* H}) &\leq 0, \\ (1 + \frac{I}{I^*} - \frac{H}{H^*} - \frac{IH^*}{I^* H}) &\leq 0, \\ (1 - \frac{R}{R^*} + \frac{H}{H^*} - \frac{HR^*}{H^* R}) &\leq 0, \\ (1 - \frac{R}{R^*} + \frac{I}{I^*} - \frac{IR^*}{I^* R}) &\leq 0. \end{aligned} \quad (18)$$

Since the arithmetic mean is greater than or equal to geometric mean, it follows that from Eq. (18) one can note that $\frac{dV}{dt} \leq 0$ whenever $R_0 > 1$. Therefore by using LaSalle Invariance principle [35], the system (1) have global asymptotically stable endemic equilibrium point for all $R_0 > 1$ and this completes the proof of Theorem 5.

Theorem 5. The proposed model (1) posses a very unique endemic equilibrium point if $R_0 > 1$ otherwise unstable.

Numerical simulation

This part aids in prediction numerically on stability of Eq. (1) through using the fourth-order Runge–Kutta scheme. Numerical experiments are investigated so as to verify analytical results. The baseline parameters for experiments of the proposed model is found Table 3. In addition, stability of the model numerically at endemic together with impact of some control parameters are investigated. Further, the study at hand explored sensitivity analysis. There are other numerical scheme such Adams–Bashforth–Moulton method, Eulers' method, and Milne method used by other authors for numerical simulation [13,15].

Sensitivity and uncertainty analysis

This is a technique deployed to examine the impact of every parameter in relation to the model output. Global sensitivity analysis in epidemiology is used to check uncertainty of each input parameter in relation to uncertainty of outcome. This methods quantify the influence whenever all input parameters are varied. PRCC determines the quantification level of uncertainty by just considering the specific problem [37]. The global sensitivity analysis technique employed in this study is called partial rank correlation coefficient (PRCC). The lowest and the highest values of PRCC are -1 and 1, respectively. Fig. 2 depicts bars which correspond to PRCC values at a instance. Also, the same figure indicates the layout of histograms for basic reproduction number. The bars are named using numbers. Every number corresponds to its parameter in the order as seen in Table 3. Parameters with positive influence against R_0 are $\lambda, \beta_1, \varepsilon, d, \omega, \alpha, \delta, \nu$, and β_2 . Any positive partial rank correlation coefficient influence positively to R_0 while the negative partial rank correlation has a negative influence against the value of R_0 . In our case the parameters θ and μ have negative PRCC values which lead to the decrease in the value of R_0 .

Through using the baseline parameters in Table 3 the value of basic reproduction number R_0 obtained is 3.2988. Also, when $\theta = 0$ while other parameters are kept as seen in Table 3, then the value of $R_0 = 8.4584$. When $\theta = 0.95$ the value of $R_0 = 0.4229$. Under this note, the wearing of PPE minimizes the COVID-19 infection. Fig. 3 depicts a positive association between R_0 and the parameter β_2 while Fig. 4 stipulates the negative correlation between R_0 and the parameter θ .

Table 3
Parameters value with source.

S/N	Parameter	Value (day ⁻¹)	Source
1	Λ	40	[14]
2	θ	0.61	[14]
3	β_1	0.54944	[38]
4	ε	0.3716	[11]
5	d	0.00011	[34]
6	μ	0.0008	[14]
7	ω	0.65	[14]
8	α	0.083	[39]
9	δ	0.2	[14]
10	ν	0.0833	[40]
11	β_2	0.05	[29]

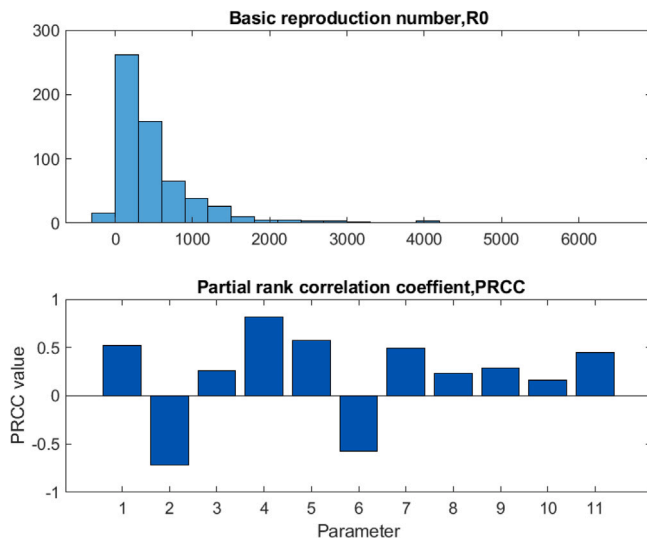


Fig. 2. Partial rank correlation coefficient (PRCC).

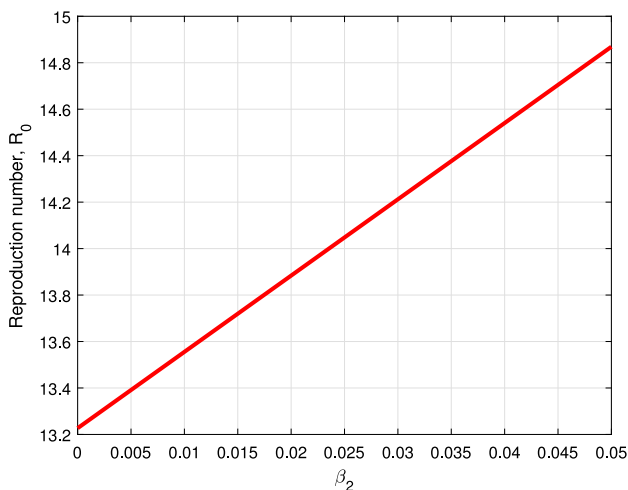


Fig. 3. Influence of β_2 on R_0 .

Dynamics of human populations

Stability of the model (1) is investigated numerically by varying initial population. Fig. 5 evinces five sub-population with an initial condition such as $S(0) = 1000$, $E(0) = 70$, $I(0) = 40$, $H(0) = 30$ and $R(0) = 20$. The susceptible sub-population starts at 1000 and decay exponentially till the point of equilibrium. The recovered sub-population grow exponential and start maintaining its equilibrium point at around

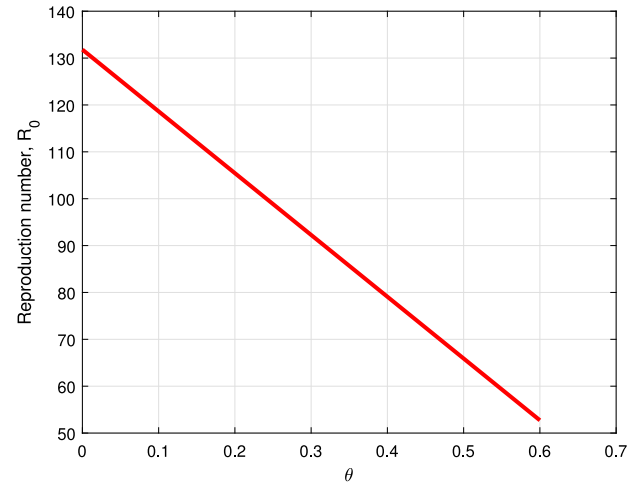


Fig. 4. Influence of θ on R_0 .

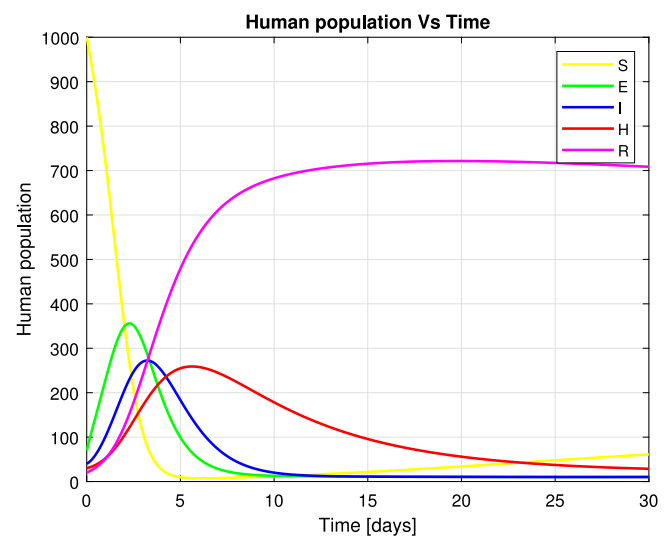


Fig. 5. Dynamics of SWEIHR sub-populations.

fifteen (15) days. The rest sub-population depicted by Fig. 5 describe the parabolic shape in the process of attaining equilibrium point.

Simulation on stability of Endemic Equilibrium Point (EEP)

We scrutinized the global stability at the endemic equilibrium point of the model system (1). The global stability can be attained whenever the model's state variables coming from distinguished initial values, varied for sometimes, convergence appeared in attaining the unique endemic numerical solution. The convergence of the model's trajectories to a common horizontal line signifies the global stability of the model system (1). Fig. 6 denotes five different trajectories originating from different assumed sub-population of the susceptible compartment such as $S(0) = 1000$, $S(0) = 900$, $S(0) = 800$, $S(0) = 700$ and $S(0) = 600$. All five trajectories converged to a common straight line after around eleven days. Figs. 7–9 depict the same results as the one stipulated in Fig. 6.

Impact of control parameters on the model

This part presents the numerical results of the model (1) when varying parameters θ , ω , and δ . Variation of aforementioned parameters

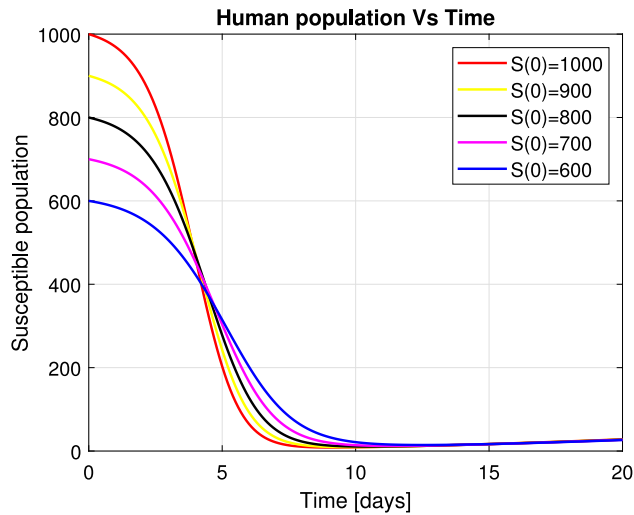


Fig. 6. Stability of the EEP for susceptible human population.

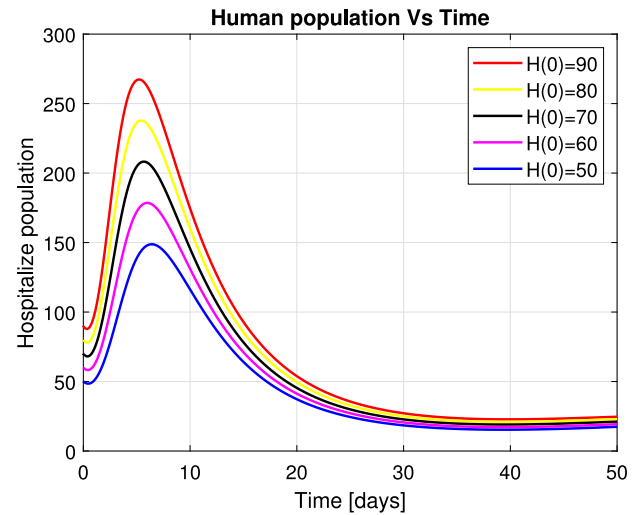


Fig. 9. Profile for stability of the EEP of hospitalized human population.

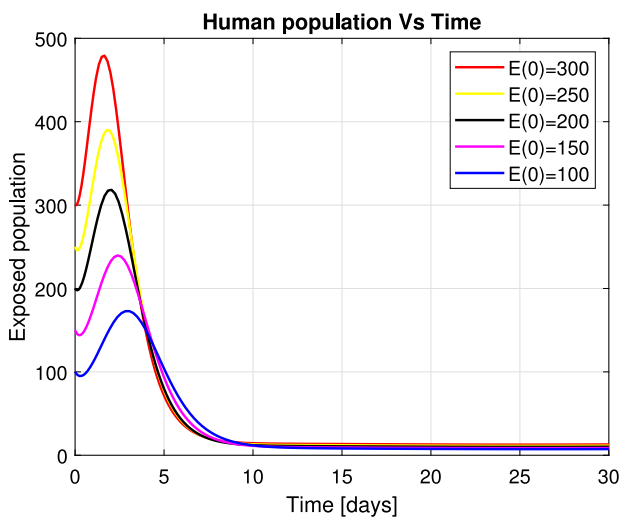


Fig. 7. Stability of the EEP for exposed human population.

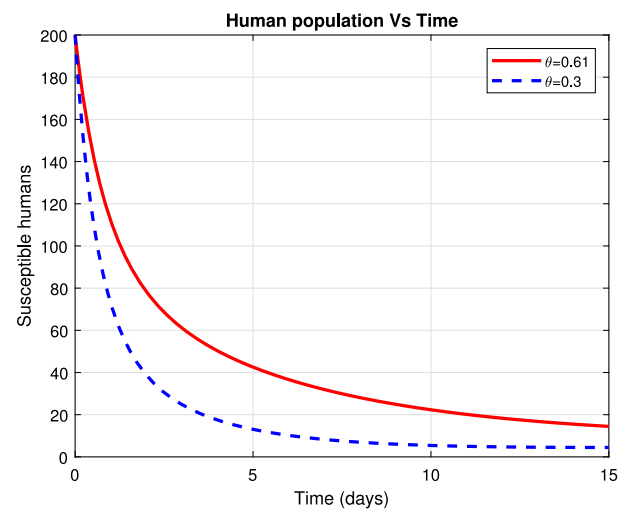
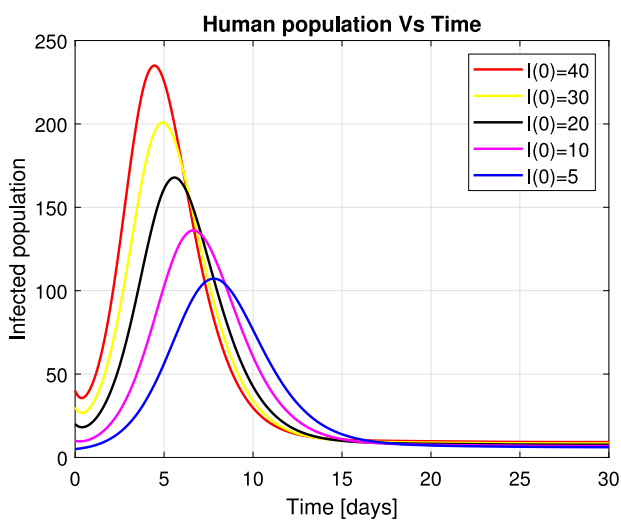
Fig. 10. Influence of θ on susceptible population.

Fig. 8. Profile for stability of the EEP of infected human population.

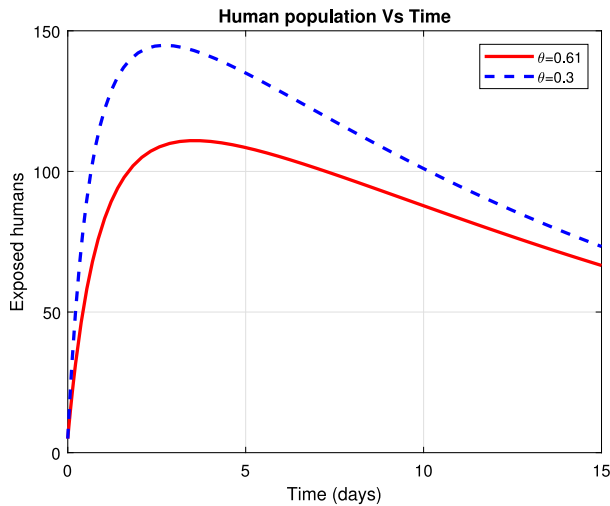
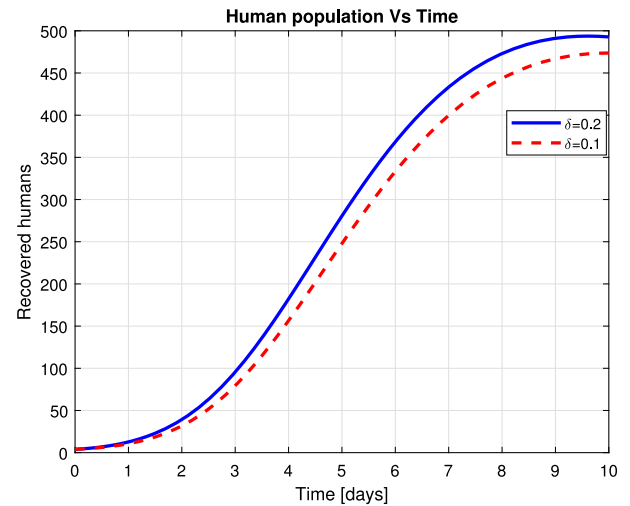
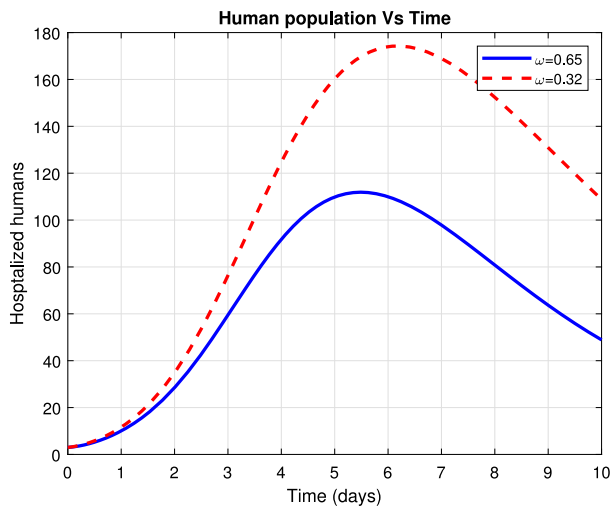
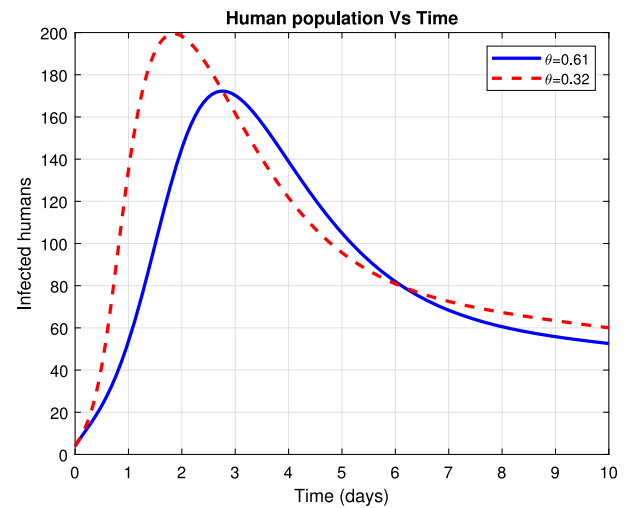
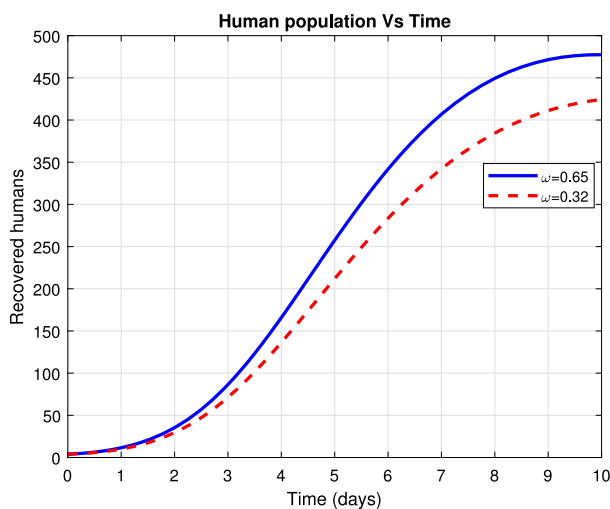
as observed in Table 3 aids in obtaining different graphical results for all state variables.

Fig. 10 shows the effect of use of PPE. Implementation PPE at a rate 0.61 helped a susceptible population to grow to around 15 individuals. Fig. 11 reveals that when PPE are worn at a rate of 0.61, exposed population reduces to about 66 individuals within only 10 days. Fig. 12 depicts the decrease in hospitalized patients to about 49 people due treatment given in the medical facilities as implemented at 65%. Fig. 13 evinces the grow of the number of the recovered population to about 447 individuals because of provision of medication in health facilities.

Fig. 14 depicts that the number of people who have recovered through acquiring natural body immunity at a rate of 0.2 is about 494. Fig. 15 shows that when θ is applied at 0.61 then the number infected individuals reduces to around 53 patients.

Discussion

The transmission dynamics of nosocomial infection for COVID-19 using a deterministic model was investigated. The parameter θ quantify the level of protection of the susceptible population when exposed to the disease. Figs. 10, 11 and 15 depicted that θ has a greater significance in reducing the spread of COVID-19 within human population. The numerical solutions obtained validated analytical results.

Fig. 11. Influence of θ on exposed population.Fig. 14. Effect of treatment (δ) recovered population.Fig. 12. Effect of ω on hospitalized humans.Fig. 15. Effect of θ on infected humans.Fig. 13. Effect of ω on recovered humans.

The stability of model (1) numerically is presented in Figs. 5 and 6–9. Positive and negative association between β_2 , θ and R_0 are shown in Figs. 3 and 4, respectively.

Conclusion

This research work proposed a deterministic model for COVID-19 nosocomial infection which was used to scrutinize the effect of personal protective equipment in reducing the load of infections. We presented the detailed analysis of the model. Positivity and boundedness of the solution have been determined through calculus technique. Further, we computed the threshold quantity by benefiting the next generation matrix. By using Metzler matrix and linearization technique the disease-free equilibrium point is found to be locally and globally asymptotically stable whenever $R_0 < 1$. Through using Lyapunov function in combination with LaSalle's Invariance Principle the endemic equilibrium point is found to be globally asymptotically stable when $R_0 > 1$. The proposed model is solved numerically by using fourth-order Runge–Kutta scheme [41] and the numerical solutions depicted that if the parameter θ is absence in the proposed model, the threshold parameter value was 8.4584. However, when the parameter is rated to be 95% the threshold parameter value decrease to around 0.4229. Hence parameter θ seem to be capable in minimization of the spread of COVID-19.

Conclusively, the model solution revealed that transmission nosocomial infection of COVID-19 can be minimized in the community through effective use personal protective equipment.

The study should be modified to Caputo fractional derivatives model for the purpose of capturing more biological phenomena such as crossover behavior and fade memory [1,42]. Further, in near future real data will be used to fit the model for the purposes of parameter estimation. The study is limited with an assumption that the total population was uniformly distributed.

CRediT authorship contribution statement

Lemjini Masandawa: Conceptualization, Formal analysis, Model formulation, Software, Data curation, Writing – original draft, Methodology, Writing – review & editing. **Silas Steven Mirau:** Supervision, Editing, Project administration. **Isambi Sailon Mbalawata:** Supervision, Editing, Project administration. **James Nicodemus Paul:** Supervision, Editing, Project administration. **Katharina Kreppel:** Supervision, Editing, Project administration. **Oscar M. Msamba:** Supervision, Editing, Project administration.

Declaration of competing interest

The authors declare that they have no known competing financial interests or personal relationships that could have appeared to influence the work reported in this paper.

Funding

No fund.

References

- Naik PA, Yavuz M, Qureshi S, Zu J, Townley S. Modeling and analysis of COVID-19 epidemics with treatment in fractional derivatives using real data from Pakistan. *Eur Phys J Plus* 2020;135(10):1–42.
- Oud MAA, Ali A, Alrabaiah H, Ullah S, Khan MA, Islam S. A fractional order mathematical model for COVID-19 dynamics with quarantine, isolation, and environmental viral load. *Adv Difference Equ* 2021;2021(1):1–19.
- Mahmoudi MR, Heydari MH, Qasem SN, Mosavi A, Band SS. Principal component analysis to study the relations between the spread rates of COVID-19 in high risks countries. *Alexandria Eng J* 2021;60(1):457–64.
- Ivorra B, Ferrández MR, Vela-Pérez M, Ramos AM. Mathematical modeling of the spread of the coronavirus disease 2019 (COVID-19) taking into account the undetected infections. The case of China. *Commun Nonlinear Sci Numer Simul* 2020;88:105303.
- Abioye AI, Peter OJ, Ogunseye HA, Oguntolu FA, Oshinubi K, Ibrahim AA, Khan I. Mathematical model of covid-19 in nigeria with optimal control. *Results Phys* 2021;28:104598.
- Shayak B, Sharma MM, Rand RH, Singh AK, Misra A. Transmission dynamics of COVID-19 and impact on public health policy. *MedRxiv* 2020.
- Peter OJ, Qureshi S, Yusuf A, Al-Shomrani M, Idowu AA. A new mathematical model of COVID-19 using real data from Pakistan. *Results Phys* 2021;104098.
- Mbogo RW, Odhiambo JW. COVID-19 Outbreak, social distancing and mass testing in Kenya-insights from a mathematical model. *Afrika Mat* 2021;1–16.
- Zamir M, Nadeem F, Abdeljawad T, Hammouch Z. Threshold condition and non pharmaceutical interventions's control strategies for elimination of COVID-19. *Results Phys* 2021;20:103698.
- Ahmad W, Abbas M, Rafiq M, Baleanu D. Mathematical analysis for the effect of voluntary vaccination on the propagation of corona virus pandemic. *Results Phys* 2021;104917.
- Ali A, Alshammari FS, Islam S, Khan MA, Ullah S. Modeling and analysis of the dynamics of novel coronavirus (COVID-19) with Caputo fractional derivative. *Results Phys* 2021;20:103669.
- Gostic K, Gomez ACR, Mummah RO, Kucharski AJ, Lloyd-Smith JO. Estimated effectiveness of symptom and risk screening to prevent the spread of COVID-19. *Elife* 2020;9:e55570.
- Baba IA, Yusuf A, Nisar KS, Abdel-Aty A-H, Nofal TA. Mathematical model to assess the imposition of lockdown during COVID-19 pandemic. *Results Phys* 2021;20:103716.
- Masandawa L, Mirau SS, Mbalawata IS. Mathematical modeling of COVID-19 transmission dynamics between healthcare workers and community. *Results Phys* 2021;29:104731.
- Yu C-J, Wang Z-X, Xu Y, Hu M-X, Chen K, Qin G. Assessment of basic reproductive number for COVID-19 at global level: A meta-analysis. *Medicine* 2021;100(18).
- Gebremeskel AA, Berhe HW, Atsaba HA. Mathematical modelling and analysis of COVID-19 epidemic and predicting its future situation in Ethiopia. *Results Phys* 2021;22:103853.
- Ahmed I, Modu GU, Yusuf A, Kumam P, Yusuf I. A mathematical model of coronavirus disease (COVID-19) containing asymptomatic and symptomatic classes. *Results Phys* 2021;21:103776.
- Naik PA, Zu J, Ghori MB, et al. Modeling the effects of the contaminated environments on COVID-19 transmission in India. *Results Phys* 2021;29:104774.
- Abdulwasaa MA, Abdo MS, Shah K, Nofal TA, Panchal SK, Kawale SV, Abdel-Aty A-H. Fractal-fractional mathematical modeling and forecasting of new cases and deaths of COVID-19 epidemic outbreaks in India. *Results Phys* 2021;20:103702.
- Moore S, Hill EM, Tildesley MJ, Dyson L, Keeling MJ. Vaccination and non-pharmaceutical interventions for COVID-19: a mathematical modelling study. *Lancet Infect Dis* 2021.
- Redhwan SS, Abdo MS, Shah K, Abdeljawad T, Dawood S, Abdo HA, Shaikh SL. Mathematical modeling for the outbreak of the coronavirus (COVID-19) under fractional nonlocal operator. *Results Phys* 2020;19:103610.
- Zhang L, Ullah S, Al Alwan B, Alshehri A, Sumelka W. Mathematical assessment of constant and time-dependent control measures on the dynamics of the novel coronavirus: An application of optimal control theory. *Results Phys* 2021;104971.
- Atangana A, Araz Si. Mathematical model of COVID-19 spread in Turkey and South Africa: theory, methods, and applications. *Adv Difference Equ* 2020;2020(1):1–89.
- Du Q, Zhang D, Hu W, Li X, Xia Q, Wen T, Jia H. Nosocomial infection of COVID-19: A new challenge for healthcare professionals. *Int J Mol Med* 2021;47(4):1.
- Park Y, Sylla I, Das AK, Codella J. Agent-based modeling to evaluate nosocomial COVID-19 infections and related policies. *Nature* 2021;3:4.
- Martos DM, Parcell B, Eftimie R. Modelling the transmission of infectious diseases inside hospital bays: implications for COVID-19. *MedRxiv* 2020.
- Lecy-Schoenherr M. How the COVID-19 pandemic may have impacted hospital acquired infection rates. 2021.
- Pham TM, Tahir H, van de Wijgert JHHM, Van der Roest B, Ellerbroek P, Bonten MJM, Bootsma MCJ, Kretzschmar ME. Interventions to control nosocomial transmission of SARS-CoV-2: a modelling study. *MedRxiv* 2021.
- Oke II, Oyebo YT, Fakoya OF, Benson VS, Tunde YT. A mathematical model for Covid-19 disease transmission dynamics with impact of saturated treatment: Modeling, analysis and simulation. *Open Access Lib J* 2021;8(5):1–20.
- Asamoah JKK, Bornaa CS, Seidu B, Jin Z. Mathematical analysis of the effects of controls on transmission dynamics of SARS-CoV-2. *Alexandria Eng J* 2020;59(6):5069–78.
- Van den Driessche P, Watmough J. Reproduction numbers and sub-threshold endemic equilibria for compartmental models of disease transmission. *Math Biosci* 2002;180(1–2):29–48.
- Patil A. Routh-hurwitz criterion for stability: An overview and its implementation on characteristic equation vectors using MATLAB. *Emerg Technol Data Min Inf Secur* 2021;319–29.
- Syafuruddin S, Noorani MSM. Lyapunov Function of SIR and SEIR model for transmission of dengue fever disease. *Int J Simul Process Model* 2013;8(2–3):177–84.
- Deressa CT, Duressa GF. Modeling and optimal control analysis of transmission dynamics of COVID-19: The case of Ethiopia. *Alexandria Eng J* 2021;60(1):719–32.
- LaSalle JP. Stability theory and invariance principles. In: *Dynamical systems*. Elsevier; 1976. p. 211–22.
- Korobeinikov A, Wake GC. Lyapunov Functions and global stability for SIR, SIRS, and SIS epidemiological models. *Appl Math Lett* 2002;15(8):955–60.
- Marino S, Hogue IB, Ray CJ, Kirschner DE. A methodology for performing global uncertainty and sensitivity analysis in systems biology. *J Theoret Biol* 2008;254(1):178–96.
- Mugisha JYT, Ssebuliba J, Nakakawa JN, Kikawa CR, Ssematimba A. Mathematical modeling of COVID-19 transmission dynamics in Uganda: Implications of complacency and early easing of lockdown. *PLoS One* 2021;16(2):e0247456.
- Aldila D. Analyzing the impact of the media campaign and rapid testing for COVID-19 as an optimal control problem in East Java, Indonesia. *Chaos Solitons Fractals* 2020;141:110364.
- Diagne ML, Rwezaura H, Tchoumi SY, Tchuenche JM. A mathematical model of COVID-19 with vaccination and treatment. *Comput Math Methods Med* 2021;2021.
- Yavuz M, Coşar FO, Günay F, Özdemir FN. A new mathematical modeling of the COVID-19 pandemic including the vaccination campaign. *Open J Model Simul* 2021;9(3):299–321.
- Ali Z, Rabiei F, Shah K, Khodadadi T. Qualitative analysis of fractal-fractional order COVID-19 mathematical model with case study of Wuhan. *Alexandria Eng J* 2021;60(1):477–89.

Poster: Mathematical Modelling of COVID-19 Transmission Dynamics Between Healthcare workers and Community

Lemjini Masandawa¹, Silas Steven Mirau² & Isambi Silon Mbalawata³

^{1, 2}The Nelson Mandela African Institution of Science and Technology (NM-AIST)

²African Institute for Mathematical Sciences, NEI Globla Secretariat, Rue KG590 ST, Kigali - Rwanda



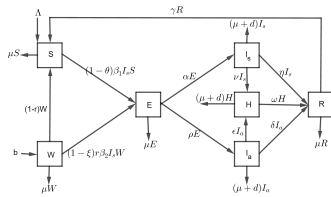
Introduction

COVID-19 is an infectious disease caused by SARS-CoV-2. It is newest kind of infectious disease posed an unprecedented threat to global public health. Healthcare workers caring for COVID-19 patients face insomnia, stigma, mental stress, physical exhaustion, separation from families, and the pain of losing patients and colleagues (Chersich et al., 2020). Many of them acquired SARS-CoV-2 and some died. From the outset of the outbreak to 8 May, 2020 there were around 152 888 infected healthcare workers with a total of 1413 death globally (Bandopadhyay et al., 2020). On other hand, as of 20 September, 2020 one study conducted in Mexico City revealed that there were around 17 531 healthcare workers who have been infected (Antonio-Villa et al., 2021).

Much researches conducted on mathematical models of COVID-19 concentrated on minimization of the disease spread among the public members. The study at hand formulated a deterministic model with focus on minimizing the COVID-19 infections among the healthcare workers and also the community at large.

Model Formulation

A mathematical model for COVID-19 between healthcare workers and community was presented. This deterministic has seven sub-population namely; Susceptible member of the community (S), Healthcare workers (W), Exposed (E), symptomatic infected (I_s), asymptomatic infected individuals (I_a), Hospitalized (H) and Recovered individuals (R).



Governing Differential Equations

$$\begin{aligned}\frac{dS}{dt} &= \Lambda + (1-r)W + \gamma R - (\mu + (1-\theta)\beta_1 I_s)S, \\ \frac{dW}{dt} &= b - \mu W - (1-r)W - (1-\xi)r\beta_2 W I_s, \\ \frac{dE}{dt} &= (1-\theta)\beta_1 I_s S + (1-\xi)r\beta_2 W I_s - (\alpha + \mu + \rho)E, \\ \frac{dI_s}{dt} &= \alpha E - (d + \nu + \mu + \eta)I_s, \\ \frac{dI_a}{dt} &= \rho E - (\mu + d + \delta + \epsilon)I_a, \\ \frac{dH}{dt} &= \nu I_s + \epsilon I_a - (\mu + d + \omega)H, \\ \frac{dR}{dt} &= \eta I_s + \omega H + \delta I_a - (\mu + \gamma)R.\end{aligned}\quad (1)$$

Theoretical Results

1. By using calculus technique the model's solutions are positive and bounded.
2. Benefiting from the next generation matrix the basic reproduction number:

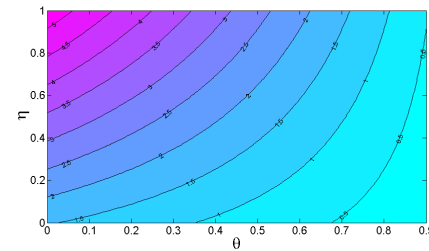
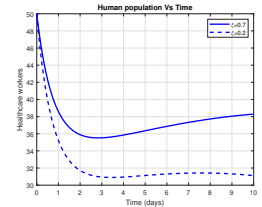
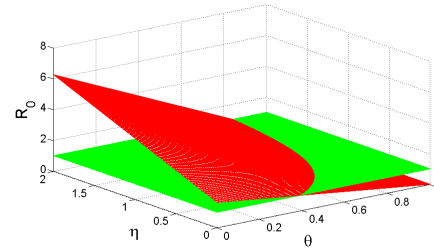
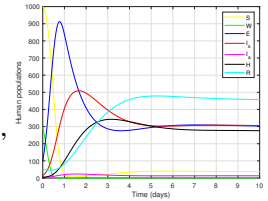
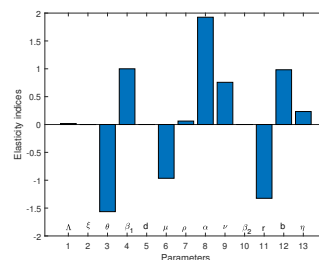
$$R_0 = \frac{\alpha\beta_1(1-\theta)((1-r)(b+\Lambda) + \Lambda\mu) + \alpha\mu(1-\xi)}{\mu(1-r+\mu)(\rho+\mu+\alpha)(\mu+\eta+d+\nu)}$$

3. Through the use of Routh-Hurwitz criterion and Metzler technique the DFE found to be LAS and GAS whenever $R_0 < 1$. Also, Lyapunov function was used to show that the EE is GAS when $R_0 > 1$.

Numerical Simulation Results

The numerical simulation was implemented through MATLAB software. Sensitivity analysis, effect some parameters and stability of the model were investigated in this study. The following figures demonstrate sensitive parameters to the model, stability of the model, effect of R_0 on the model, effect of PPE on the model and contour plot for the effect η and θ on R_0 , respectively.

Sensitivity Analysis



Conclusion and Recommendation

In this current work, a deterministic model for the transmission dynamics of COVID-19 between healthcare workers and the community that includes the protective measures with waning immunity is derived and analyzed both theoretically and numerically. This work recommends the adequate provision of Personal protective equipment to healthcare workers so to maintain this important workforce. In the future this model will be linked with vaccine compartment.